Form and Function in the *Scn1b*-null Cerebellar Cortex: Implications for Epileptic Encephalopathy

By

Jesse J. Winters

A dissertation submitted in partial fulfillment
of the requirements for the degree of
Doctor of Philosophy
(Neuroscience)
in the University of Michigan
2017

Doctoral Committee:

Professor Lori L. Isom, Chair
Assistant Professor Asim A. Beg
Professor Roman J. Giger
Research Associate Professor James Offord
Professor Jack M. Parent

Table of Contents

Acknowledgements

This work would not have been possible without the technical, professional, and intellectual support of my advisor, the members of my laboratory, and my dissertation committee. Here, I would like to acknowledge three mentors in particular, Dr. Lori L. Isom, Dr. James Offord and Dr. Roman J. Giger.

I would like to thank Lori for her exceptional patience. I know that I presented a unique mentorship challenge during my time as her graduate student, and she gave me the opportunity to overcome the shortcomings in my approach to science and the experimental failures that resulted. Her continued support afforded me the opportunity to learn and to grow into a competent, independent scientist. I am grateful that she did not give up on me or facilitate my giving up on myself. Additionally, her value for work-life balance permitted me to achieve my goals in the laboratory while simultaneously being present for and taking care of my children.

Secondly, I would like to acknowledge and appreciate Jim for the time he spent with me in organizing and improving my experimental approach. His constructive criticism and the rigor that he demonstrates in reviewing data are instructive and inspirational.

Finally, I would not be where I am without the guidance and support of my mentor and friend, Roman. My research project in his laboratory permitted me to gain an education in laboratory technique, experimental design, scientific writing and presentation. Together, the publication of our findings and his generous recommendation qualified me for entrance into the prestigious and competitive University of Michigan Ph.D. Program in Neuroscience. Moreover, he lent me invaluable support during the most difficult and trying part of my graduate school experience. I am sincerely grateful to Roman for believing in my capabilities and standing by me when I needed him.

List of Figures

Chapter I

Developmental and Regulatory Functions of Na^+ Channel Non-pore-forming β Subunits

(Portions of this chapter have been published in Current Topics in Membranes 2016, doi:10.1016/bs.ctm.2016.07.003)

Voltage-gated Na^+ channels (VGSCs) isolated from mammalian neurons are heterotrimeric complexes containing one pore-forming α subunit and two non-pore-forming β subunits. In excitable cells, VGSCs are responsible for the initiation of action potentials. VGSC β subunits are type I topology glycoproteins, containing an extracellular amino-terminal immunoglobulin (Ig) domain with homology to many neural cell adhesion molecules (CAMs), a single transmembrane segment, and an intracellular carboxyl-terminal domain. VGSC β subunits are encoded by a gene family that is distinct from the α subunits. While α subunits are expressed in prokaryotes, β subunit orthologs did not arise until after the emergence of vertebrates. β subunits regulate the cell surface expression, subcellular localization, and gating properties of their associated α subunits. In addition, like many other Ig-CAMs, β subunits are involved in cell migration, neurite outgrowth, and axon pathfinding and may function in these roles in the absence of associated α subunits. In sum, these multifunctional proteins are critical for both channel regulation and central nervous system development.

1. Introduction to the β Subunits

Voltage-gated Na^+ channels (VGSCs), anticipated by the classic voltage clamp experiments of Hodgkin and Huxley, were first discovered and biochemically-isolated from rat brain over 30 years ago. The purified constituents included one large (~260 kD) α subunit and two much smaller (~33 to 36 kD) β subunit proteins (Beneski & Catterall, 1980; Hartshorne &

Catterall, 1984; Hartshorne, Messner, Coppersmith, & Catterall, 1982; Hodgkin & Huxley, 1952). Although Na^+ currents can be measured by expression of an α subunit alone, e.g. in *Xenopus* oocytes (Goldin et al., 1986; Noda et al., 1986) in order to approximate physiological kinetics and gating properties, β subunits need to be co-expressed (Isom et al., 1992, 1995). Mammalian VGSCs are heterotrimeric complexes (Messner & Catterall, 1985). At the center of each channel is a pore-forming α subunit, flanked by one non-covalently associated β subunit (β1 or β3) and one covalently-associated β subunit (β2 or β4) (Hartshorne & Catterall, 1981; Isom et al., 1992, 1995; Morgan et al., 2000; Yu et al., 2003). As components of the VGSC complex, β subunits function in ion conduction by regulating channel expression at the cell surface, anchoring the complex to intracellular proteins, and by directly modulating the gating properties of the α subunit (Aman et al., 2009; Bennett, Makita, & George, 1993; Brackenbury et al., 2010; Chen et al., 2004; Isom et al., 1992, 1995, 1995b; Kazarinova-Noyes et al., 2001; Kazen-Gillespie et al., 2000; Ko, Lenkowski, Lee, Mounsey, & Patel, 2005; Lopez-Santiago, Brackenbury, Chen, & Isom, 2011; Lopez-Santiago et al., 2007; McEwen, Meadows, Chen, Thyagarajan, & Isom, 2004; Medeiros-Domingo et al., 2007; Patino et al., 2009; Watanabe et al., 2008; Yu et al., 2003; Zhou, Potts, Trimmer, Agnew, & Sigworth, 1991). In addition, β1 subunits have now been shown to modulate currents carried by voltage-gated K^+ channels (VGKCs), expanding the known β subunit functions outside of the realm of Na^+ channel physiology (Brackenbury, Yuan, O'Malley, Parent, & Isom, 2013; Deschenes & Tomaselli., 2002; Marionneau et al., 2012; Nguyen et al., 2012). Beyond that, it is now clear that in the CNS β subunit proteins are involved in a wide array of developmental functions that may be independent of the VGSC complex (Brackenbury et al., 2008, 2013; Brackenbury & Isom, 2011b; Davis, Chen, & Isom, 2004; Fein, Wright, Slat, Ribera, & Isom, 2008; Patino et al., 2011). β subunits each contain an extracellular immunoglobulin (Ig) domain, common to many cell-adhesion molecules (CAMs), with important roles in brain development (Isom et al., 1995; Maness & Schachner, 2007). This feature makes them unique amongst ion channel subunits and places them in the Ig-superfamily of CAMs. Binding partners include other VGSC β subunits, CAMs such as contactin and neurosfascin-186 (NF186), and extracellular matrix proteins such as tenascin (Malhotra, Thyagarajan, Chen, & Isom, 2004; McEwen & Isom, 2004;

Ratcliffe, Westenbroek, Curtis, & Catterall, 2001; Srinivasan, Schachner, & Catterall, 1998; Xiao et al., 1999). Finally, β1 interacts with ankyrins. This interaction may regulate VGSC subcellular localization and brain development (Malhotra et al., 2002, 2004; Malhotra, Kazen-Gillespie, Hortsch, & Isom, 2000). In sum, VGSC β subunits are promiscuous and multifunctional. This chapter will review the known regulatory and developmental functions of the VGSC β subunits, β1, β2, β3, β4, and β1B.

2. *β Subunit Evolution, Genes, and Structure*

2.1 Genes and Evolution

Ancestral orthologs to the mammalian VGSC β subunits have accompanied α subunits in the genome since the evolution of early vertebrate species (Chopra, Watanabe, Zhong, & Roden, 2007; Vilella et al., 2009). Mammalian β subunits are glycoproteins encoded by a gene family distinct from that of the α subunits, with the genes *SCN1B* through *SCN4B* encoding β1 through β4, respectively (Isom et al., 1992, 1995; Morgan et al., 2000; Qin et al., 2003; Yu et al., 2003). The gene *SCN1B* also encodes the secreted splice variant β1B, originally called β1A (Kazen-Gillespie et al., 2000a; Patino et al., 2011). While VGSC α subunit orthologs are expressed in prokaryotes, the β subunits evolved much later. In prokaryotes, VGSC α subunit genes are closely related to those of voltage-gated Ca^{2+} channels. Bacterial Na^{+} channels and Ca^{2+} channels are each composed of 6 transmembrane repeats that form homotetramers to construct the ion-conducting pore. They have a high degree of sequence similarity, especially in the pore domains, exhibit similar pharmacological profiles, and ultimately share common descent from VGKCs (Catterall, 2000; Goldin, 2001; Ren et al., 2001). By contrast, the VGSC β subunits share sequence homology and common ancestry with other proteins that have V-type Ig domains, including myelin P_0 (McCormick et al., 1998). β subunits are present in mammals, birds, and fish, but are absent from invertebrates (Chopra et al., 2007; Isom et al., 1992; Patino et al., 2009; Ren et al., 2001). β subunits were notably absent from purified VGSCs of the electric organ and brain of *Electrophorus electricus* (electric eel), shown to consist of α subunits

alone (Miller, Agnew, & Levinson, 1983; Sutkowski & Catterall, 1990). The recently reported *Electrophorus electricus* genome provided the opportunity to search for sequences homologous to the human proteins (Gallant et al., 2014). Our pBLAST analysis reveals orthologs to all four human β subunits. Perhaps in *Electrophorus electricus* these proteins serve functions separate from the VGSC complex. A β1 ortholog is expressed in the electric organ of the weakly electric fish *Sternopygus macrurus*. This ortholog modulates the properties of human Nav1.4 as well as the orthologous α subunit smNav1.4b, accelerating the rate of inactivation (Liu, Ming-Ming, & Zakon, 2007). The genome of another teleost, *Danio rerio* (zebrafish), contains six β subunit genes, homologous to β2, β3, and two duplicates each of β1 and β4, respectively (Chopra et al., 2007; Fein et al., 2008). Remarkably, important structural features of mammalian β subunits, including the extracellular Ig domain, an intracellular tyrosine-phosphorylation site in β1, and potential sites for N-linked glycosylation, are conserved in the zebrafish and electric eel orthologs (Chopra et al., 2007; Gallant et al., 2014). Zebrafish *scn1b* and *scn2b* have several splice variants and, similar to mammalian *SCN1B* encoding β1B, the zebrafish *scn1b* splice variants have variable carboxyl-termini (Chopra et al., 2007; Fein, Meadows, Chen, Slat, & Isom, 2007). Analysis of the zebrafish genome suggested that β2/β4 and β1/β3 subunits arose from the duplication of two distinct precursor genes early in vertebrate evolution (Chopra et al., 2007). In agreement with this estimate, no genes homologous to the sequences of zebrafish and human β subunits exist in the genomes of the invertebrate filter-feeding tunicates *Ciona intestinalis* and *Ciona savignyi* (sea squirts) (Azumi et al., 2003; Chopra et al., 2007; Du Pasquier, Zucchetti, & De Santis, 2004). The *Drosophila melanogaster* VGSC is composed of the pore-forming α subunit *paralytic* and the associated subunit *tipE*, but this protein is not homologous to vertebrate β subunits (Li, Waterhouse, & Zdobnov, 2011). Vertebrate genomes including jawless fishes, cartilaginous fishes, ray-finned fishes, and lobe-finned fishes all have predicted β subunit orthologs (Amemiya et al., 2013; Shin et al., 2014; Smith et al., 2013; Venkatesh et al., 2014; Vilella et al., 2009). The genomes of *Gallus gallus* (chicken) and other birds reveal that they have only 3 β subunit genes, with β1 being absent from all available sequences (Hillier, Miller, Birney, Warren, & Hardison, 2004; Vilella et al., 2009). Figure 1.1 shows a phylogenetic tree of selected vertebrate and invertebrate species, revealing homologous genes to human

SCN1B-SCN4B found in the sequenced genomes of those organisms. Note that the vertebrate jawless fish, *Petromyzon marinus* (sea lamprey) is the most evolutionarily distant species from humans that possesses a predicted β subunit ortholog. This finding suggests that these proteins arose in early fishes at least 500 million years ago. Notably, orthologs to *MPZ*, the human gene which encodes myelin P_0, occur in ray-finned fish genomes but not in more distantly-related jawless fishes or in invertebrates (Vilella et al., 2009). This corresponds with the evolutionary origin of myelin, the insulating sheath that is a necessary feature of saltatory axonal conduction, which characterizes the nervous systems of hinged-jawed fishes and their descendants, but is absent in jawless fishes such as lampreys and hagfish (Zalc, Goujet, & Colman, 2008). Myelinated axons have specialized structures, the nodes of Ranvier, where VGSC complexes, including β subunits, are highly concentrated (Buffington & Rasband, 2013; Chen et al., 2002, 2004; Kaplan, Cho, Ullian, & Isom, 2001; Patino et al., 2009). This could explain why genes encoding these proteins emerged alongside myelin proteins. Myelin P_0, one of the most abundant proteins in the peripheral myelin sheath, shares a highly homologous Ig domain with VGSC β subunits and is predicted to have a common ancestral gene (Vilella et al., 2009).

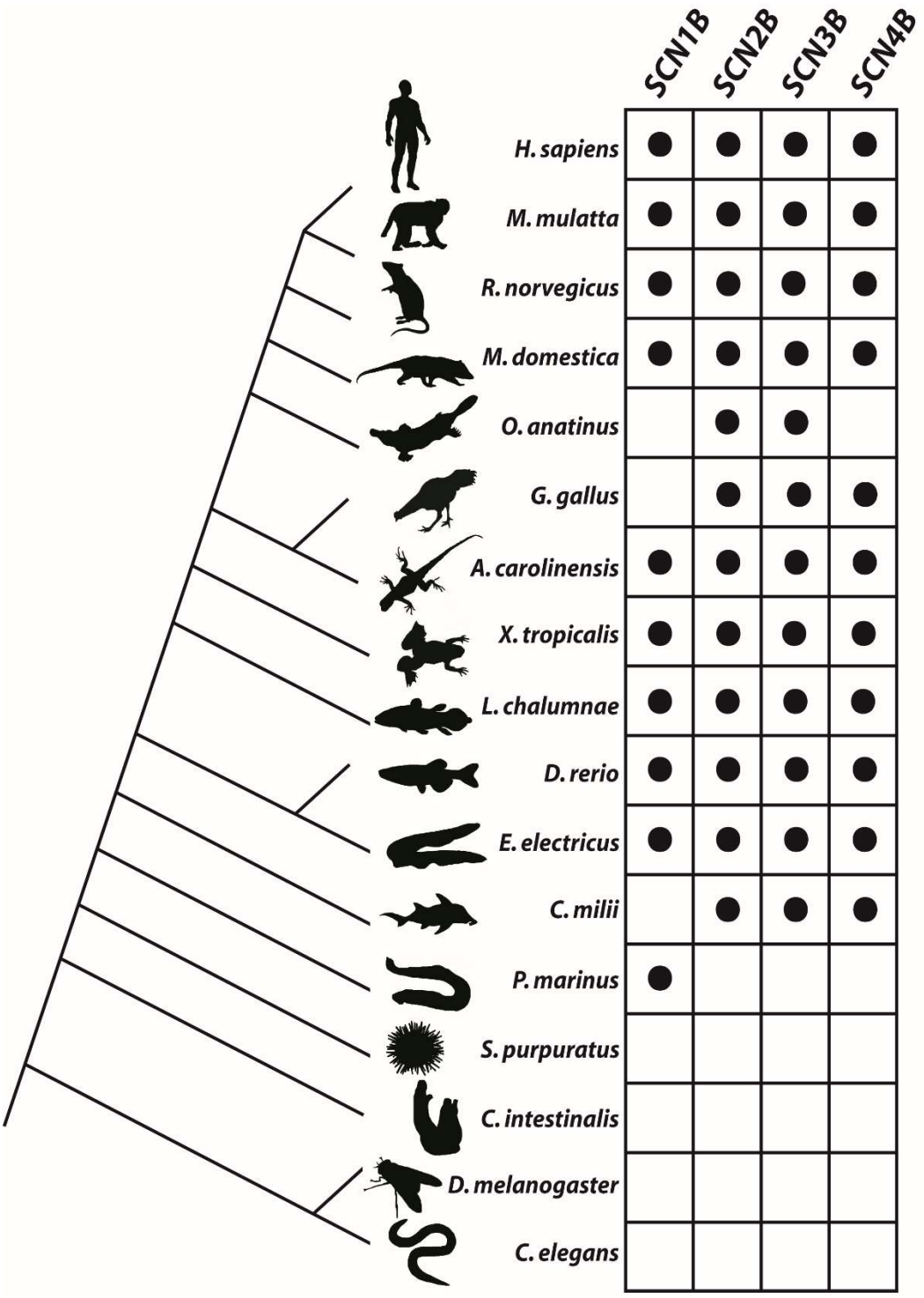

Figure 1.1 Phylogenetic tree of selected vertebrate and invertebrate species showing genes homologous to human *SCN1B-SCN4B*. *Macaca mulatta* = rhesus macaque (Gibbs et al., 2007); *Rattus norvegicus* = Norway rat; *Monodelphis domestica* = opossum (Mikkelsen et al., 2007); *Ornithorhynchus anatinus* = duck-billed platypus (Warren et al., 2008); *Gallus gallus* = chicken (Hillier et al., 2004); *Anolis carolinensis* = anole lizard (Alföldi et al., 2011); *Xenopus tropicalis* =

western clawed frog (Hellsten et al., 2010); *Latimeria chalumnae* = coelacanth (Amemiya et al., 2013); *Danio rerio* = zebrafish (Chopra et al., 2007; Fein et al., 2008); *Electrophorus electricus* = electric eel (Gallant et al., 2014); *Callorhinchus milii* = elephant shark (Venkatesh et al., 2014); *Petromyzon marinus* = sea lamprey (Smith et al., 2013); *Strongylocentrotus purpuratus* = sea urchin (Sodergren et al., 2006); *Ciona intestinalis* = sea squirt (Azumi et al., 2003); *Drosophila melanogaster* = fruit fly (Adams et al., 2000); *Caenorhabditis elegans* = nematode (The C. elegans Sequencing Consortium, 1998). Homologous genes and evolutionary history were analyzed using Ensembl (Vilella et al., 2009).

2.2 Structure

The structural features of VGSC β subunits predict diverse intracellular and extracellular interactions with ion channels, adhesion molecules, and cytoskeletal elements. Figure 1.2 diagrams the structures of β1 and β2, illustrating many of these important features. Mammalian β1, β2, β3, and β4 are type I topology transmembrane proteins, each having an extracellular amino-terminus containing an Ig domain, a single transmembrane segment, and an intracellular carboxyl-terminus (Isom, 2001). By contrast, β1B, formed by in-frame extension of the *SCN1B* third exon into intron 3, shares the extracellular amino-terminal domain of β1 but lacks a transmembrane domain, and has instead an alternate carboxyl-terminus (Kazen-Gillespie et al., 2000a; Patino et al., 2011). This results in a soluble protein that is secreted from the cell. Two subunits, β1 and β3, which share 57% sequence homology, interact exclusively in a non-covalent manner, via their amino- and carboxyl-termini, with the associated α subunit (McCormick et al., 1998; Meadows, Malhotra, Stetzer, Isom, & Ragsdale, 2001; Morgan et al., 2000; Spampanato et al., 2004). β2 and β4, which share 35% sequence identity, each interact covalently with the α subunit by means of a single extracellular disulfide bond between cysteine residue 26 of β2 or cysteine residue 28 of β4 (residue 58 from the initiator methionine) and one of the cysteine residues in the α subunit S5-S6 loops (Buffington & Rasband, 2013; Chen et al., 2012; Gilchrist, Das, Van Petegem, & Bosmans, 2013; Hartshorne & Catterall, 1984; Hartshorne et al., 1982; Messner & Catterall, 1985; Yu et al., 2003). The extracellular Ig domain, common to all five β subunits, is homologous to the V-type Ig loop motifs of members of the Ig-superfamily of CAMs (Ig-CAMs) (Isom & Catterall, 1996; Kazen-Gillespie et al., 2000; McCormick et al., 1998; Morgan et al., 2000; Yu et al., 2003). Figure 1.3 compares the

structures of the V-type Ig-CAMs N-CAM, L1, neurofascin, NrCAM, contactin, and myelin P_0 with the VGSC β subunits. Molecules of the Ig-superfamily are characterized by one or more tandem Ig-domain repeats with homology to the motif first identified in Ig proteins of the immune system. Neural Ig-CAMs, including N-CAM, L1, and contactin, bind homophilically and heterophilically and mediate important developmental processes such as neurite outgrowth, axon fasciculation, and cell migration (Crossin & Krushel, 2000; Vaughn & Bjorkman, 1996; Williams & Barclay, 1988). Sequence analysis of the β2 Ig loop shows remarkable homology to the third Ig repeat of the CAM contactin (Isom et al., 1995). The β1 and β3 Ig loops show homology to another Ig-CAM, myelin P_0 (Isom et al., 1995; McCormick et al., 1998; Morgan et al., 2000) (Figure 1.3). The recently reported β3 and β4 extracellular domain crystal structures revealed that the Ig loop of each β subunit, containing multiple β-sheets, is formed by a disulfide bridge between two cysteine residues (Gilchrist et al., 2013; Namadurai et al., 2014). This structure is consistent with V-type Ig domains (Vaughn & Bjorkman, 1996). An additional intramolecular disulfide bridge, unique to β3, results in further protein stability. Interestingly, the β3 crystal structure showed the formation of homodimers and homotrimers. Since Nav1.5 contains multiple sites for interaction with β3, it follows that it may form oligomeric complexes (Namadurai et al., 2014).

β subunits contain recognition sequences that subject them to sequential proteolytic cleavage by BACE1 (β-secretase) and γ-secretases, resulting in the release of amino-terminal and carboxyl-terminal fragments (H. K. Wong et al., 2005). This processing has important consequences. In particular, β1-mediated neurite outgrowth requires γ-secretase activity (Brackenbury & Isom, 2011a). β2-cleavage by γ-secretase leads to translocation of the intracellular domain (ICD) to the nucleus and subsequent changes in VGSC gene expression (Kim et al., 2007). Finally, the carboxyl-termini of β1 and β2 interact with the cytoskeleton-linked proteins ankyrinG and ankyrinB (Malhotra et al., 2000, 2002). This interaction, which may be critical to localizing channel proteins to specific cellular domains, is disrupted in β1 by phosphorylation of an intracellular tyrosine residue (Malhotra et al., 2002, 2004). Together, the extracellular and intracellular features of β subunit structures equip them for involvement in a diverse range of cellular functions.

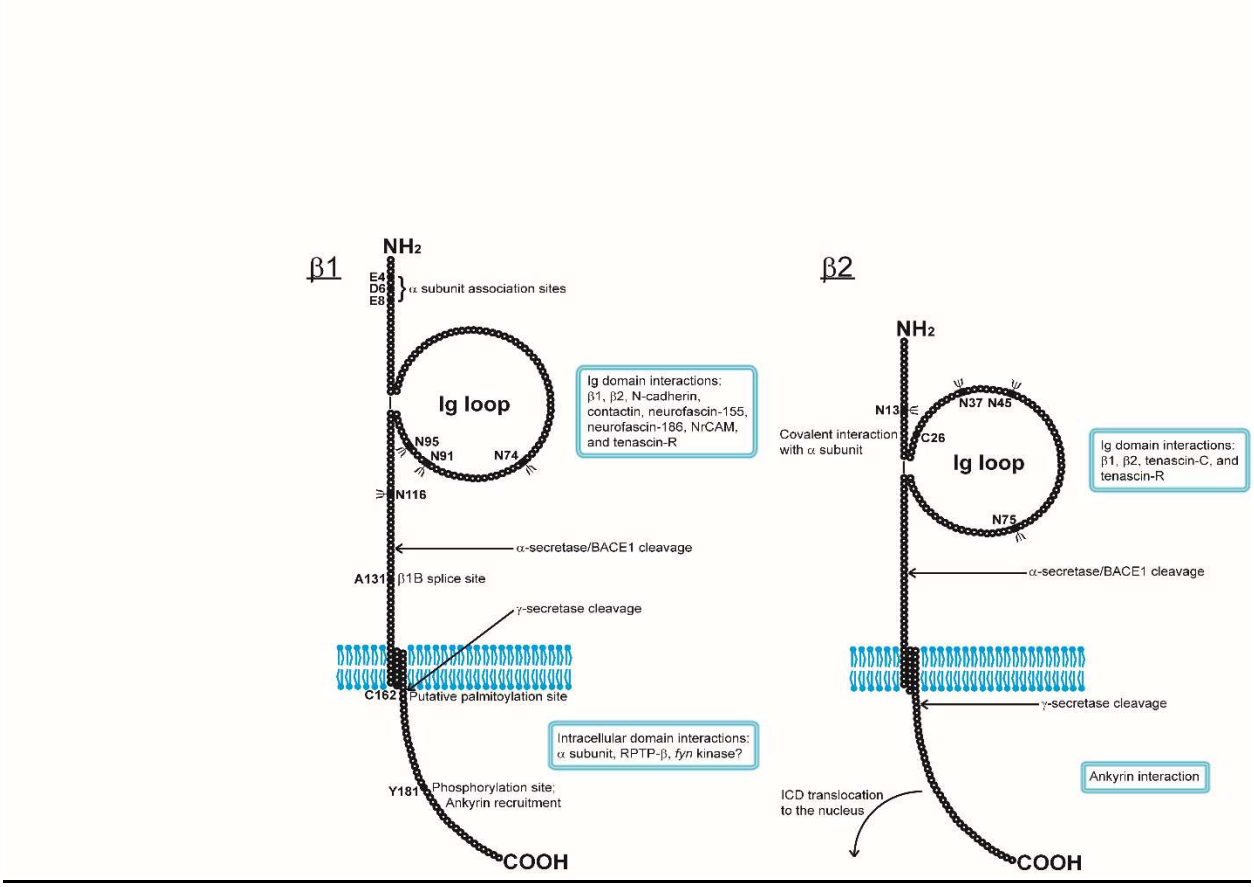

Figure 1.2 Structural features of β1 and β2. Features shown for β1 include extracellular sites for α subunit interaction (McCormick et al., 1998), N-linked glycosylation (ψ) sites (McCormick et al., 1998), the splice site for β1B indicating the first residue (A131) that is not shared by the splice variant (Kazen-Gillespie et al., 2000a; Patino et al., 2011; Qin et al., 2003), a putative palmitoylation site (McEwen & Isom, 2004), secretase cleavage sites (H. K. Wong et al., 2005), and a tyrosine phosphorylation site (Y181) which interacts with ankyrin (Malhotra et al., 2002, 2004). Boxes indicate the known Ig domain homophilic interaction (Malhotra et al., 2000) and heterophilic interactions with β2, N-cadherin, contactin, neurofascin-155 and -186, NrCAM (McEwen & Isom, 2004; Ratcliffe et al., 2001), and tenascin-R (Xiao et al., 1999) and intracellular domain interactions with the α subunit (Spampanato et al., 2004), RPTP-β (Ratcliffe et al., 2000), and, potentially, *fyn* kinase (Brackenbury et al., 2008; Malhotra et al., 2002, 2004). Features shown for β2 include N-linked glycosylation (ψ) sites (Isom et al., 1995), the cysteine residue (C26) that interacts covalently with the associated α subunit (Chen et al., 2012), and secretase cleavage sites (H. K. Wong et al., 2005). Also noted is the translocation of the cleaved β2 intracellular domain (ICD) to the nucleus (Kim et al., 2007). Boxes indicate known Ig domain homophilic interactions (Malhotra et al., 2000) and heterophilic interactions with β1 (McEwen & Isom, 2004), tenascin-C and tenascin-R (Srinivasan et al., 1998; Xiao et al., 1999) as well as the intracellular ankyrin interaction (Malhotra et al., 2000).

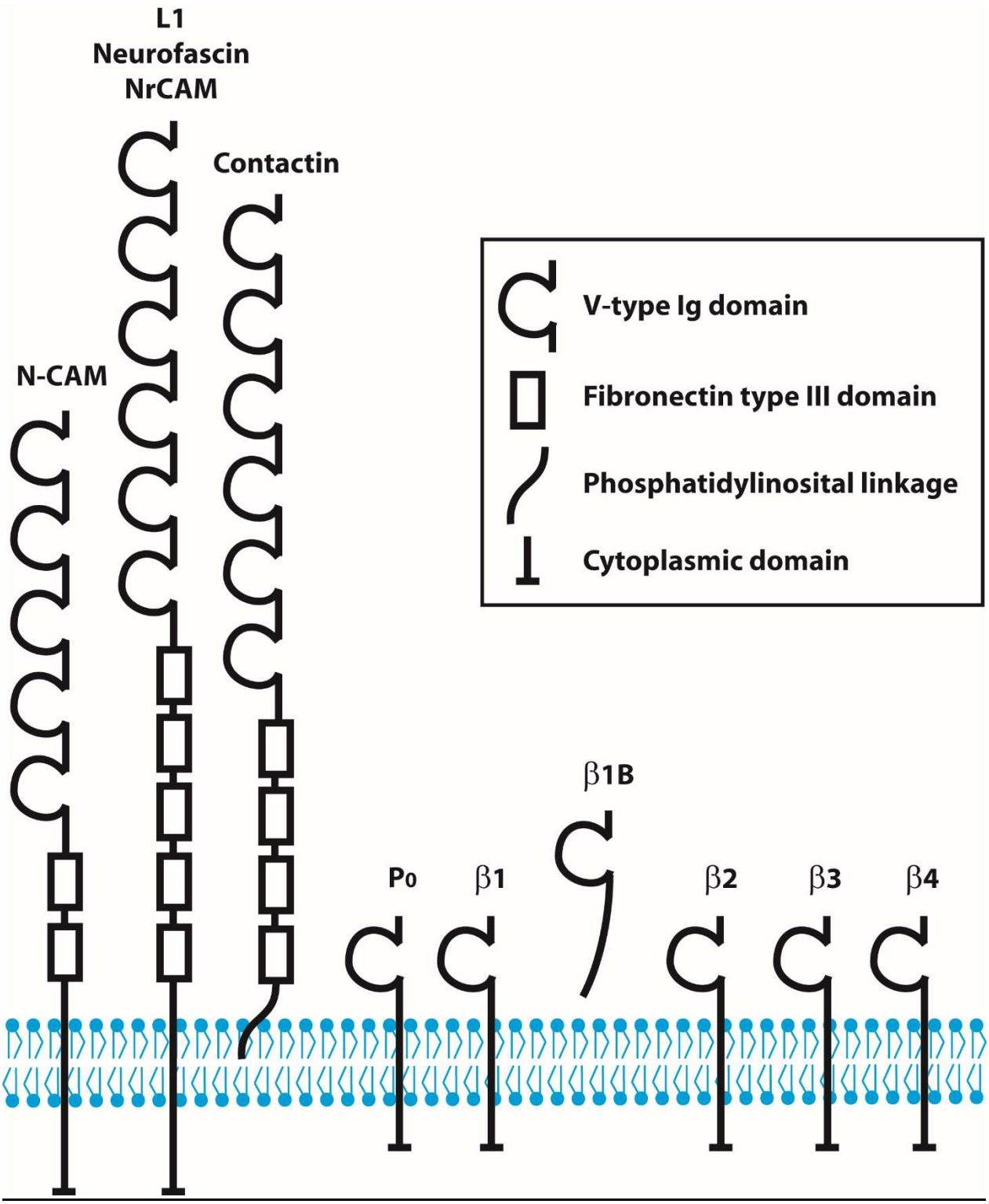

Figure 1.3 Comparison of VGSC β subunits with other V-type members of the Ig superfamily of CAMs.

3. β Subunit Expression, Localization, and Posttranslational Modification

3.1 Expression

Specific combinations of VGSC α and β subunits (and other proteins of the channelome complexes in which they reside) contribute to the particular physiological characteristics of divergent cell types. A model of such a complex is represented in Figure 1.4, which shows an α subunit associated with β1 and β2 to form a heterotrimer in addition to potential interacting partners that make up the channelome. Along with other molecular components of these channel complexes, VGSC β subunits are highly expressed in excitable cells of the CNS, peripheral nervous system (PNS), heart and skeletal muscle (Brackenbury & Isom, 2011a; Isom et al., 1992, 1995; Lopez-Santiago et al., 2006, 2011; Maier et al., 2004; Morgan et al., 2000; Yu et al., 2003). VGSC β subunits are also expressed in non-excitable cells, including astrocytes and radial glia, vascular endothelial cells, and cancer cells (Andrikopoulos et al., 2011; Aronica et al., 2003; Chioni, Brackenbury, Calhoun, Isom, & Djamgoz, 2009; Davis et al., 2004; Diss et al., 2008; Fein et al., 2008; Oh & Waxman, 1995). In a mouse model of breast cancer, β1 is postulated to enhance adhesion and increase tumor growth and invasion (Nelson, Millican-Slater, Forrest, & Brackenbury, 2014; Patel & Brackenbury, 2015). Reactive astrocytes in a rat temporal lobe epilepsy model and those associated with human pathologies show increased β1 protein expression, which might affect their ability to migrate toward an area of CNS injury (Aronica et al., 2003; Gorter, van Vliet, da Silva, Isom, & Aronica, 2002). In zebrafish, however, the *SCN1B* orthologs *scn1ba* and *scn1bb,* are differentially expressed in cells of the CNS and PNS, with *scn1ba* expression being greatest in neurons and skeletal muscle cells and *scn1bb* being expressed in Schwann cells, supporting cells of the olfactory pit and inner ear, and CNS myelinating glia (Fein et al., 2007, 2008). In addition, β subunit expression is developmentally regulated, with certain subunits generally decreasing during development and others generally increasing (Sutkowski & Catterall, 1990). In rodents, β1B and β3 are highly expressed prenatally with decreasing abundance after birth (Kazen-Gillespie et al., 2000a; Patino et al., 2011; Shah, Stevens, Pinnock, Dixon, & Lee, 2001). By contrast, β1 and β2 expression increases during

postnatal development and remains high in adulthood (Isom et al., 1995; Kazen-Gillespie et al., 2000; Patino et al., 2011). The developmental time course of β4 expression is unknown, but it is expressed postnatally in rat (Yu et al., 2003). Notable exceptions to these generalities exist. For example, β1B expression is maintained in adult heart and β3 continues to be expressed in adult dorsal root ganglion (DRG) neurons (Kazen-Gillespie et al., 2000a; Takahashi et al., 2003).

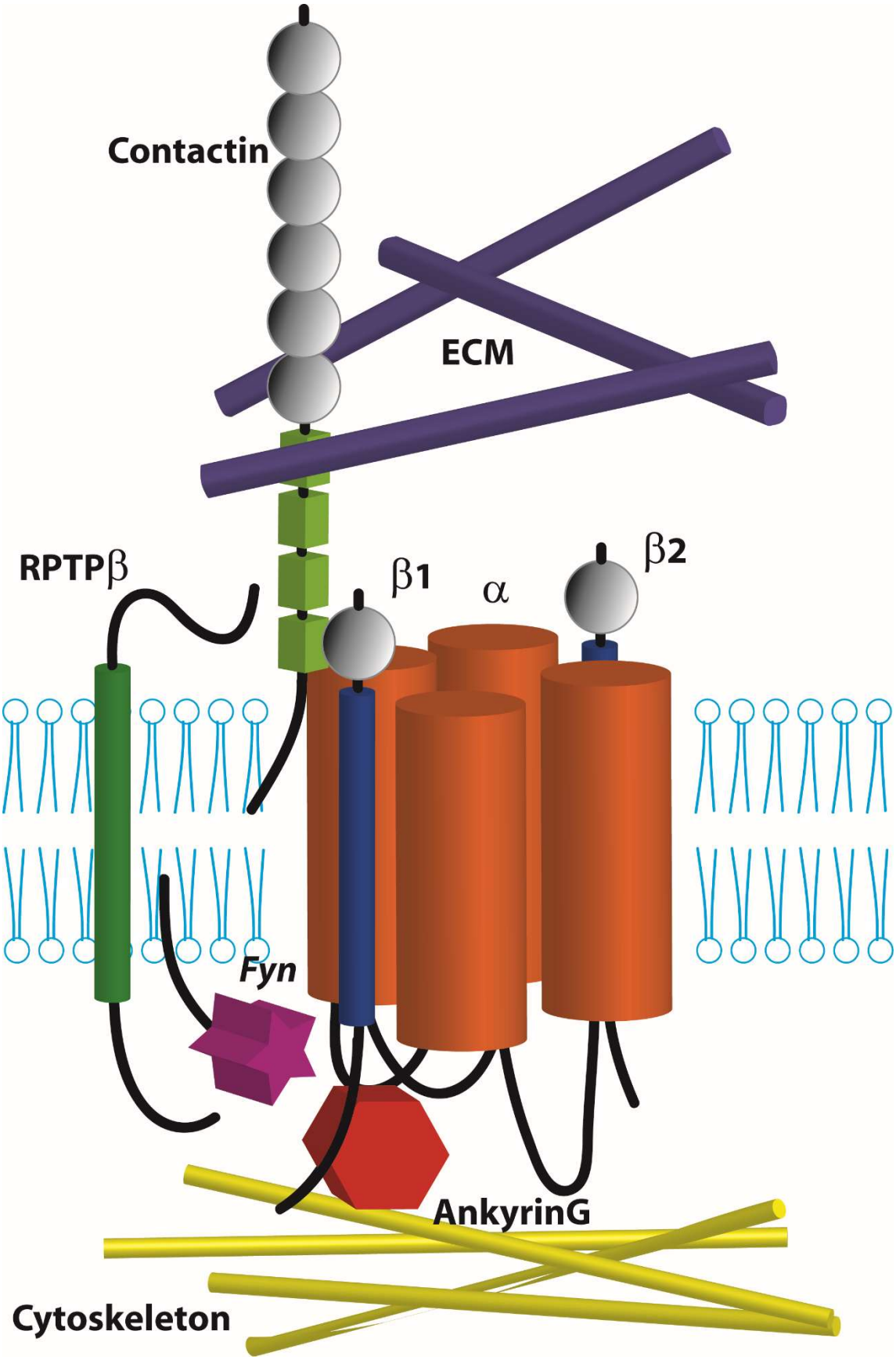
Contactin
ECM
RPTPβ
β1
α
β2
Fyn
AnkyrinG
Cytoskeleton

Figure 1.4 Model of the VGSC complex along with potential neuronal β subunit-interacting proteins. At the center is the pore-forming α subunit, composed of four contiguous domains (orange cylinders). β1 and β2 (blue cylinders) are represented flanking the α subunit, each with one extracellular Ig domain (grey sphere). Contactin, which has 4 fibronectin type-III domains (green rectangles) and 6 tandem Ig-domains (grey spheres), is shown anchored to the membrane adjacent to β1. ECM proteins (purple tubes), such as tenascin-C and tenascin-R, which are known partners for β1 and β2, are positioned above the complex. AnkyrinG (red hexagon), which binds to the intracellular domains of α and β1, is shown associated with the cytoskeleton (yellow filaments). Finally, the kinase *fyn* (pink star) and RTPβ (green cylinder) appear to the left of the complex near their sites of interaction with the β1 carboxyl-terminus.

3.2 Subcellular Localization in Neurons

As components of VGSCs, β subunits localize to subcellular compartments where they engage in specialized tasks. In neurons, these compartments include the axon initial segment (AIS) and the nodes of Ranvier. β subunits may also be present in the dendrites of certain neurons, such as subicular neurons, which have reduced dendritic arborization in a *Scn1b* mutant mouse (Reid et al., 2014). Viewed ultrastructurally, Nav1.6 localizes to presynaptic and postsynaptic membranes in the cortex and cerebellum (Caldwell, Schaller, Lasher, Peles, & Levinson, 2000). It is likely, though it has not been shown, that β subunits associate with the Nav1.6 channel complex at these synapses. The AIS, a specialized neuronal structure at the base of an axon near the soma, is the site of action potential initiation. Within this structure neuronal subtypes have diverse molecular compositions (Yoshimura & Rasband, 2014). In cortical neurons, Nav1.6 is enriched in the distal AIS along with VGKCs, while Nav1.2 is localized to the proximal AIS (Hu et al., 2009; Yoshimura & Rasband, 2014). Depending on the subtype, specific VGSC α and β subunits localize at high density to the neuron's AIS along with the cytoskeletal adaptor protein ankyrinG, and CAMs such as β1 binding partners NrCAM and NF186. β2 and β4 localize to the AIS in some neuronal subtypes (Buffington & Rasband, 2013; Chen et al., 2012). Nodes of Ranvier are axonal structures found in the gaps between myelinated segments. They are necessary for rapid, long-distance electrical signaling by means of saltatory conduction. A high density of ion channels and CAMs, including VGSC α and β subunits, are localized to nodes of Ranvier in CNS and PNS. In the CNS, β1 and β2 are localized

to optic nerve nodes of Ranvier, with a subset also expressing β4 (Buffington & Rasband, 2013; Kaplan et al., 2001; O'Malley, Shreiner, Chen, Huffnagle, & Isom, 2009; Patino et al., 2009). In the PNS, β1 and β2 localize to nodes of Ranvier in the sciatic nerve, while β4 localizes to most nodes of Ranvier in the dorsal and ventral spinal cord roots (Buffington & Rasband, 2013; Chen et al., 2002, 2004). Of note, an important binding partner for β1, the Ig-CAM contactin, is transiently colocalized with VGSCs at newly-formed PNS nodes of Ranvier and persistently colocalized at CNS nodes of Ranvier from development to adulthood (Kazarinova-Noyes et al., 2001). During neuronal development, another subcellular structure, the axon growth cone, has been shown to express CAMs, including β1 (Brackenbury et al., 2010). The axon growth cone is the dynamic, growing tip which senses its environment by means of cell adhesion and intracellular signaling to accurately direct axon pathfinding (Lowery & Van Vactor, 2009).

3.3 Subcellular Localization in Cardiomyocytes

VGSC β subunits are differentially localized to specialized subcellular domains of cardiomyocytes. Intercalated disks, formed at junctions between cardiomyocytes, are necessary for mechanical and electrical coupling. Transverse (T)-tubules are invaginations of the plasma membrane, linking it to the sarcoplasmic reticulum to allow for efficient Ca^{2+}-induced Ca^{2+} release upon stimulation (Brette & Orchard, 2003). β1 has been shown to localize to both intercalated disks and T-tubules in ventricular cardiomyocytes, and to intercalated discs in atrial cardiomyocytes (Kaufmann et al., 2013; Maier et al., 2004; Malhotra et al., 2001, 2004). β2 has been alternately reported to localize to intercalated disks or to T-tubules in ventricular cardiomyocytes (Maier et al., 2004; Malhotra et al., 2001). In the atrium, β2 is localized to T-tubules (Kaufmann et al., 2013). β3 localizes to T-tubules in ventricular cardiomyocytes and to intercalated disks in the atrium (Kaufmann et al., 2013; Maier et al., 2004). β4, by contrast, localizes to intercalated disks in ventricular cardiomyocytes (Maier et al., 2004). β1B is also expressed in atrial and ventricular cardiomyocytes, and may be particularly important in junctions between cells (Kazen-Gillespie et al., 2000a). Nav1.5 is highly expressed at intercalated disks, and β1B has been shown to regulate these α subunits in heterologous cells,

increasing peak Na^+ current and negatively shifting the voltage-dependence of activation and inactivation (H. Watanabe et al., 2008).

3.4 Glycosylation

N-linked glycosylation sites of VGSC β subunits are conserved across highly divergent species (Chopra et al., 2007). Approximately one-third of the total β subunit molecular weight is glycosylation. The Ig domain of each of these proteins contains 3 or 4 N-linked glycosylation sites (Figure 1.2; Isom et al., 1992; Messner & Catterall, 1985). The potential importance of glycosylation in β subunit function has been demonstrated in heterologous systems. In Chinese hamster ovary (CHO) cells lacking the capacity for sialylation, a prominent type of glycosylation in VGSC proteins, β1 is unable to modulate the gating of Nav1.2, Nav1.5, or Nav1.7 (Johnson et al. 2004). In the same type of assay, β2 modulates Nav1.5 in a sialic acid-dependent manner, but modulates Nav1.2 even without sialic acid (D. Johnson & Bennett, 2006). These *in vitro* studies suggest that glycosylation is likely to be important for the modulation and increased cell surface expression of certain α subunits by their partner β subunits. Notably, myelin P_0, which has homology to β subunit Ig domains, requires glycosylation for its homophilic interactions (Filbin & Tennekoon, 1993). This suggests that β subunit CAM functions may also depend critically on carbohydrate components.

3.5 Phosphorylation

β1 is regulated by phosphorylation of its carboxyl-terminal domain. Basal tyrosine phosphorylation of β1 can be detected in rat brain membranes, and a tyrosine residue at position 181 is phosphorylated *in vitro* (Figure 1.2; Malhotra et al., 2002). In *Drosophila* S2 cells expressing a β1 mutant construct (β1Y181E) which mimics phosphorylation, CAM functions are intact but interaction with ankyrinG is disrupted (Malhotra et al., 2002). β1Y181E increases cell surface expression of α in transfected Chinese hamster lung (CHL) fibroblasts, but does not modulate Na^+ current as β1 does (McEwen et al., 2004). In cardiomyocyes, tyrosine-

phosphorylated β1 colocalizes with tetrodotoxin (TTX)-resistant Nav1.5 at intercalated disks, while non-phosphorylated β1 localizes at T-tubules, where the TTX-sensitive channels, Nav1.1, Nav1.3, and Nav1.6 are known to reside (Malhotra et al., 2004). This suggests that tyrosine-phosphorylation may regulate the subcellular localization of β1, as well as its interactions with other proteins within the cell. A screen for phosphorylated proteins in mouse synaptosomes revealed that β1 is also phosphorylated on threonine residues, but the functional impact of this modification remains unknown (Trinidad et al., 2012). Finally, both α and β1, but not β2, interact with receptor protein tyrosine phosphatase β (RPTPβ), in a developmentally regulated manner resulting in altered VGSC function (Ratcliffe et al., 2000). Data suggest that RPTPβ is a member of the VGSC signaling complex along with β subunits and other Ig-CAMs (Figure 1.4; Ratcliffe et al., 2000).

3.6 Proteolytic Regulation

The transmembrane VGSC β subunits are targets for sequential proteolytic cleavage by BACE1 and γ-secretase (Figure 1.2). First, BACE1 cleaves and releases the Ig-loop-containing extracellular domain, which may function as a soluble CAM (H. K. Wong et al., 2005). The β1 construct β1Fc and the secreted β1B subunit have been proposed to function in this way (Davis et al., 2004; McEwen & Isom, 2004; Patino et al., 2011). Following that, γ-secretase cleavage releases the intracellular domain (ICD) into the cytoplasm (H. K. Wong et al., 2005). Pharmacological inhibition of γ-secretase prevents neurite outgrowth mediated by homophilic β1-β1 interactions, suggesting a role for the β1 ICD in signal transduction (Brackenbury & Isom, 2011b). The cleaved β2 ICD has been shown to translocate to the nucleus, leading to increased *SCN1A* mRNA expression and Nav1.1 protein levels *in vitro* (Figure 1.2; Kim et al., 2007). *Scn1b*-null mice have increased levels of *Scn3a* and *Scn5a* mRNA in the heart (Lin et al., 2015; Lopez-Santiago et al., 2007). This may result from the loss of β1 ICD regulation of *Scn3a* and *Scn5a* transcription in the nucleus. No function is yet known for the β3 and β4 ICDs.

4. β Subunits Modulate α Subunit Localization and Function

4.1 Modulation in Heterologous Cells

Expression of VGSC α and β subunits in heterologous cells has provided much of what we know about the functions and interactions of these proteins. Results in these systems are not always consistent with what is seen in the physiological context of the neuron or cardiomyocyte but have, nevertheless, yielded valuable insights. Early VGSC studies expressing Nav1.2 in *Xenopus* oocytes revealed Na^+ currents that activated and inactivated much more slowly than those recorded in neurons (Auld et al., 1988; Goldin et al., 1986; Joho et al., 1990). The first suggestion that modulatory proteins were necessary to achieve physiological currents came from co-injection of α subunit mRNA with low-molecular weight mRNA isolated from rat brain into oocytes (Auld et al., 1988; Krafte et al., 1990). Recordings from these cells showed increased Na^+ current density, more rapid inactivation, and altered voltage-dependence of inactivation, mimicking Na^+ currents recorded from neurons. Because VGSC α subunits purified from rat brain to theoretical homogeneity contained β subunits, these were predicted to be the modulatory proteins encoded in the low-molecular weight mRNA (Hartshorne & Catterall, 1984; Hartshorne et al., 1982). The cDNAs for β1 and β2 were subsequently cloned, and mRNAs encoding these proteins were co-expressed in oocytes along with Nav1.2 (Isom et al., 1992, 1995, 1995b). Co-expression of Nav1.2 with β1 revealed increased peak Na^+ current density (2.5-fold), negatively-shifted voltage dependence of inactivation (~19 mV), and accelerated inactivation compared with Nav1.2 alone (Isom et al., 1992). Co-expression of Nav1.2 with β2 also led to increased Na^+ current density (1.8- to 2.9-fold) and accelerated channel inactivation. Additionally, β2 expression in the absence of α increased the oocyte surface area, likely by stimulating the fusion of intracellular vesicles with the plasma membrane. The largest Na^+ current levels (3.7-fold) were achieved when all three subunits were co-expressed. Most importantly, co-expression of Nav1.2 with both β1 and β2 resulted in rapidly inactivating currents similar to those recorded from neurons (Isom et al., 1995, 1995b). β1 also modulates K^+ currents carried by the K^+ channels Kv1.1, Kv1.2, Kv1.3, Kv1.6, Kv4.2, and Kv7.2 when co-expressed in oocytes (Deschenes & Tomaselli., 2002; Nguyen et al., 2012). In

this regard, the Kv4.2 channel complex immunoprecipitated from mouse brain contains VGSC β1. Furthermore, knockdown of β1 in isolated cortical neurons resulted in reduced A-type K^+ currents and prolonged action potential waveforms (Marionneau et al., 2012). These experiments show that β subunits are capable of promiscuous alteration of ion channel function.

Mammalian cell lines have been used extensively to study VGSC physiology. These heterologous cells provide a more physiological context than *Xenopus* oocytes, but nevertheless do no fully recapitulate the VGSC properties seen in neurons and cardiomyocytes. Co-expression of Nav1.2 with β1 in CHL cells recapitulates the results seen in oocytes with regard to increased peak current density. β1 also causes negative shifts in the voltage dependence of activation (2-11 mV) and inactivation (10-12 mV) although these effects are smaller than those measured in oocytes (Isom et al., 1995; Patino et al., 2009). The modulatory and localization effects exerted by β1 on Nav1.2 in mammalian cells are further amplified by interaction with other Ig-superfamily CAMs (Kazarinova-Noyes et al., 2001; McEwen et al., 2004). For example, when contactin is co-expressed with Nav1.2 and β1 in CHL cells, α subunit surface expression and Na^+ current density are both increased dramatically (~4-fold) over that seen with just Nav1.2 and β1 (Kazarinova-Noyes et al., 2001). Co-expression of NF186 with Nav1.2 and β1 also increases the expression of α subunits on the cell surface beyond that seen with Nav1.2 and β1 alone (McEwen et al., 2004). Co-expression of Nav1.2 with β2 in CHL cells results in Na^+ currents that are reduced or unchanged compared to Nav1.2 expressed alone (Kazarinova-Noyes et al., 2001; McEwen et al., 2004). This result is in disagreement with experiments conducted in oocytes. However, when β1 and β2 are both co-expressed with Nav1.2, β2 increases cell surface expression of α subunits above that seen with Nav1.2 and β1 alone. Thus, at least in this heterologous system, β2 requires expression of β1 to exert its effects (Kazarinova-Noyes et al., 2001). When co-expressed with Nav1.3 in CHO cells, either β1 or β3 induced a negative shift (~10 mV) in the voltage of inactivation without affecting the rate of inactivation. β2 co-expression had no effect on Nav1.3 in these cells (Meadows, Chen, Powell, Clare, & Ragsdale, 2002). In rodent development β3 and Nav1.3 are expressed at their highest levels early, so the interaction of these two subunits could be relevant physiologically

(Shah et al., 2001). β3 co-expressed with Nav1.5 in CHO cells, results in a negative shift in the voltage dependence of inactivation and slows the rate of inactivation (Ko et al., 2005). In human embryonic kidney (HEK) cells, co-expression of β4 with either Nav1.2 or Nav1.4 leads to a negative shift (6-7 mV) in the voltage dependence of activation (Yu et al., 2003). Co-expression of β4 with Nav1.1 in HEK cells has the same effect but also increases the amount of non-inactivating current (Aman et al., 2009). Co-expression of Nav1.5 and β4 in HEK cells induces a negative shift in the voltage of inactivation (Medeiros-Domingo et al., 2007). Resurgent current, the influx of Na^+ through VGSCs during membrane repolarization in neurons, has been proposed to involve the intracellular domain of β4 as a blocking particle of the open channel (Bean, 2005; Grieco, Malhotra, Chen, Isom, & Raman, 2005). Indeed, in HEK cells a β4 peptide was able to mediate resurgent current when coexpressed with Nav1.7, but not Nav1.6, (Chen et al., 2008; Theile & Cummins, 2011). Co-expression of β1B with Nav1.2 in CHL cells, reveals a strong increase in α subunit surface expression and Na^+ current density with only a subtle effect on channel activation and inactivation (Kazen-Gillespie et al., 2000a). By contrast, when co-expressed in CHO cells β1B has no effect on cell surface localization of Nav1.3 or its Na^+ current density, despite both proteins being preferentially expressed in prenatal brain (Patino et al., 2011). β1B, which is also expressed in heart, interacts in an interesting way with Nav1.5, remaining at the cell surface along with the α subunit and increasing its expression there (Patino et al., 2011; H. Watanabe et al., 2008). Thus β1B may function as a soluble CAM in some contexts and, in others, as an α subunit-modulator.

4.2 Modulation in Native Cells

The best experimental representation of VGSC physiology is found by investigating the native channels in neurons and cardiomyocytes. In acutely isolated primary cells and tissue slices, β subunit regulatory effects on α subunit function and surface expression are more subtle than in heterologous systems and differ between cell types. *Scn1b*-null mice lack both β1 and β1B subunits. These mice exhibit spontaneous seizures, ataxic gait, and premature death (Chen et al., 2004). Recordings from P10-18 *Scn1b*-null acutely isolated hippocampal

pyramidal (excitatory) neurons and bipolar (inhibitory) neurons showed no differences in Na^+ current properties compared to neurons from wildtype animals (Chen et al., 2004; Patino et al., 2009). By contrast, slice recordings from similarly-aged *Scn1b*-null brain reveal hyperexcitability in hippocampal CA3 neurons (Patino et al., 2009). Because brain slices preserve intact dendrites and axons, β1 and β1B in these neuronal processes, not just the soma, may be important in regulating the cell's activity. Immunofluorescence experiments show a reduction in Nav1.1 and an increase in Nav1.3 in *Scn1b*-null CA3 neurons relative to wildtype neurons (Chen et al., 2004). P16 *Scn1b*-null brain slices display epileptiform activities in cortical and hippocampal extracellular field potential recordings (Brackenbury et al., 2013). These effects may require the presence of neuronal processes since they are not apparent in acutely-isolated cells. In slice recordings, cerebellar granule neurons (CGNs) from P12-13 *Scn1b*-null mice have reduced resurgent current compared to wildtype controls, but normal transient current. Thus, loss of β1 and β1B results in reduced CGN excitability. These cells also have reduced Nav1.6 at the AIS with concomitant increase in Nav1.1 (Brackenbury et al., 2010). Acutely-dissociated *Scn1b*-null dorsal root ganglion (DRG) neurons, by contrast, are hyperexcitable (Lopez-Santiago et al., 2011). *Scn1b*-null ventricular myocytes have increased Na^+ current, and *Scn1b*-null mice exhibit prolonged QT and RR intervals. These cardiac cells also have increased *Scn5a* mRNA, Nav1.5 protein, and [^{3}H]-STX binding to cell surface channels compared to wildtype (Lopez-Santiago et al., 2007). Moreover, deletion of *Scn1b* in the heart, results in increased TTX-sensitive Na^+ currents and higher expression of *Scn3a*, encoding Nav1.3 (Lin et al., 2015). Together, these data clearly demonstrate that β1 and β1B are important regulators of α subunit function and subcellular localization, *in vivo*. Importantly, shRNA-mediated knockdown of *Scn1b* results in the reduction of K^+ current carried by Kv4, and β1 co-immunoprecipitates with Kv4.2 from mouse brain (Marionneau et al., 2012). Furthermore, prolonged action potentials and increased repetitive firing measured in *Scn1b*-null cortical pyramidal neurons supports a link between the β1 and β1B subunits and K^+ current (Brackenbury et al., 2013; Marionneau et al., 2012).

Unlike *Scn1b*-null mice, *Scn2b*-null mice do not have seizures or die early, but rather have increased susceptibility to pharmacologically induced seizures. Nevertheless, compared

to wildtype, acutely-dissociated hippocampal neurons from *Scn2b*-null mice exhibit a negative shift in the voltage dependence of inactivation and significantly-decreased Na^+ current density. Measurement of cell surface [^{3}H]-STX binding in *Scn2b*-null brain neurons is decreased, while [^{3}H]-STX binding in *Scn2b*-null brain membranes is unchanged, showing the importance for this β subunit as an α subunit chaperone (Chen et al., 2002). In the peripheral nervous system, a subset of *Scn2b*-null DRG neurons have reduced Nav1.7 Na^+ current density and slowed rates of activation and inactivation (Lopez-Santiago et al., 2006). Thus, like β1 and β1B, β2 has different roles depending on the cell-type in which it is expressed.

Scn3b-null mice have defects in cardiac excitability. Specifically, ventricular and atrial tachycardia and fibrillation occur in stimulated Langendorff-perfused *Scn3b*-null, but rarely wildtype, hearts (Hakim et al., 2008, 2010).

Transfection experiments carried out in cultured hippocampal neurons and CGNs suggest that β4 promotes resurgent Na^+ current (Aman et al., 2009; Bant & Raman, 2010; Bean, 2005; Grieco et al., 2005). This is an important adaptation for high-frequency firing exhibited by certain types of neurons, such as Purkinje cells (Burgess et al., 1995; Raman, Sprunger, Meisler, & Bean, 1997). In acutely-dissociated hippocampal CA3 neurons, which lack endogenous β4, addition of a peptide consisting of the carboxyl-terminal portion of β4 generates resurgent current (Grieco et al., 2005). Knockdown of β4 expression in CGNs by siRNA reduces resurgent current and decreases repetitive action potential firing (Bant & Raman, 2010). These data implicate the intracellular domain of β4 as an open-channel blocking particle that allows for resurgent current in neurons (Grieco et al., 2005). Evidence suggests that Nav1.6 contributes strongly to resurgent current in Purkinje neurons and DRG neurons (Cummins, Dib-Hajj, Herzog, & Waxman, 2005; Raman & Bean, 1997). Despite this, in HEK cells co-expression of Nav1.6 and β4 is not sufficient to produce resurgent current (Chen et al., 2008). This suggests that other proteins or cellular processes found in neurons are required for physiological responses. These data support the emerging understanding that β subunits impact neuronal and cardiac physiology in a manner that is dependent on the particular cell type.

5. β Subunits are CAMs that Have Roles in Brain Development

5.1 CAM Functions

Members of the Ig superfamily are neural recognition molecules involved in developmental functions ranging from axon growth and guidance to synaptogenenesis (Maness & Schachner, 2007). VGSC β subunits each have an extracellular Ig domain with homology to the V-set of Ig-CAMs (Figure 1.3; Isom et al., 1995). These subunits, especially β1, have been shown experimentally to function as CAMs. *Drosophila* S2 cells transfected to express β1 or β2 orm aggregates, showing that these molecules adhere to one another homophilically. Visualized by immunofluorescence, *Drosophila* ankyrin is recruited to sites of contact between these cells. Ankyrin-recruitment occurs in the presence of full-length β subunits, but not when truncated β1 or β2 constructs lacking the intracellular carboxyl-terminal domain are expressed (Malhotra et al., 2000). Homophilic binding is disrupted in the epilepsy-linked mutant β1C121W, which lacks a cysteine residue that normally forms a critical disulfide bridge for Ig-loop formation (Meadows et al., 2002; Wallace et al., 1998). This suggests that in human patients loss of cell adhesive functions may contribute to *SCN1B*-linked pathologies. *In vitro* experiments have shown that β1 also interacts with other neuronal and glial CAMs (Figure 1.2). These include contactin, N-cadherin, neurofascin-155 (NF155), neurofascin-186 (NF186), NrCAM, and VGSC β2 (Malhotra et al., 2004; McEwen & Isom, 2004; Ratcliffe et al., 2001). β1 also interacts with the extracellular matrix protein tenascin-R (Xiao et al., 1999). β2 participates in homophilic as well as heterophilic binding, *in vitro*, with partners including β1 and the extracellular matrix proteins tenascin-R and tenascin-C (Figure 1.2; Malhotra et al., 2000; McEwen & Isom, 2004; Srinivasan et al., 1998; Xiao et al., 1999). Both β1 and β2 regulate migration of transfected CHL cells away from tenascin-R (Xiao et al., 1999). These data were the first evidence that β1 and β2 could function in cell migration. While β3 homophilic binding leading to cellular aggregation was not observed in transfected *Drosophila* S2 experiments, a more recent study reported trans-homophilic interactions between β3 subunits expressed in HEK cells (McEwen, Chen, Meadows, Lopez-Santiago, & Isom, 2009; Yereddi et al., 2013). In contrast to β1, β3 does not associate with either contactin or ankyrinG in transfected CHL cells

(McEwen et al., 2009). With the exception of VGSC α subunit proteins, no known binding partners for β4 have been reported. In agreement, β1 and β2, but not β4, influence neurite outgrowth (Davis et al., 2004). β subunit involvement in this process will be described in detail below. Taken together, these data indicate that β subunits are functional adhesion molecules similar to other Ig-CAMs like NCAM and L1.

5.2 Neurite Outgrowth

Extensive experimental evidence has been collected showing a role for β1 in neurite outgrowth, at least in CGNs. CGNs extend longer neurites when grown on monolayers of CHL fibroblasts expressing β1 than on mock-transfected CHL cells. Importantly, *Scn1b*-null CGNs do not produce longer neurites in this assay, suggesting that *trans*-homophilic binding is required (Davis et al., 2004). β1-mediated neurite outgrowth also does not occur in CGNs isolated from contactin-null mice. These mice have reduced β1 protein expression, further implying a functional connection between contactin and β1. Interestingly, RPTPβ, which associates with β1, has previously been demonstrated to promote neurite outgrowth through interactions with contactin and NrCAM (Peles et al., 1995; T. Sakurai et al., 1997). EGF receptor and FGF receptor signaling have been implicated in L1-mediated adhesion and NCAM-mediated neurite outgrowth, respectively (Islam, Kristiansen, Romani, Garcia-Alonso, & Hortsch, 2004; Niethammer et al., 2002) Investigation of the intracellular signaling cascade responsible for β1-mediated neurite outgrowth shows that EGF and FGF receptor kinase inhibitors fail to reduce the effect, so a separate pathway is likely involved. When grown on β1-expressing monolayers CGNs isolated from *fyn*-null mice do not extend longer neurites (Brackenbury et al., 2008). In detergent-resistant membrane fractions solubilized from mouse brain F*yn*, a member of the src family of tyrosine kinases. associates with β1 subunit polypeptides (Brackenbury et al., 2008). Contactin, a glycosylphosphatidylinositol-linked CAM, also associates with this membrane fraction (Krämer et al., 1999). These data suggest a model in which β1-β1 *trans*-homophilic binding, combined with β1-contactin heterophilic interactions in *cis,* within lipid rafts results in transmembrane signaling to induce neurite extension via a mechanism involving *fyn* kinase

(Brackenbury & Isom, 2011b). The model of the VGSC complex shown in Figure 1.4 includes these and other important interacting partners. β1-mediated neurite outgrowth is abrogated in the absence of Nav1.6 or following TTX treatment. Thus, for neurite outgrowth neuronal activity seems to be a requirement. Significantly, TTX treatment has no inhibitory effect on FGF-mediated neurite outgrowth, further implicating a separate signaling cascade (Brackenbury et al., 2010). Proteolytic processing of β1 is also important, as pharmacological inhibition of γ-secretase activity prevents β1-mediated neurite outgrowth (Brackenbury & Isom, 2011b). In cultured breast cancer cells that express β1, *trans*-homophilic interaction with β1-expressing CHL cells promotes the outgrowth of neurite-like extensions (Nelson et al., 2014). Thus, β1 may have developmental functions outside of the nervous system. β1B-expressing CHL cells induce neurite outgrowth to the same degree as those expressing β1 (Patino et al., 2011). Thus, it is proposed that either β1 or the secreted splice variant β1B can interact with neuronal β1 and its associated complex to induce neurite extension. By contrast, β2-expressing CHL monolayers reduce neurite outgrowth of CGNs and β4 subunits appear to have no effect on neurite outgrowth in this assay (Davis et al., 2004).

5.3 Scn1b in CNS development

From an early postnatal stage, the *Scn1b*-null mouse CNS exhibits significant morphologic abnormalities, suggesting roles for β1 and β1B in brain development (Brackenbury et al., 2008, 2013). Immunohistochemical analysis showed fewer nodes of Ranvier in the optic nerve. This defect corresponds with reduced optic nerve conduction velocity. Analysis at the ultrastructural level detected abnormalities in nodal architecture in the spinal cord, sciatic nerve, and optic nerve (Chen et al., 2004). At P14, the *Scn1b*-null cerebellar cortex exhibited defects when visualized by immunofluorescence. The external germinal layer (EGL), where CGNs first appear and proliferate, has increased thickness and increased total number of 4',6-diamidino-2-phenylindole (DAPI)-positive cells compared to wildtype littermates. By contrast, the number of recently-divided, 5-bromo-2'-deoxyuridine (BrdU)-labeled cells was not different. These data suggest that *Scn1b*-null CGNs have slowed migration from the EGL inward

through the cerebellar cortex to populate the granule cell layer. Axon pathfinding and parallel fiber fasciculation of CGNs are also abnormal in *Scn1b*-null cerebellum. In the normal mouse cerebellar cortex, these axons extend from the granule layer outward through the molecular layer (ML) where they bifurcate and form the tightly-bundled parallel fibers. In the mutant mouse, some of these axons in the ML deviate from their normal trajectory. Most noticeably, the parallel fibers are highly defasciculated (Brackenbury et al., 2008). It is noteworthy that contactin-null mice, which are *Scn1b* hypomorphs, also have cerebellar microorganization defects, ataxia, and early death, further suggesting a link between β1 and this Ig-CAM (E O Berglund et al., 1999; Brackenbury et al., 2010). CNS defects are already apparent in *Scn1b*-null cerebellar cortex at P5, prior to the onset of behavioral seizures and elevated cFos-expression in the cortex and hippocampus (Brackenbury et al., 2013). CGNs migrate and extend their axons along the processes of astrocytes known as Bergmann glia (BG), which express β1, *in vivo* (Brackenbury et al., 2008). These cells may act as partners for β1 *trans*-homophilic binding *in vivo*, similar to β1-expressing CHL cells, which promote neurite outgrowth in cultured CGNs *in vitro*. Brain defects are not limited to the cerebellum of *Scn1b*-null mice. DiI-labeled *Scn1b*-null axons of the corticospinal tract (CST) exhibit abnormal pathfinding and defasciculation (Brackenbury et al., 2008). At P5, the *Scn1b*-null hippocampus has several abnormal features as detected by immunohistochemistry. Mutant hippocampus shows ectopic Prox1-expressing cells and increased cellular proliferation in the hilus of the dentate gyrus (DG). Additionally, the *Scn1b*-null DG shows dispersion compared to wildtype. The microorganization of interneurons is unusual in the DG of these mice, as well, with parvalbumin-labeled cell bodies being spread laterally rather than being tightly arranged. Axon outgrowth and pathfinding are abnormal in the *Scn1b*-null hippocampus compared to wildtype (Brackenbury et al., 2013). Finally, pyramidal neurons in the *Scn1b*-null subiculum have reduced dentritic arborization (Reid et al., 2014). Zebrafish *scn1bb* morphants also have defective axon pathfinding in the olfactory nerve (Fein et al., 2008). This finding, together with the defects observed across the CNS and PNS of early postnatal *Scn1b*-null mice, and the seizures, ataxia, and early death that follow, highlight the importance of β1 and β1B for normal neurological development. Thus, it is not surprising that human mutations in *SCN1B* have disastrous, sometimes fatal consequences.

6. β Subunit Gene Mutations Are Linked to Epilepsy and Cardiac Arrhthmia

6.1 Epilepsy

VGSC β subunit gene mutations are linked to epilepsy syndromes, cardiac arrhythmias, and other pathological conditions. Epilepsy is a neurological disorder characterized by recurrent, unprovoked seizures, and events of excessive hypersynchronous action potential firing in one or more brain regions. They can have many causes, but a large percentage of cases are idiopathic and likely genetic (Stafstrom & Carmant, 2015). Channelopathies, including mutations in VGSC α subunits, are responsible for many of these idiopathic epilepsy syndromes. Human mutations in *SCN1B* have been linked to generalized epilepsy with febrile seizures plus (GEFS+) and the severe pediatric epileptic encephalopathy Dravet syndrome (DS) (Audenaert et al., 2003; Escayg & Goldin, 2010; Ogiwara et al., 2012; Patino et al., 2009; Wallace et al., 1998, 2002). In DS, children in the first years of life present with frequent febrile seizures followed by afebrile seizures, cognitive decline, ataxia, and high risk of sudden unexpected death due to epilepsy (SUDEP). Apnea and cardiac arrhythmia have been proposed to be significant causes of SUDEP (Surges & Sander, 2012). *SCN1A* mutations resulting in haploinsufficiency have been determined to be responsible for most incidences of DS (Claes et al., 2001; Escayg et al., 2000; Meisler & Kearney, 2005; Shi et al., 2009; Sugawara et al., 2001). However, homozygous *SCN1B* mutations have been found in at least two patients with DS, with one of these shown to be loss-of-function (Ogiwara et al., 2012; Patino et al., 2009). In addition to GEFS+, other epilepsy syndromes, including temporal lobe epilepsy (TLE) and early onset absence epilepsy (EOAE) have been linked to human mutations in *SCN1B* (Audenaert et al., 2003; Scheffer et al., 2007). A β1B-specific *SCN1B* mutation, the trafficking-deficient G257R, has been discovered in two separate cases of idiopathic epilepsy (Patino et al., 2011). However, most of the epilepsy-linked mutations in *SCN1B* map to extracellular residues in the Ig domain shared by both β1 and β1B (Brackenbury & Isom, 2011b). For example, the first *SCN1B* mutation to be associated with GEFS+ was the β1(C121W) mutation that replaces one of the cysteine residues in the disulfide

bridge that holds together the Ig-loop domain (Wallace et al., 1998). Further epilepsy-linked mutations in *SCN1B* include R85C, R125C, and many others (O'Malley & Isom, 2015).

β1 and β1B are multifunctional proteins with varying effects on VGSC physiology depending on developmental and cell-type specific contexts. Impaired regulation of Na^+ current likely contributes to the mechanism of *SCN1B*-linked epilepsy. In addition, all *SCN1B*-linked epilepsy mutations identified to date, except for the one specific to β1B, are located in residues of the extracellular Ig-loop (Audenaert et al., 2003; Meadows et al., 2002; Patino et al., 2009; Scheffer et al., 2007; Wallace et al., 1998). Given the strength and quantity of experimental evidence demonstrating adhesive functions for β1/β1B, it is reasonable to suggest that loss of these functions might be an important contribution to the CNS neuronal network hyperexcitability underlying *SCN1B*-linked seizures and epilepsy.

6.2 Cardiac Arrhythmia

Channelopathies, including mutations in VGSC α subunits, especially Nav1.5, have also been linked to cardiac arrhythmias. Such mutations are linked to long QT syndrome (LQTS), Brugada syndrome, and fatal ventricular fibrillation (VF) (Remme & Bezzina, 2010). Human mutations in *SCN1B*, *SCN2B*, and *SCN3B* have all been associated with Brugada syndrome, which carries a high risk of sudden cardiac death due to VF (Ishikawa & Takahashi, 2012; Riuró et al., 2013; H. Watanabe et al., 2008). Other mutations in *SCN1B*, *SCN2B*, *SCN3B*, and *SCN4B* have been linked to atrial fibrillation (AF) (Li et al., 2013; Olesen et al., 2011; Watanabe et al., 2009). Further, a mutation in *SCN4B* has been linked to long QT syndrome (LQTS), in which slowed repolarization can lead to arrhythmia and VF (Medeiros-Domingo et al., 2007). These findings suggest that all VGSC β subunits are important for healthy cardiac function in humans.

In addition to epilepsy and cardiac arrhythmias, β subunits have been implicated in a number of other pathological conditions, including sudden infant death syndrome (SIDS), neuropathic pain, neurodegenerative diseases such as Huntington's disease (HD) and multiple sclerosis (MS), and even cancer (O'Malley et al., 2009). Recent reviews provide a detailed

treatment of the roles β subunits have in pathophysiology (Calhoun & Isom, 2014; O'Malley & Isom, 2015).

7. Scn1b and Development of the Cerebellar Cortex

As described above, patients with Dravet syndrome present with recurrent, intractable seizures, ataxia, and delayed or impaired cognitive development. The *Scn1b*-null mouse model of Dravet syndrome developed in our laboratory begins to display frequent, spontaneous seizures at P10 (C. Chen et al., 2004). These mutants also have an apparent ataxic gait, which could correspond to defects in the formation and/or function of the cerebellar cortex. Indeed, significant micro-organizational defects have been uncovered in this region of the *Scn1b*-null brain (Brackenbury et al., 2008, 2013). The discussion that follows will broadly describe the development of the mouse cerebellar cortex, the phenotypical deficits that emerge from perturbation of development in spontaneous and transgenic mutants, functional defects in Purkinje cell activity that impact motor coordination, and a characterization of what is currently understood about the role of *Scn1b* in the cerebellum within the context of the larger field of developmental neurobiology.

7.1 Development and Connectivity of the Cerebellar Cortex

The murine cerebellum forms from dorsal rhombomere 1 of the hindbrain around embryonic day 9 (E9). Purkinje cells become post-mitotic between E11 and E13, migrate radially from the ventricular zone on the dorsal surface of the fourth ventricle, and form a transient multilayer beneath the external germinal layer. The external germinal layer covers the outer surface of the developing cerebellum. This region first appears around E15, and remains an active mitotic area of dividing granule cell precursors for more than 2 postnatal weeks. The major lobes form, divided by a series of shallow fissures, by about E18. These early developmental processes, especially before E12.5 are stimulated spatially and temporally by secreted molecules such as Wnt1 and FGF8 under the direction of important transcription factors including *Otx2*, *En2*, and *Pax2* (Hatten & Heintz, 1995; Sillitoe & Joyner, 2007). A leading

hypothesis proposes that Purkinje cells, anchored to the deep cerebellar nuclei by their axons, are positioned at the bases of these fissures. Granule cell precursor proliferation then causes the lobes to expand outward and assume their ultimate shape (J Altman & Bayer, 1997). The cerebellar cortex largely develops its characteristic 3-layered structure and connectivity during the first three postnatal weeks. From the most interior, these layers are the densely-populated internal granule layer, the Purkinje cell layer, which is composed of the Purkinje cell somata, and the molecular layer, which is home to the massive fan-shaped dendritic structures of the Purkinje cells. Near the time of birth, Purkinje cells disperse into a single monolayer that will form the middle layer of the cerebellar cortex. At the same time, granule cell precursors begin to exit the cell cycle and migrate along the processes of Bergmann glia down through the molecular layer, past the Purkinje cell bodies and into the nascent internal granule layer. The two classes of molecular layer interneurons, stellate and basket cells, arise from the ventricular zone, proliferate in-transit and migrate through the white matter into the internal granule layer and outward into their final resting positions in the molecular layer. This process mostly occurs during the first postnatal week. Also early in postnatal development, foliation of the lobe surfaces begins to take place and results in the development of 10 distinct lobules visible in the sagittal plane through the cerebellar vermis (J Altman & Bayer, 1997; Larsell, 1970; Sillitoe & Joyner, 2007).

Purkinje cells, which are the sole efferent projections from the cerebellar cortical circuit to the deep cerebellar nuclei, are stimulated directly by two different excitatory inputs, those of the parallel fibers and those of the climbing fibers (Palay & Chan-Palay, 1974). Densely clustered in the internal granule layer, the granule cells receive excitation from nuclei in the brainstem and spinal cord by means of the mossy fibers. In turn, granule cells project their bifurcated axons making up the parallel fibers, and form glutamatergic synapses throughout the dendritic extensions of multiple Purkinje cells during the first few weeks of life. Secondly, the climbing fibers arising from neurons positioned in the inferior olives each innervate and form a separate class of glutamatergic synapses onto an individual Purkinje cell's soma and major dendritic branches (Apps & Garwicz, 2005). This arrangement of mono-innervation of the Purkinje cell by the climbing fiber proceeds in a series of steps beginning early in postnatal

development. Initially, a number of climbing fibers form synaptic contacts onto the soma starting at around E18 (Mason & Gregory, 1984; Palay & Chan-Palay, 1974). Then, between P3 and P7, a single climbing fiber will become strengthened (Hashimoto & Kano, 2003; Kano et al., 1995). During the second and third postnatal weeks, translocation of this strengthened climbing fiber's synaptic connections from the soma to the major dendrites takes place. Finally, the somatic synapses are eliminated (Hashimoto, Ichikawa, Kitamura, Watanabe, & Kano, 2009). In addition to these excitatory connections, two types of interneurons, the stellate and basket cells, form GABAergic synapses onto distinct Purkinje cell domains. Stellate cells migrate into scattered positions throughout the molecular layer and form synapses at relatively distal positions on the Purkinje cell dendritic arbor. By contrast, basket cells are positioned at or near the Purkinje cell layer and form synapses onto the soma, proximal dendrites and axon initial segment (AIS). The process of GABAergic synapse-formation begins around P7 and continues at a rapid pace for about the first three postnatal weeks (Takayama, 2005). Together, these local cellular constituents and afferent projections converge onto and influence the firing behavior of the Purkinje cells, which indirectly guide motor functions and modulate forebrain activity through their GABAergic connections with neurons in the deep cerebellar nuclei (Sillitoe & Joyner, 2007).

7.2 Mechanisms and Consequences of Cerebellar Cortical Malformation

A number of now-classic spontaneous mouse mutants have been described, which demonstrate the behavioral impacts of cerebellar malformation. Many such mutants undergo severe reduction or complete absence of critical cell-types in the cerebellar cortex. For example, Lurcher mice lose all Purkinje cells starting at two weeks of age, then subsequently nearly all granule cells disappear (Caddy & Biscoe, 1979). These mice express a gain-of-function mutation in *Grid2*, the gene encoding the GluRδ2 ionotropic glutamate receptor, resulting in an ataxic gait (Fortier, Smith, & Rossignol, 1987; Zuo et al., 1997). Deletion of *Grid2* results in a mild loss of granule cells and reduced synaptic contacts between parallel fibers and Purkinje

cells. These mice also have motor coordination defects (Kashiwabuchi et al., 1995). The Staggerer mouse carries a homozygous loss-of-function mutation in the gene *Rora*, which is highly expressed in Purkinje cells (Hamilton et al., 1996; Ino, 2004; Nakagawa, Watanabe, & Inoue, 1997; Sashihara, Felts, Waxman, & Matsui, 1996). Prior to P5, Staggerer mice begin to lose Purkinje cells, which reduce in number to about 25% of wildtype. As with Lurcher mice, they subsequently experience a loss of essentially all granule cells (Sonmez & Herrup, 1984). Behaviorally, Staggerer mice display even more profound motor deficiencies than Lurcher mice (Lalonde, 1987; Lalonde et al., 1996; Lalonde, Bensoula, & Filali, 1995). A third mutant, commonly referred to as the Reeler mouse, exhibits a disruption in the gene *reln*, encoding the extracellular matrix protein reelin (Beckers et al., 1994; D'arcangelo et al., 1995). *Reln* mRNA is highly expressed in granule cells but not in Purkinje cells (Schiffmann, Bernier, & Goffinet, 1997). In agreement with this, the main cytological defect in Reeler mouse development is a nearly complete disappearance of granule cells following the second postnatal week (Caviness Jr & Rakic, 1978). Reeler mice also show a loss of about half of their Purkinje cells (Heckroth, Goldowitz, & Eisenman, 1989). As expected, these mice are ataxic and prone to loss of balance (Lalonde, Hayzoun, Derer, Mariani, & Strazielle, 2004). Another classic ataxic mutant mouse, Weaver, contrasts with the aforementioned spontaneous mutants in that cerebellar morphology is largely normal prior to granule cell degeneration around the time of birth (Goldowitz & Smeyne, 1995; Signorini, Liao, Duncan, Jan, & Stoffel, 1997). This mutation, which occurs in *Girk2*, affects an inward-rectifying K^+ channel that is highly expressed in the cerebellum and midbrain (Patil et al., 1995). These mutants demonstrate major examples of developmental defects in the cerebellum that result in profound motor abnormalities. It is also worth noting that at least three of them, Lurcher, Staggerer, and Weaver, are susceptible to tonic-clonic seizures (Eisenberg & Messer, 1989; Seyfried & Glaser, 1985). Purkinje cells send the sole efferent projections from the cerebellar cortex. Thus, any disruption of Purkinje cell development or function, or any loss of cells which excite or inhibit Purkinje cells or alteration in the synapses they form onto Purkinje cells can result in motor deficits.

A transgenic mouse that was generated as a model of spinocerebellar ataxias affecting humans is the SCA1/Q82 mouse, which is driven specifically in Purkinje cells by the *Pcp2/L7*

promoter (Burright et al., 1995). *SCA1*, encoding ataxin-1, carries a varying number of CAG repeats in human patients with adult-onset degeneration in the cerebellum and brainstem, resulting in ataxia (H. B. Clark & Orr, 2000). In contrast to the developmental mutants described above, the SCA1/Q82 mice do not lose large numbers of cells. Instead, by one year of age they have smaller, less dendritically complex Purkinje cells which contain ataxin-1 aggregates (Vig et al., 1998). These mice begin to show ataxia near three months of age following the onset of Purkinje cell pathology (H. Clark et al., 1997).

The Immunoglobulin-superfamily of cell adhesion molecules (Ig-CAMs) are a class of proteins which exhibit one or a number of tandem extracellular Ig-loops. Cell adhesion molecules (CAMs) such as these are expressed on the cell surface where they mediate homophilic and heterophilic interactions with molecular components of other cells and the extracellular matrix. Ig-CAMs are implicated in neurite outgrowth, axon fasciculation, and cell migration, among other important functions during nervous system development (Maness & Schachner, 2007). Loss-of-function mutations in mice demonstrate substantial consequences for brain development, and cerebellar development is no exception. Contactin is a glyosylphosphotidyl inositol (GPI)-anchored Ig-CAM composed extracellularly of a sequence of four fibronectin type III (FNIII) domains and six tandem Ig-loops (Erik O Berglund & Ranscht, 1994; Brümmendorf, Michael Wolff, Frank, & Rathjen, 1989). These domains allow for heterophilic interactions with ligands, including Ig-CAMs such as VGSC β1 (Buttiglione et al., 1998; Morales et al., 1993; T. Sakurai et al., 1997). Like many related molecules, contactin is known to promote neurite outgrowth (Durbec, Gennarini, Goridis, & Rougon, 1992; Gennarini G, Durbec P, Boned A, Rougon G, 1991). Similar to β1, contactin is strongly expressed in the postnatal mouse cerebellar cortex (Faivre-Sarrailh, Gennarini, Goridis, & Rougon, 1992). At P0, P11, and P16, contactin is expressed in the granule cell precursors of the external granule layer and in the developing parallel fibers, and it is maintained in the granule cells of the internal granule layer. By contrast, immunoreactivity for contactin is not observable in Purkinje cell somata or processes. Contactin-null mice exhibit a progressive ataxic gait starting at around P10, have a small body size compared to wild-type littermates, and die by P18 (E O Berglund et al., 1999). These characteristics are very similar to those of *Scn1b*-null mice (C. Chen et al.,

2004). Brain sections collected from P15 contactin-null mice have normal development of cerebellar folia and layers of the cerebellar cortex but have misorientation and less compact fasciculation of PFs (E O Berglund et al., 1999). It is noteworthy that *Scn1b*-null mutants share these developmental abnormalities in the cerebellar cortex. Contactin has considerable sequence homology to VGSC β subunits, especially β2 (L L Isom et al., 1995). Furthermore, contactin-null mice are β1 hypomorphs, strengthening the hypothesis that these two Ig-CAMs have closely related functions (Brackenbury et al., 2010).

7.3 The Scn1b-null Cerebellar Cortex

Similar to contactin-null mice (E O Berglund et al., 1999), *Scn1b*-null mice are born in expected Mendelian ratios, and are indistinguishable at P0 from wildtype and heterozygous littermates (C. Chen et al., 2004). In agreement with a role in cerebellar cortical development, β1 expression is highest in postnatal brain. By contrast, β1B is most-highly expressed during embryological development of the brain (Kazen-Gillespie et al., 2000b; Patino et al., 2011). It remains possible that *Scn1b*-null mice have delays in neuronal migration and axon pathfinding that precede P0, but these are likely subtle in effect. The cerebellar cortex mostly develops postnatally, and *Scn1b* null mice have notable defects by P5 (Brackenbury et al., 2013). Defects in the developmental processes that take place prenatally in the cerebellar formation would be predicted to have behavioral consequences, particularly with regard to gait. The secreted splice variant β1B is much more highly expressed in the prenatal cerebellum than β1, and it is reasonable to hypothesize that it could participate in the early organization of the cerebellar cortex (Kazen-Gillespie et al., 2000b; Patino et al., 2011). This has not been examined directly, but transgenic mice which express β1B on a *Scn1b*-null background do not rescue the overt phenotypes of the animals (unpublished observations). Behavioral analysis of motor coordination has not been carried out in these mutants, however. Further characterization of these mice is necessary to determine what, if any, contribution β1B gives to cerebellar development and function.

In common with other Ig-CAM mutants, *Scn1b*-null mice exhibit substantial micro-organizational defects in the cerebellar cortex throughout postnatal development (Brackenbury et al., 2008, 2013). *Scn1b* mRNA is strongly expressed throughout the postnatal cerebellar cortex. In contrast with contactin, however, β1 is highly enriched in Purkinje cells as well as granule cells. Granule cells, which first arise and proliferate in the transient external granule layer on the surface of the molecular layer of the cerebellar cortex, have a deficiency in migration into the *Scn1b* null internal granule layer (Brackenbury et al., 2008, 2013). This process occurs along the fibers of Bergmann glia, which have their cell bodies arranged amongst the Purkinje cells in the Purkinje cell layer. This defect measurable by P5 of postnatal development, with a significantly thicker external granule layer, more densely populated with newborn granule neurons, (Brackenbury et al., 2013). Nevertheless, a prominent internal granule layer forms even in the absence of *Scn1b* expression.

8. Concluding Remarks

Descendent from and sharing structural homology with a family of proteins possessing V-like Ig domains and having diverse developmental functions in the nervous system, β1, β2, β3, β4, and β1B might be thought of as Ig superfamily CAM proteins which, in excitable cells, also regulate ion channel function. Indeed, the VGSC β subunits are expressed in non-excitable cells like astrocytes, oligodendrocyte precursor cells, and radial glia (Cahoy et al., 2008). Like their cousins, the Ig-superfamily CAMs contactin, L1, and NCAM, these proteins, especially β1/β1B, are critical for development of the CNS. They localize in neurons at specialized intracellular structures like the AIS and nodes of Ranvier, where they link other CAMs and extracellular matrix molecules with appropriate VGSC α subunits, VGKCs, and cytoskeletal proteins. The importance of β subunits, especially those encoded by *Scn1b*, in this role is highlighted by the catastrophic pathological conditions that can occur when they are mutated. *Scn1b*-null mice, like contactin-null mice, exhibit ataxia and altered cerebellar microorganization, and both mutants have radically shortened lives. Ongoing research seeks to determine whether β1 and β1B participate in other developmental processes common to Ig-

superfamily CAMs, such as synaptogenesis. Most-importantly, *SCN1B* mutations are linked to serious human pathologies, including epileptic encephalopathy. Because these syndromes, especially DS, are usually caused by *SCN1A* mutations, there is a tendency to presume that *SCN1A*- and *SCN1B*-linked epileptic encephalopathy have the same underlying mechanism. However, we do not yet know whether loss of crucial adhesive functions of β1 and β1B contributes to the seizures, ataxia, and severe cognitive impairment of *SCN1B*-linked DS. VGSC β subunits are multi-functional, regulating VGSC α subunit transcription, localization, and function and contributing to key aspects of CNS development as CAMs. It might, therefore, be predicted that loss of function of *SCN1B* leads to even more severe epileptic encephalopathy than *SCN1A*-linked DS. Additional cases will need to be evaluated before such a determination can be made.

Ataxia has been observed in *Scn1b*-null mice since they were first developed in the lab (C. Chen et al., 2004). This is consistent with the progressive ataxia seen in patients with Dravet syndrome. Moreover, cognitive impairments in Dravet syndrome patients, including hyperactivity and features of autism, may implicate involvement of the cerebellum (Battaglia et al., 2013; Guzzetta, 2011). Defects in the micro-organization of the *Scn1b*-null cerebellar cortex are visible early in postnatal development, but it is not known whether these abnormalities are sufficient to explain the motor coordination phenotype they exhibit (Brackenbury et al., 2008, 2013). Spontaneous mutants such as Lurcher and Staggerer show substantial cell loss, especially Purkinje cell loss, resulting in ataxia (Lalonde & Strazielle, 2007). Purkinje cells are the sole efferent neurons which project from the cerebellar cortex. Defective axon migration and pathfinding of granule cells, which form prolific glutamatergic synapses onto Purkinje cell dendrites, could be contributing to reduced Purkinje cell activity, but Ig-CAMs are involved in a variety of other processes including synaptogenesis (Crossin & Krushel, 2000). Furthermore, intrinsic Purkinje cell function could be compromised in *Scn1b*-null mice, perhaps due to a reduction in VGSC α subunit expression at the AIS. We hypothesized that *Scn1b* may be essential for normal Purkinje cell function. We further hypothesized that β1/β1B may regulate the formation of synapses. The discovery that *Scn1b* is critical for cerebellar cortex function

would provide insight into the underlying neurobiology behind Dravet syndrome and its comorbidities.

Chapter II

Reduced excitability in Purkinje cells and cerebellar cortical interneurons correlates with ataxia in a mouse model of *SCN1B*-linked Dravet syndrome

Introduction

Voltage-gated Na^+ channels (VGSCs) are heterotrimers composed of a single pore-forming α subunit and two β subunits (R P Hartshorne & Catterall, 1981; L L Isom et al., 1992, 1995; Messner & Catterall, 1985; Morgan et al., 2000; Yu et al., 2003). In neurons, these complexes are necessary for the initiation and propagation of action potentials. VGSC β subunits functionally modulate α subunits and regulate their subcellular localization (Aman et al., 2009; Bennett et al., 1993; Brackenbury et al., 2010; C. Chen et al., 2004; L L Isom et al., 1995, 1992; Lori L. Isom et al., 1995; Kazarinova-Noyes et al., 2001; Kazen-Gillespie et al., 2000a; Ko et al., 2005; Lopez-Santiago et al., 2007, 2011; McEwen et al., 2004; Medeiros-Domingo et al., 2007; Patino et al., 2009; H. Watanabe et al., 2008; Yu et al., 2003; J. Zhou et al., 1991). In addition, these proteins, especially β1, play developmental roles in the brain including axon pathfinding and cell migration (Brackenbury et al., 2008, 2013; C. Chen et al., 2004; Fein et al., 2008; Patino et al., 2011). β1, encoded by *SCN1B*, functions as an immunoglobulin-superfamily cell adhesion molecule (Ig-CAM) (L L Isom et al., 1995; Jyoti Dhar Malhotra et al., 2000; Maness & Schachner, 2007). β1B, a secreted splice variant, mainly expressed embryonically in brain, is encoded by the same gene (Kazen-Gillespie et al., 2000a; Patino et al., 2011). Along with the associated VGSC complex, β1 is expressed axonally, at highest concentrations at the axon initial segment (AIS) and within nodes of Ranvier (Brackenbury et al., 2008; Kaplan et al., 2001; Patino et al., 2009). β1 may also be found in dendrites of certain neurons (Reid et al., 2014). Mutations in *SCN1B* are associated with generalized epilepsy with febrile seizures plus (GEFS+) and the severe epileptic encephalopathy Dravet syndrome (DS)

(Audenaert et al., 2003; Kruger et al., 2016; Laurence S Meadows et al., 2002; Ogiwara et al., 2012; Patino et al., 2009, 2011; Scheffer et al., 2007; Wallace et al., 1998, 2002; Wimmer et al., 2010). While DS is most commonly caused by heterozygous loss-of-function mutations of the α subunit gene *SCN1A* resulting in haploinsufficiency, the disorder can also be caused by homozygous loss-of-function *SCN1B* mutations (L Claes et al., 2001; A Escayg et al., 2000; Meisler & Kearney, 2005; Patino et al., 2009; Shi et al., 2009; Sugawara et al., 2001). Children with this catastrophic disorder present with intractable seizures, intellectual disability, and autism spectrum disorders in the first years of life (Dravet, Bureau, Oguni, Fukuyama, & Cokar, 2005). In addition, patients present with ataxia that progresses with development (Scheffer, 2012).

Developmental processes in the brain such as neurite outgrowth, cell migration, and synaptogenesis rely on homophilic and heterophilic interactions of Ig-CAMs such as neurofascin, contactin, and L1 (Ango, di Cristo, et al., 2004; Buttermore et al., 2012; Crossin & Krushel, 2000; Vaughn & Bjorkman, 1996; Williams & Barclay, 1988). β1 participates in homophilic adhesion as well as heterophilic adhesion with other partners including neurofascin, contactin, and VGSC β2 (Jyoti D Malhotra et al., 2004; McEwen & Isom, 2004; Charlotte F. Ratcliffe et al., 2001). Moreover, *trans*-homophilic β1 adhesion promotes neurite outgrowth in cultured cerebellar granule neurons (CGNs) (Davis et al., 2004). This function requires contactin, NaV1.6, and *fyn* kinase (Brackenbury et al., 2008; Davis et al., 2004). *Scn1b*-null mice, which model DS, have spontaneous seizures at P10, are ataxic, and die by approximately P20, with abnormal development throughout the brain (Brackenbury et al., 2008, 2013; C. Chen et al., 2004). In the cerebellar cortex, *Scn1b*-null cerebellar granule neurons (CGNs) have delayed migration into the internal granular layer (IGL) and the parallel fibers, composed of the axons of CGNs, exhibit pathfinding errors and defasciculation. Disruptions such as these, which have already begun by P5, prior to the onset of seizures in the mice, may contribute to the cognitive and motor disabilities that are clinical hallmarks of DS (Brackenbury et al., 2013). Furthermore, dysfunction of the cerebellum may be of consequence for hippocampal function and seizures (Krook-Magnuson, Szabo, Armstrong, Oijala, & Soltesz, 2014; Rochefort, Arabo, Andre, et al., 2011).

The mouse cerebellar cortex is composed of a relatively simple, well characterized circuit that largely develops over the first 3 postnatal weeks (Joseph Altman, 1972; De Zeeuw et al., 2011; Eccles, 1967). Purkinje cells, which project the only output from the circuit, receive molecularly-distinguishable excitatory synaptic inputs from parallel fibers and climbing fibers. In addition, two classes of interneurons, basket cells and stellate cells, form GABAergic inhibitory synapses onto PCs. Basket interneurons selectively target the PC soma, proximal dendrites, and AIS where their axon collaterals make up the large, basket-shaped pinceau synapse (Ango, di Cristo, et al., 2004; Somogyi & Hámori, 1976)., Mice lacking neurofascin, a binding partner of β1, have disorganization of pinceau synapses and severe ataxia (Buttermore et al., 2012). Importantly, β1 protein is localized at the Purkinje cell AIS, along with its associated VGSC α subunits. The degree to which β1 is expressed in other PC compartments such as dendrites remains unknown. Many related Ig-CAMs are expressed pre- and post-synaptically where they instruct the formation and function of synapses. Using antibody markers of distinct classes of excitatory and inhibitory synapses formed between parallel fibers, climbing fibers, and molecular layer interneurons, it is possible to determine the densities at which they have formed in postnatal cerebellar sections. A role for *Scn1b* in the formation of excitatory and inhibitory synapses has not been previously investigated. We hypothesized that β1 and/or β1B might serve a function in the organization of one or more classes of synapses in the cerebellar cortex which could be contributing to the ataxia that has been observed in *Scn1b*-null mice.

Scn1b-null Purkinje cell function has not been investigated. These efferent projection neurons are solely responsible for conveying cerebellar cortical signals to the deep cerebellar nuclei and thus to rest of the nervous system. Considering the significant comorbid symptoms presented by DS, attaining a better understanding of the role of *Scn1b* in the development and function of the cerebellar cortex is critical. Here, we report that *Scn1b*-null Purkinje cells and molecular layer interneurons are hypoexcitable and show the first characterization of the *Scn1b*-null mouse's ataxic gait. We further show that loss of *Scn1b* does not result in abnormal PC morphology or reduced numbers of excitatory and inhibitory synapses formed between parallel fibers, climbing fibers, or basket interneurons and the Purkinje cell compartments that

they target. We conclude that *Scn1b* is required for healthy intrinsic function of Purkinje cells and interneurons in the cerebellar cortex and propose that these defects are responsible for the ataxia exhibited by *Scn1b*-null mice.

Materials and Methods

1. *Animals:*

Scn1b +/+ and *Scn1b -/-* littermate mice were bred from *Scn1b+/-* mice congenic on the C57BL/6 background for more than 20 generations. Animals were housed at the University of Michigan in the Unit for Laboratory Animal Medicine in accordance with University of Michigan Institutional Animal Care and Use Committee (IACUC) guidelines.

2. Gait analysis:

P16 *Scn1b +/+* and *Scn1b -/-* littermate mice were subjected to footprint analysis of gait (Becker et al., 1988). Paws were painted with non-toxic, washable paint. Blue was used for hindpaws, and red was used for forepaws. A strip of paper was laid in the floor of a customized open-topped chamber, into which each mouse was introduced and allowed to walk to the other side. Mice were given repeated attempts to walk naturally to produce a series of at least 3 clear footprints along the paper until this was achieved, with fresh paint added to their paws each time. Lines were hand-drawn between similar places on each footpad and measurements were recorded of stride lengths, stride widths, and angles of step for both hindpaws and forepaws.

3. *Immunohistochemistry:*

Littermate mice were anesthetized at P10 or P14 and transcardially perfused with cold PBS followed by 4% paraformaldehyde. Brains were removed and postfixed overnight at 4° C, cryprotected in 10% sucrose followed by 30% sucrose, then frozen in isopentane between -20° and -30° C. Frozen brains were stored at -80° C until they were sectioned. 50 μm parasagittal cryostat sections were collected in cold PBS for free-floating immunohistochemistry. Sections were blocked for 3 hours at room temperature in 0.1 M PB with 10% goat serum and 0.3% Triton X-100 followed by incubation with primary antibodies for about 42 hours at room temperature with gentle rocking. Primary antibodies used in this study were as follows: anti-VGLUT1 (guinea

pig; 1:2000; Millipore), anti-VGLUT2 (mouse; 1:1000; Millipore), anti-VGAT (rabbit; 1:500; Synaptic Systems), anti-VGAT (mouse; 1:500; Synaptic Systems), anti-calbindin (mouse; 1:400; Sigma), anti-calbindin (rabbit; 1:400, Cell Signaling Technology), and anti-parvalbumin (rabbit; 1:400; Abcam). Sections were washed with 0.1M PB and incubated overnight at room temperature with Alexa fluor-conjugated secondary antibodies (Invitrogen or Life Technologies). Finally, sections were washed, mounted onto microscope slides using Prolong® Gold with DAPI (Invitrogen), and coverslipped.

4. *Microscopy and image analysis:*

Immunohistochemistry-stained sections were imaged using a Nikon A1R laser scanning confocal microscope with 20x and 60x objectives. Z-stack images were acquired using NIS-Elements A1R software. For *in vivo* synapse data, these confocal z-stacks were analyzed in Bitplane Imaris. In brief, the 'Create Surface' feature was used to manually surround regions of interest (i.e. calbindin+ Purkinje cell somata) plane-by-plane. The 'create new spots' feature was applied to the channel corresponding to the appropriate synaptic marker (i.e. VGAT signal) within this region of interest. At a set size and threshold, the number of 'spots' was quantified and densities were calculated using the calculated surface area of the region of interest.

5. Transmission electron microscopy:

Scn1b +/+ and *Scn1b* -/- mice at P14 were anesthetized with isoflurane and transcardially-perfused with a mixture of 3% paraformaldehyde (Electron Microscopy Sciences) and 2.5% glutaraldehyde (Ted Pella) in 0.1 M Sorensen's buffer. Cerebellar lobule 4/5 sections were dissected and postfixed at 4^0C overnight in perfusion solution. They were then incubated for 1 hour in OsO_4 (1% solution in 0.1 M Sorensen's buffer) and embedded in epoxy resin. Ultrathin (75 nm) sections were cut at the University of Michigan Imaging Laboratory Core and visualized with a JEOL JSM 1400 transmission electron microscope.

5. *Synaptosome fractionation:*

Cerebella were dissected from wild-type P14 mice and homogenized in a solution with a final concentration of 1.25 M sucrose. In an ultracentrifuge tube, this homogenate (H) was overlayed with a 1M sucrose solution and then a 0.32M sucrose solution to form a three-step gradient. Tubes were spun in an ultracentrifuge at 100,000 x g for 3 hours at 4° C. The synaptosome fraction (S) was collected from the 1.25M:1M interface and resuspended in buffer (pH 6.0) containing 1% Triton® X-100, gently rotated for 30 minutes, and spun at 40,000 x g for 30 minutes at 4° C to pellet the synaptic junction fraction. This pellet was resuspended in buffer (pH 8.0) containing 1% Triton® X-100, gently rotated for 30 minutes, and spun again at 40,000 x g for 30 minutes at 4° C to pellet the post-synaptic fraction. This final pellet was resuspended in 5% SDS. Sample buffer containing β-mercaptoethanol and dithiothreitol **(**DTT) was added to each sample. Then samples were heated to 85° C for 10 minutes and stored at -20° C until Western blot experiments were performed.

6. *Western blot analysis:*

Synaptosome fractions were loaded onto 10% polyacrylamide gels and separated by SDS-PAGE, then transferred to nitrocellulose membranes. Membranes were blocked at room temperature for 2-3 hours in TBS-Tween buffer (TBST) containing 1% bovine serum albumin (BSA) and 2.5% nonfat dry milk then incubated overnight at 4° C with primary antibodies as follows: anti-synaptophysin (rabbit; 1:10,000; Millipore), anti-PSD95 (mouse; 1:2000; Thermo Scientific), and anti-β1 (rabbit; 1:1000; Cell Signaling Technology). HRP-conjugated secondary antibodies were applied for 2-3 hours at room temperature. Chemiluminescent detection was accomplished using the Thermo Scientific reagents Supersignal® West Dura (synaptophysin) or Supersignal® West Fempto (PSD95 and β1) to detect immunoreactive bands.

7. Preparation of cerebellar slices:

All animal procedures adhered to NIH guidelines and were approved by the University of Michigan Committee on the Use and Care of Animals. Acute cerebellar slices were prepared using similar procedures as described previously (Brackenbury et al, 2013). In brief, the brain was removed rapidly following euthanasia by isoflurane inhalation and decapitation. Both transverse (coronal) and parasagittal cerebellar slices (~250 μm) were prepared from postnatal day (P) 14 - 20 WT or *Scn1b*-/- mice in ice-cold, oxygenated "slicing" solution saturated with 95% O_2 /5% CO_2. The slicing solution contained (in mM): 110 sucrose; 62.5 NaCl; 2.5 KCl; 6 $MgCl_2$; 1.25 KH_2PO_4; 26 $NaHCO_3$; 0.5 $CaCl_2$ and 20 D-glucose (pH 7.35-7.4 when saturated with 95% O_2 /5% CO_2 at room temperature of 22 – 25 ^oC). Slices were incubated initially in the same slicing solution for >30 min at room temperature and then in the mixture (1:1) of the "slicing" solution and artificial cerebrospinal fluid (ACSF), the latter contains (in mM): 125 NaCl; 2.5 KCl; 1 $MgCl_2$; 1.25 KH_2PO_4; 26 $NaHCO_3$; 2 $CaCl_2$ and 20 D-glucose, (pH 7.35-7.4) in a holding chamber aerated continuously with 95% O_2 /5% CO_2 at 25 ^oC for at least another 30 min before finally transferred to ACSF.

8. Electophysiological recording:

A given cerebellar slice was transferred to a recording chamber where it was superfused (2-3 ml/min) with (ACSF) bubbled continuously with 95% O_2 /5% CO_2. Purkinje cells or interneurons (molecular layer) of lobule 4/5 or 6 in cerebellar slices were visually identified based on their size, shape and location using a NIKON E600FN upright microscope equipped with Nomarski optics (x 40 water immersion objective). For recording of action potential (AP) firing, the recording electrodes had a resistance of 3-6 MΩ when filled with the potassium gluconate (K-Gluconate)-based pipette solution consisted of (in mM): 140, K-gluconate; 4, NaCl; 0.5, $CaCl_2$; 10, HEPES; 5, EGTA, 5 phophocreatine; 2, Mg-ATP and 0.4, GTP (pH 7.2-7.3 adjusted with KOH). Repetitive firing pattern and frequency of APs of individual neurons were examined using whole cell current-clamp recording technique. Repetitive AP firing was evoked by injections of a series of 1500 ms depolarizing currents varying from -60 pA to 180 pA at 10 pA-step from their resting

membrane potentials. For recording spontaneous synaptic responses in Purkinje cells, whole cell voltage-clamp recording techniques were used with two different pipette solutions. For recording spontaneous inhibitory postsynaptic currents (sIPSCs), the pipette solution consisted of (in mM): 140, CsCl; 4, NaCl; 0.5, $CaCl_2$; 10, HEPES; 5, EGTA, 2, Mg-ATP and 0.4, GTP (pH 7.3 adjusted with CsOH). sIPSCs were recorded at a holding potential of -70 mV in the presence of 6-Cyano-7-nitroquinoxaline-2,3-dione (CNQX, 10 µM) and amino-5-phosphonopentanoic acid (APV, 50 - 100 µM) in the external solution to block glutamate receptor-mediated synaptic responses. For recordings of miniature IPSCs (mIPSCs), 0.5 µM tetrodotoxin (TTX) was added subsequently to the external solution in addition to CNQX and APV to block spontaneous firing-evoked release of neurotransmitters. For recording spontaneous excitatory postsynaptic currents (sEPSCs), the pipette solution consisted of (in mM): 140, K-gluconate; 4, NaCl; 0.5, $CaCl_2$; 10, HEPES; 5, EGTA, 2, Mg-ATP and 0.4, GTP (pH 7.3 adjusted with KOH). sEPSCs were recorded at a holding potential of -70 mV in the presence of bicuculline (10 µM) in the external solution to block $GABA_A$ receptor-mediated synaptic responses. Similarly, miniature EPSCs (mEPSCs) were recorded in the presence of 0.5 µM TTX in the external solution in addition to bicuculline. Signals were amplified with a Multiclamp 700B amplifier (Molecular Devices, Sunnyvale, CA) and filtered at 2-4 kHz and digitized at 20 kHz for off-line analysis. Data were acquired with a Digidata 1440A interface and analyzed using pClamp10 offline. All experiments were carried out at room temperature of 22-25 ^oC. Data were analyzed offline as described previously (Brackenbury et al, 2013).

9. *Statistics:*

Continuous variables with normal distribution were compared for significant differences using a 2-tailed student's t-test or, in the case of synaptic puncta, repeated-measures ANOVA. The latter analysis was conducted in Graph Pad Prism 7.0. Statistical significance of $P < 0.05$ is indicated by *. $P < 0.01$ is indicated by **. $P < 0.001$ is indicated by ***.

Results

1. Scn1b-null mice exhibit an ataxic gait

We used footprint analysis to characterize the abnormal gait phenotype of *Scn1b* null mice compared to wildtype littermates at P16 , an age at which the mice clearly show abnormal motor coordination (C. Chen et al., 2004). Using this technique, we measured the stride length, stride width, and angle. Stride lengths, measured from either hindlimb prints (Figure 2.1C; wildtype, 38.4 $\pm$ 1.36 mm vs. *Scn1b*-null, 34.3 $\pm$ 1.32 mm; N = 9 wildtype and 8 null; P = 0.577) or forelimb prints (Figure 2.1B; wildtype, 38.3 $\pm$ 1.51 mm vs. *Scn1b*-null, 35.0 $\pm$ 1.00 mm; N = 9 wildtype and 8 null; P = 0.451) were not significantly different between genotypes. In contrast, *Scn1b*-null mice have greater stride widths, especially with the forepaws (Figure 2.1 D and E; wildtype hindpaw, 18.9 $\pm$ 0.86 mm vs. *Scn1b*-null hindpaw, 20.6 $\pm$ 0.85 mm; N = 9 wildtype and 8 null; P = 0.19; wildtype forepaw, 11.3 $\pm$ 0.38 mm vs. *Scn1b*-null forepaw, 17.5 $\pm$ 1.00 mm; N = 9 wildtype and 8 null; P < 0.000). We found that *Scn1b*-null mice walk with their forepaws nearly at the same width as their hindpaws. As expected, wildtype mice walk with a substantially wider hindpaw stance than forepaw stance (cite previous work). Thus, the ratio between forepaw and hindpaw widths is significantly higher, closer to 1.0, for *Scn1b*-null mice compared to wildtype (Figure 2.1F; wildtype ratio, 0.60 $\pm$ 0.017; *Scn1b*-null ratio, 0.85 $\pm$ 0.027; N = 9 wildtype and 8 null, P = 0.000). *Scn1b*-null mice are considerably smaller than their wildtype littermates at comparable ages (Chen 2004), thus we dissected and measured the lengths of the humerus and femur bones to incorporate these differences into the analysis of forelimb and hindlimb gait, respectively. Bone lengths were significantly shorter in *Scn1b*-null compared to wildtype mice. *Scn1b*-null femurs were 8% shorter (wildtype, 9.79 $\pm$ 0.14 mm vs. *Scn1b*-null, 9.04 $\pm$ 0.23 mm; N = 6; P = 0.019). *Scn1b*-null humeri were 5% shorter (wildtype, 8.67 $\pm$ 0.06 mm vs. *Scn1b*-null, 8.20 $\pm$ 0.14 mm; N = 6; P = 0.011). We next normalized the data for stride widths to the relevant limb bone to obtain a more accurate idea of the positioning of the limbs during walking. We found that *Scn1b*-null mice exhibit a significantly wider stance with both the forepaws, adjusted for humerus length (wildtype, 1.00 $\pm$ 0.03 vs. *Scn1b*-null, 1.64 $\pm$ 0.09; N = 9 wildtype and 8 null; P = 0.000) and the hindpaws, adjusted for femur length (wildtype, 1.00 $\pm$ 0.05 vs. *Scn1b*-null, 1.18 $\pm$ 0.05; N = 9 wildtype and 8 null; P = 0.016). Finally,

we measured the angle formed by 3 consecutive steps made by each mouse. In agreement with the observed difference in width of forepaw and hindpaw stances between genotypes, we found significantly different angles of forepaw steps (Figure 2.1G; wildtype, 116.8° ± 3.08° vs. *Scn1b*-null, 87.8° ± 3.39°; N = 9 wildtype and 8 null; P = 0.000) and hindpaw steps (Figure 2.1H; wildtype, 89.6° ± 3.72° vs. *Scn1b*-null, 79.3° ± 2.93°; N = 9 wildtype and 8 null; P = 0.048). The *Scn1b*-null forepaw and hindpaw angles of step were more similar to one another than the wildtype angles of step. Consequently, the ratio between the forepaw angle and the hindpaw angle was significantly higher for wildtype than for *Scn1b*-null mice (Figure 2.1I; wildtype, 1.31 ± 0.028 vs. Scn1b-null, 1.11 ± 0.23; N = 9 wildtype and 8 null; P = 0.000). Taken together, gait analysis shows a significant difference in gait parameters between wildtype and *Scn1b*-null mice at P16, suggesting that *Scn1b* deletion may have consequences for cerebellar function.

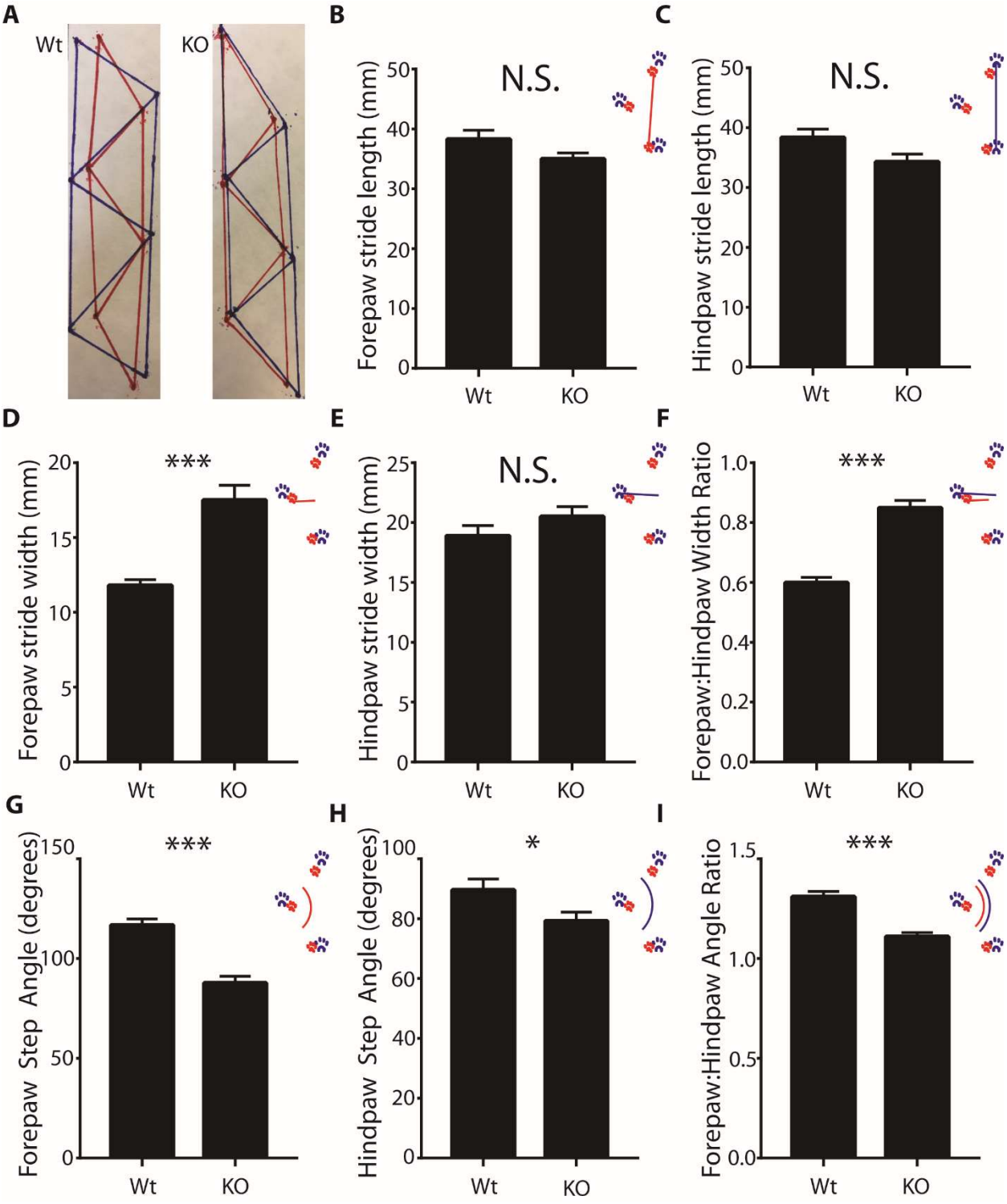

Figure 2.1 *Scn1b*-null mice exhibit an ataxic gait. A, Representative examples of footprint analyses from wildtype and null mice showing hindpaw prints in blue and forepaw prints in red. Hand-drawn lines connecting the paw prints were made in the corresponding colors. B, Mean forepaw stride length. C, Mean hindpaw stride length. D, Mean ratio between each individual

animal's forepaw and hindpaw stride length. E, Mean forepaw stride width. F, Mean hindpaw stride width. G, Mean ratio between each individual animal's forepaw and hindpaw stride width showing that *Scn1b*-null mice position their forepaws nearly as widely as their hindpaws in contrast to wildtype mice. H, Mean forepaw step angle. I, Mean hindpaw step angle. J, Mean ratio between each individual animal's forepaw step angle and hindpaw step angle illustrating that *Scn1b*-null mice have a similar angle of step between forepaws and hindpaws, while wildtype mice do not.

2. Scn1b-null Purkinje cells and interneurons are hypoexcitable.

Purkinje cells represent the sole efferent neurons from the cerebellar cortex. Abnormal development or function of these cells can have dramatic effects on behavior, most notably motor coordination (Lalonde & Strazielle, 2007). We measured action potential firing rates in Purkinje cells under current clamp with increasing ranges of injected current from 0 pA to 180 pA. As shown in Figure 2.2, we found an increase in the threshold to fire an action potential and a marked reduction in the frequency of firing in *Scn1b*-null Purkinje neurons in cerebellar slices across the range of currents. 12 of 26 *Scn1b*-null Purkinje cells examined failed to fire repetitively, while only 3 of 17 wildtype Purkinje cells failed to do so. We also measured action potential firing rates in molecular layer interneurons in wildtype and *Scn1b*-null cerebellar slices, as shown in Figure 2.3. These cells also had an increased threshold for firing an action potential and were hypoexcitable. Figure 2.4 summarizes the mean frequencies of AP firing in Purkinje cells (top) and molecular layer interneurons (bottom) at a range of current injections from -60 pA to 180 pA. Figure 2.5 A and B show the mean maximal firing rates measured in Purkinje cells and interneurons, respectively. In both Purkinje cells and interneurons, the maximal firing rates are significantly reduced in *Scn1b*-null slices recordings. We conclude that *Scn1b* is essential for the high-frequency activities which characterize these cerebellar cortical neurons.

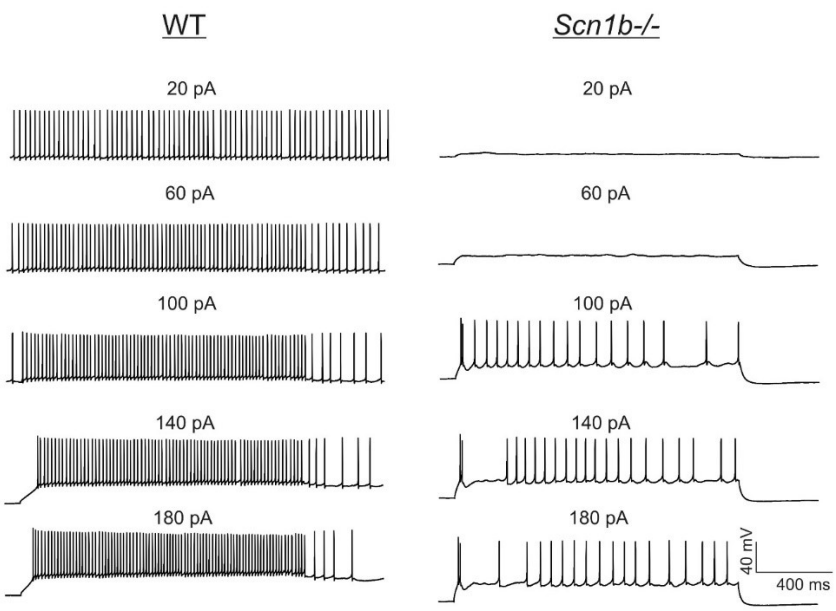

Figure 2.2 Purkinje cells from *Scn1b*-null mice have an increased threshold and reduced firing frequency. Representative traces showing evoked repetitive firing of Purkinje cells in cerebellar slices from wildtype (Left) and *Scn1b*-/- (Right) mice. Repetitive AP firing was evoked by injections of 1500 ms pulse currents of -60 pA to +180 pA (only 20 pA -180 pA-evoked responses are shown). Note that stronger depolarizing current injections are required for evoking repetitive firing in Purkinje cells from *Scn1b*-/- mice. Each trace is a representative example of wildtype (n = 10) and *Scn1b*-/- (n = 14) mice.

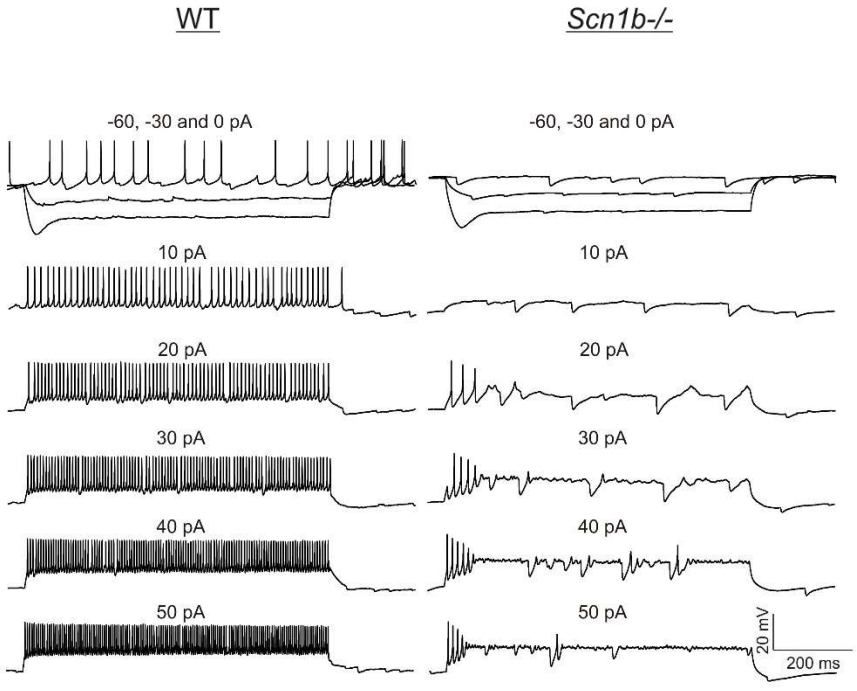

Figure 2.3 Molecular layer interneurons from *Scn1b*-null mice have an increased threshold and reduced firing frequency. Representative traces showing evoked repetitive firing of an interneurons in lobule 4/5 in parasagittal cerebellar slices from wildtype (Left) and *Scn1b*-/- (Right) mice, respectively. Repetitive AP firing was evoked by injections of 1500 ms pulse currents of -60 pA to +180 pA (only selected -60 pA to 50 pA-evoked responses are shown). Note that stronger depolarizing current injections are required for evoking repetitive firing in interneurons from *Scn1b*-/- mice. Each trace is a representative example of WT (n = 3) and *Scn1b*-/- (n = 3) mice.

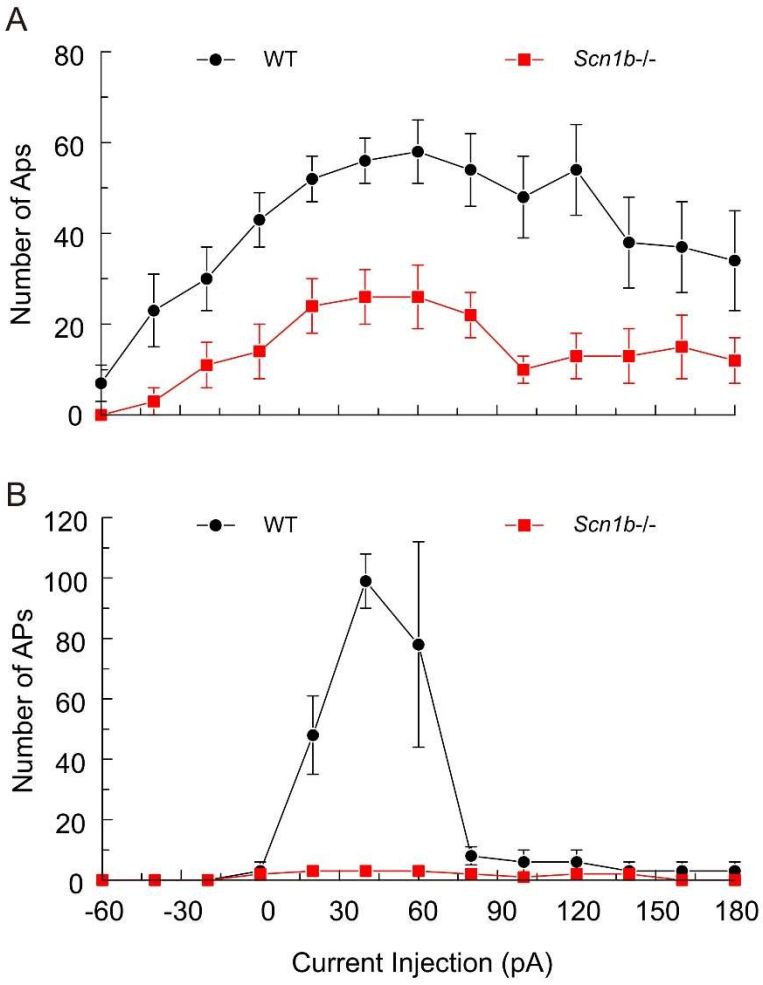

Figure 2.4 Purkinje cells and interneurons from *Scn1b*-null mice show a reduction in AP firing frequency at all stimulation intensity. APs in Purkinje cells (A) or interneurons (B) from wildtype or *Scn1b*-/- neurons were evoked by injections of 1500 ms currents varying from -60 pA to 180 pA. The input–output curves were constructed as number of AP firing vs. stimulation intensity (current injection). All values are mean ± SE of individual recordings from wildtype (n = 10) and *Scn1b*-/- (n = 14) mice for Purkinje cells and 3 wildtype and *Scn1b*-/- mice, respectively, for interneurons.

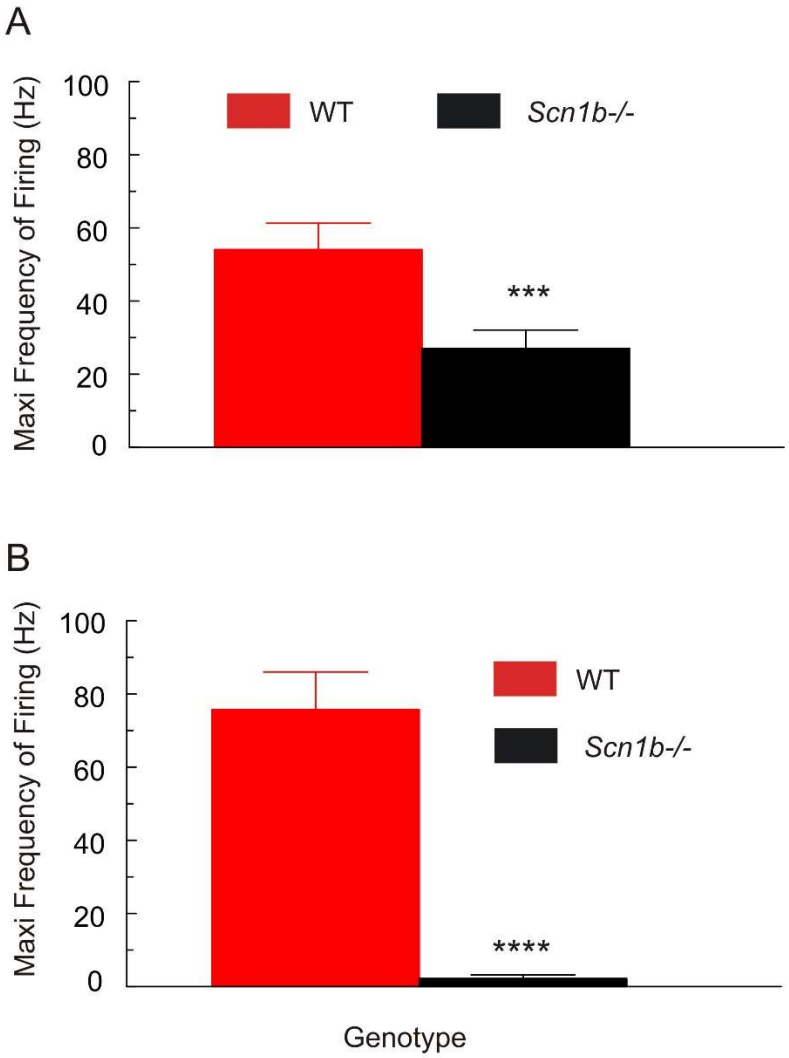

Figure 2.5 *Scn1b*-null Purkinje cells and interneurons display reduced maximum firing frequencies. A, Maximal frequency of APs in Purkinje cells evoked by current injections of -60 to 180 pA. B, Maximal frequency of APs in interneurons evoked by current injections of -60 to 180 pA. Each value is a mean ± SEM of 10 – 14 mice (Purkinje cells) or 3 mice interneurons). Differences between wildtype and *Scn1b*-/- mice are statistically significant, ***, $p<0.005$; ****, $p<0.001$, Student's *t*-test.

3. Scn1b-null Purkinje cells show aberrant bursting activity.

In mice, Purkinje cells develop their complex dendritic morphology, synaptic connections, and mature firing patterns over the first three postnatal weeks (Joseph Altman, 1972). As shown in Figure 2.2, wildtype current clamp recordings showed sustained tonic firing

of single action potentials that increased in frequency with increased injections of current. In *Scn1b*-null Purkinje cell recordings, we observed two instances of aberrant bursting activity. These two recordings, one from a cerebellar slice taken at P15 and one at P19, are displayed in Figure 2.6. We did not observe this behavior in any of our age-matched wildtype control Purkinje cells. This type of burst firing has been described previously in spontaneously firing rat Purkinje cells at P12 but not in adulthood (Cingolani, Gymnopoulos, Boccaccio, Stocker, & Pedarzani, 2002; Crepel, 1972). In the previous report, it was uncovered that this type of firing pattern was dependent on small conductance Ca^{2+}-activated K^+ channels (SK channels), which are highly expressed during early postnatal ages but not in the adult cells (Cingolani et al., 2002). This bursting activity may represent an indication of a developmental delay in Purkinje cells in the absence of *Scn1b*.

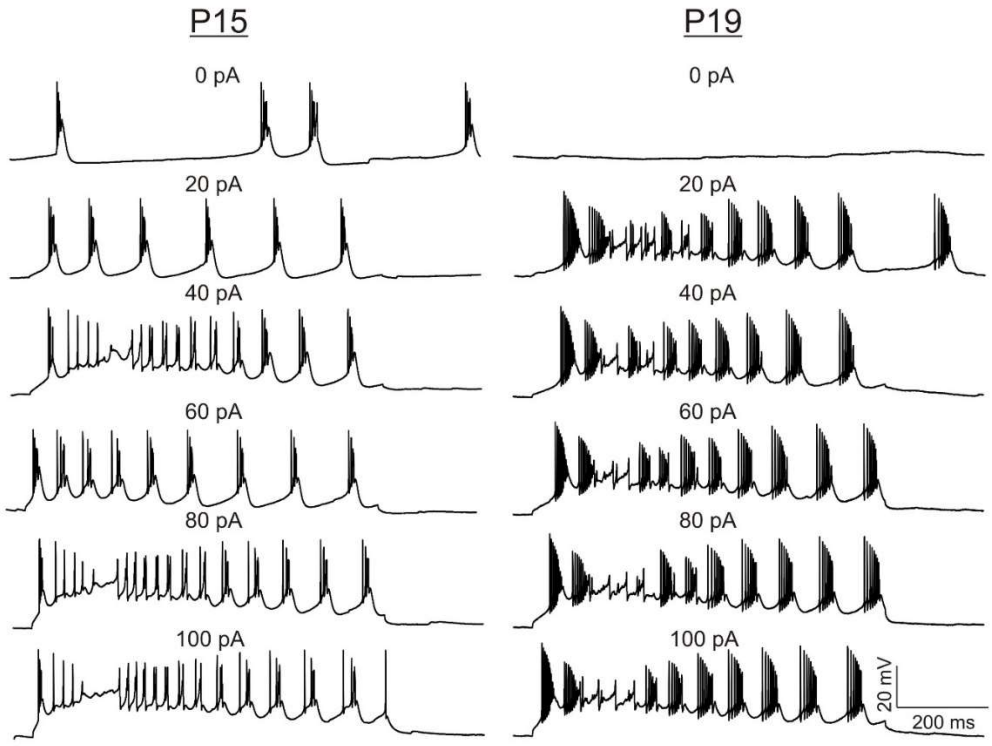

Figure 2.6 *Scn1b*-null Purkinje cells show aberrant bursting activity. Two cases of burst firing seen in Scn1b-null Purkinje cells under current clamp. We did not observe this behavior in any wildtype Purkinje cells from which we recorded action potentials.

4. Scn1b-null mice have morphologically normal Purkinje cells.

We hypothesized that *Scn1b*-null Purkinje cells might have less mature morphological features compared to age-matched wildtype animals. The cerebellar cortex is composed of 3 histological layers: the Molecular Layer (ML), Purkinje cell layer, and granule cell layer. Previous work has shown that *Scn1b*-null mice exhibit abnormal or delayed granule neuron migration into the Granule cell layer (Brackenbury et al., 2008, 2013). Furthermore, we have previously reported abnormal pathfinding of many CGN axons, in the developing *Scn1b*-null mouse (Brackenbury et al., 2008, 2013). However, in spite of these abnormalities, the *Scn1b* null cerebellar cortex largely develops normally comparably to wildtype littermates. At P14, for example, the *Scn1b*-null cerebellar cortex appears normal in most respects, with a densely-populated layer of granule cells overlayed by a single layer of Purkinje cell bodies, each extending a complex dendritic arbor into ML, complete with secondary and tertiary branches and populous dendritic spines. We observed no difference between genotypes in the thickness of the Purkinje cell layer or the number of Purkinje cells, at P14 (Data not shown). In order to determine whether there could be subtle structural differences in *Scn1b*-null Purkinje cells, we labeled parasaggital sections with anti-calbindin and measured Purkinje cell somatic surface areas, primary dendrite widths, and the angle at which the primary dendrites extend from the surface of the cells. We found no significant difference in the surface area of Purkinje cell somata in lobule 4/5 between genotypes (wildtype, 2291 $\pm$ 78 μm^2 vs. *Scn1b*-null, 2402 $\pm$ 100 μm^2; N = 6; P = 0.382, Table 2.1), lobule 6 (wildtype, 2175 $\pm$ 60 μm^2 vs. *Scn1b*-null, 2035 $\pm$ 86 μm^2; N = 6; P = 0.186, Table 2.1), or lobule 8 (wildtype, 2476 $\pm$ 55 μm^2 vs. *Scn1b*-null, 2343 $\pm$ 80 μm^2; N = 6; P = 0.174, Table 2.1). We also found no significant difference in the width of the primary dendrites in lobule 4/5 between genotypes (wildtype, 3.69 $\pm$ 0.19 μm vs. *Scn1b*-null, 3.45 $\pm$ 0.18 μm; N = 6, P = 0.382, Table 2.1), lobule 6 (wildtype, 3.36 $\pm$ 0.15 μm vs. *Scn1b*-null, 3.35 $\pm$ 0.11 μm; N = 6, P = 0.959, Table 2.1), or lobule 8 (wildtype, 3.31 $\pm$ 0.39 μm vs. *Scn1b*-null, 3.42 $\pm$ 0.18 μm; N = 6, P = 0.659, Table 2.1). Finally, we found no significant difference in the angle of the primary dendrite between genotypes, with 90 ^{o} defined as perpendicular to the

Purkinje cell layer, in lobule 4/5 (wildtype, 76.68 ± 1.51° vs. *Scn1b*-null, 78.75 ± 1.17°; N = 6, P = 0.300, Table 2.1), lobule 6 (wildtype, 71.55 ± 1.88° vs. *Scn1b*-null, 75.93 ± 2.11°; N = 6, P = 0.154, Table 2.1), or lobule 8 (wildtype, 74.98 ± 2.27° vs. *Scn1b*-null, 73.39 ± 2.70°; N = 6, P = 0.662, Table 2.1). In sum, Purkinje cells are largely comparable in morphology between wildtype and *Scn1b*-null mice.

	Wildtype			**Knockout**		
	Lobule 4/5	**Lobule 6**	**Lobule 8**	**Lobule 4/5**	**Lobule 6**	**Lobule 8**
Somatic surface area (μm²)	2291 ± 78	2175 ± 60	2476 ± 55	2402 ± 100	2035 ± 86	2343 ± 80
Primary dendrite width (μm)	3.69 ± 0.19	3.36 ± 0.15	3.31 ± 0.39	3.45 ± 0.18	3.35 ± 0.11	3.42 ± 0.18
Primary dendrite angle (°)	76.68 ± 1.51	71.55 ± 1.88	74.98 ± 2.27	78.75 ± 1.17	75.93 ± 2.11	73.39 ± 2.70

Table 2.1 *Scn1b*-null mice have morphologically normal Purkinje cells.

5. β1 is not post-synaptically enriched at excitatory synapses.

Since many Ig-CAMs are localized to pre- and post-synaptic membranes where they are positioned to contribute to synaptic organization and function, we wondered where β1 localizes with respect to synapses. VGSC α and β subunits are enriched in rodent synaptosomal preparations (Beneski & Catterall, 1980; Robert P Hartshorne & Catterall, 1984; Robert P Hartshorne et al., 1982). To ask whether β1 subunits are enriched in post-synaptic fractions of synaptosomes, we prepared homogenates from P14 wildtype mouse cerebellum and fractionated them as described in Methods. Western blot analysis with anti-β1 revealed that β1 protein is expressed in the homogenate (H) and synaptosome (S) fractions. To determine whether β1 is expressed post-synaptically, we isolated the post-synaptic density (PSD) fraction from these synaptosome preparations. As shown in Figure 2.7, Western blot analysis showed that the PSD fraction strongly expresses the post-synaptic protein PSD-95 but not the pre-

synaptic protein synaptophysin. In comparison to the S fraction, the PSD fraction is almost completely depleted of β1. This result suggests that β1 is not enriched post-synaptically in excitatory synapses of the mouse cerebellum, which express post-synaptic densities. In contrast, expression of β1 subunits at the Purkinje cell AIS, which is a post-synaptic target for basket cells, is well known (Kruger et al., 2016; Jyoti Dhar Malhotra et al., 2000; McEwen et al., 2004). Thus, a post-synaptic role for β1 at specific types of synapses cannot be ruled out.

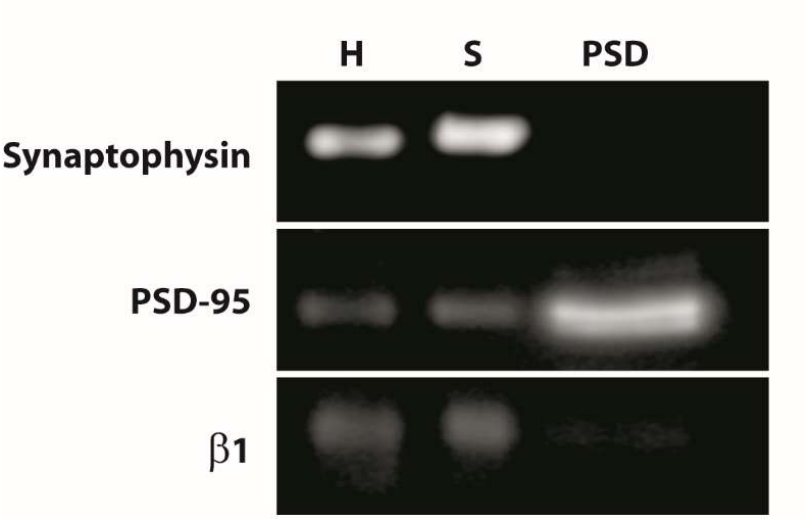

Figure 2.7 β1 is not post-synaptically enriched. Results of representative Western blots using anti-synaptophysin, anti-PSD95, and anti-β1 antibodies in fractionated wildtype synaptosome preparations. H = homogenate; S = synaptosome fraction; PSD = post-synaptic fraction

6. Scn1b-null mice have normal density of parallel fiber-Purkinje cell synapses.

The mossy fibers, afferent projections from outside of the cerebellum, form synaptic connections with CGNs. During the first weeks of postnatal development, the CGNs project their axons outward through the molecular layer (ML) of the cerebellar cortex where they bifurcate to form the densely bundled parallel fibers (Eccles, 1967). These axons interact with PC dendritic spines to form glutamatergic synapses, which can be specifically labeled with anti-Vglut1 antibodies. We used anti-Vglut1 to evaluate the density of parallel fiber synaptic boutons in the outer ML of parasagittal cerebellar sections taken from wildtype and *Scn1b*-null mice at P14. We found no difference between the genotypes in lobule 4/5 (Figure 2.8C;

wildtype, 9.8 ± 0.59 puncta/100μm^3 vs. *Scn1b*-null, 8.2 ± 0.49 puncta/100 μm^3; N = 6; P = 0.38), lobule 6 (Figure 2.8D; wildtype, 9.8 ± 0.69 puncta/100 μm^3 vs. *Scn1b*-null, 8.5 ± 0.54 puncta/100 μm^3; N = 6; P = 0.56), or lobule 8 (Figure 2.8E; wildtype, 11.7 ± 0.64 puncta/100 μm^3 vs. *Scn1b*-null, 10.4 ± 0.57 puncta/100 μm^3; N = 6; P = 0.51).

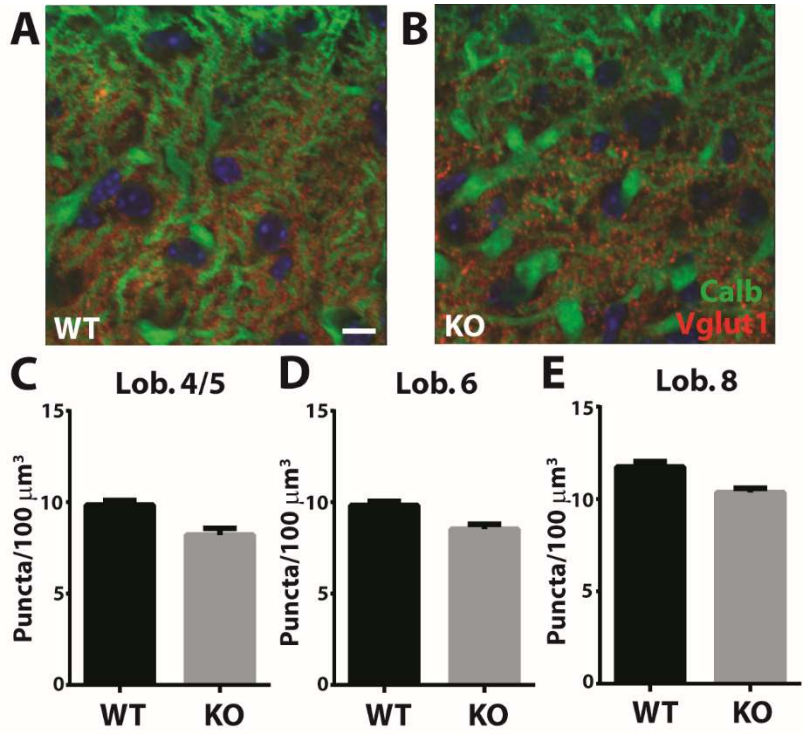

Figure 2.8 *Scn1b*-null mice have a normal density of parallel fiber-Purkinje cell synapses. A and B, representative images (180X), labeled with anti-calbindin (green) and anti-Vglut1 (red) antibodies, captured from the outer molecular layer of wildtype and knockout cerebellar cortex, respectively. Scale bar = 20 μm. Graphs show the mean number of Vglut1+ puncta per 100 μm^3 in wildtype and knockout lobules 4/5 (C), 6 (D), and 8 (E). N = 6. Error bars represent SEM.

7. Scn1b-null mice have normal climbing fiber synapse density.

The second afferent projection which forms excitatory synapses onto Purkinje cells is composed of the climbing fibers (Eccles, 1967). In postnatal mouse development, these axons initially form synapses onto PC somata and major dendritic branches. After about postnatal week 3, the somatic synapses are no longer present, and each PC is innervated by a single

climbing fiber (M. Watanabe & Kano, 2011). The synapses formed by climbing fibers can be specifically labeled with anti-Vglut2 antibody. Using this marker, we examined the quantity of climbing fiber synaptic puncta on both the PC somata and the PC primary dendrite in parasagittal cerebellar sections from wildtype and *Scn1b*-null mice at P14. We found no significant difference in the density of somatic climbing fiber synaptic puncta in lobule 4/5 (Figure 2.9C; wildtype, 1.16 $\pm$ 0.15 puncta/100 μm^2 vs. *Scn1b*-null, 1.81 $\pm$ 0.16 puncta/100 μm^2; N = 6; P = 0.10), lobule 6 (Figure 2.9D; wildtype, 1.74 $\pm$ 0.19 puncta/100 μm^2 vs. *Scn1b*-null, 1.58 $\pm$ 0.19 puncta/100 μm^2; N = 6; P = 0.75), or lobule 8 (Figure 2.9E; wildtype, 0.94 $\pm$ 0.12 puncta/100 μm^2 vs. *Scn1b*-null, 1.16 $\pm$ 0.17 puncta/100 μm^2; N = 6; P = 0.61). We also found no difference in the density of dendritic climbing fiber synaptic puncta in lobule 4/5 (Figure 2.9F; wildtype, 2.49 $\pm$ 0.19 puncta/100 μm^2 vs. *Scn1b*-null, 3.02 $\pm$ 0.23 puncta/100μm^2; N = 6; P = 0.31), lobule 6 (Figure 2.9G; wildtype, 2.93 $\pm$ 0.17 puncta/100 μm^2 vs. *Scn1b*-null, 3.08 $\pm$ 0.23 puncta/100 μm^2; N = 6; P = 0.68), or lobule 8 (Figure 2.9H; wildtype, 2.56 $\pm$ 0.16 puncta/100 μm^2 vs. *Scn1b*-null, 3.14 $\pm$ 0.24 puncta/100 μm^2; N = 6; P = 0.46). As the mouse cerebellar cortex develops, the climbing fibers extend outward into the ML along the PC dendritic arbors. To determine whether there is a defect in this process in the null mice, we measured the range of the Vglut2+ puncta and expressed it as a percentage of the total ML starting from the base of the PCs. We observed no difference in this range between the genotypes in lobule 4/5 (Figure 2.9I; wildtype, 68.1 $\pm$ 2.4% vs. *Scn1b*-null, 68.9 $\pm$ 1.7%; N = 4; P = 0.88), lobule 6 (Figure 2.9J; wildtype, 61.8 $\pm$ 2.5% vs. *Scn1b*-null, 61.1 $\pm$ 1.9%; N = 4; P = 0.92), or lobule 8 (Figure 2.9K; wildtype, 64.5 $\pm$ 1.8% vs. *Scn1b*-null, 62.7 $\pm$ 1.9%; N = 4; P = 0.67). We conclude that climbing fiber-PC synapses develop normally in mice lacking *Scn1b*.

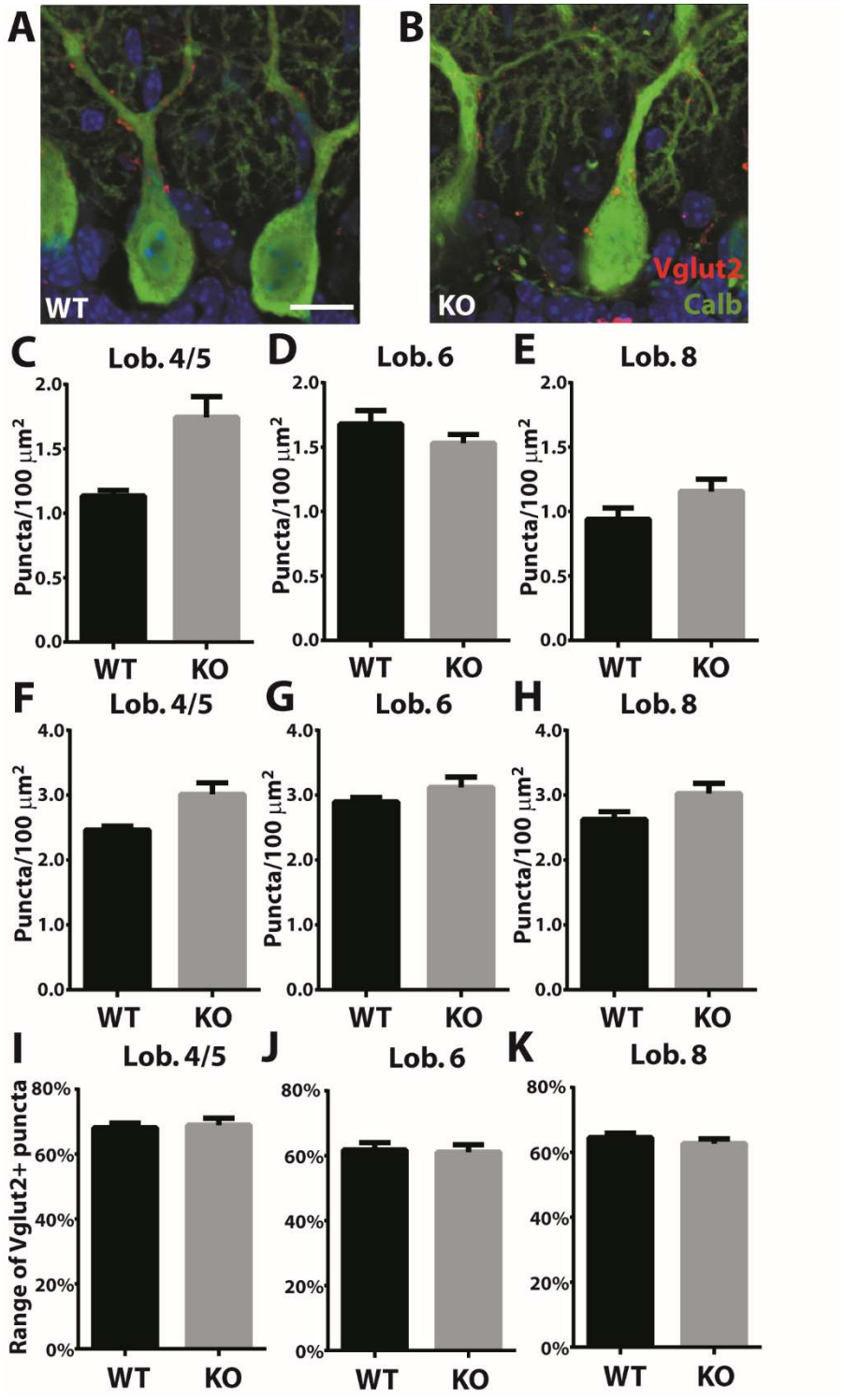

Figure 2.9 *Scn1b*-null mice have a normal density of climbing fiber synapses. A and B, representative images (180X), labeled with anti-calbindin (green) and anti-Vglut2 (red) antibodies, showing Purkinje cell somata and proximal dendrites of wildtype and knockout cerebellar cortex, respectively. Scale bar = 20 μm. Graphs C, D, and E show the mean density of Vglut2+ puncta per 100um^2 of Purkinje cell somatic surface in wildtype and knockout lobules

4/5, 6, and 8, respectively. Graphs F, G, and H show the mean density of Vglut2+ puncta per 100um^2 of Purkinje cell primary dendritic surface in wildtype and knockout lobules 4/5, 6, and 8, respectively. Graphs I, J, and K show the mean range of Vglut2+ puncta measured from the base of the Purkinje cell bodies outward toward the surface of the cerebellar cortex in wildtype and knockout lobules 4/5, 6, and 8, respectively. N = 6. Error bars represent SEM.

8. Scn1b-null mice have comparable densities of GABAergic synapses formed between basket interneurons and Purkinje cell somata at P10 and at P14.

Two classes of ML interneurons form GABAergic synapses with PCs, stellate cells and basket cells. Situated adjacent to the PCs, the basket cells innervate their somata and proximal dendrites between about P7 and P18 in the mouse. Basket cell axons extend collaterals that construct a specialized, basket-shaped structure directly onto the PC AIS called a Pinceau synapse (Bayer & Altman, 1987; Somogyi & Hámori, 1976). This synaptogenic process begins at ~P16 and remains incomplete until P30 or later (Ango, di Cristo, et al., 2004; Buttermore et al., 2012). While *Scn1b*-null mice do not survive long enough to form the Pinceau synapse, basket cells prolifically form synapses onto Purkinje cell somata earlier than the time of death in these mice. In order to determine the contribution of β1 subunits to basket cell synapse-formation, we analyzed the number of VGAT+ puncta on the somatic surface of PCs at P10 and 14. We found no significant difference in the density of GABAergic synaptic puncta in lobule 4/5 (Figure 2.10C; wildtype, 3.70 $\pm$ 0.31 puncta/100 μm^2 vs. *Scn1b*-null, 3.52 $\pm$ 0.27 puncta/100 μm^2; N = 6; P = 0.67), lobule 6 (Figure 2.10D; wildtype, 3.54 $\pm$ 0.42 puncta/100 μm^2 vs. *Scn1b*-null, 3.24 $\pm$ 0.27 puncta/100 μm^2; N = 6; P = 0.56), or lobule 8 (Figure 2.10E; wildtype, 2.58 $\pm$ 0.14 puncta/100 μm^2 vs. *Scn1b*-null, 3.12 $\pm$ 0.45 puncta/100 μm^2; N = 6; P = 0.28) at P10. In agreement, we found no significant differences in their density in lobule 4/5 (Figure 2.11C; wildtype, 2.99 $\pm$ 0.13 puncta/100 μm^2 vs. *Scn1b*-null, 2.65 $\pm$ 0.36 puncta/100 μm^2; N = 6; P = 0.40), lobule 6 (Figure 2.11D; wildtype, 3.27 $\pm$ 0.39 puncta/100 μm^2 vs. *Scn1b*-null, 2.65 $\pm$ 0.34 puncta/100 μm^2; N = 6; P = 0.26), or lobule 8 (Figure 2.11E; wildtype, 2.80 $\pm$ 0.26 puncta/100 μm^2 vs. *Scn1b*-null, 3.30 $\pm$ 0.50 puncta/100 μm^2; N = 6; P = 0.40) at P14. Viewed ultrastructurally at P14, wildtype and *Scn1b*-null synaptic boutons appear comparable in size and density. Representative examples are shown in Figure 2.11 F and G. Based upon these

experiments, we conclude that *Scn1b* is expendable for the formation of basket interneuron-Purkinje cell synapses, *in vivo*. However, a potential role in the organization of the Pinceau synapse cannot be evaluated.

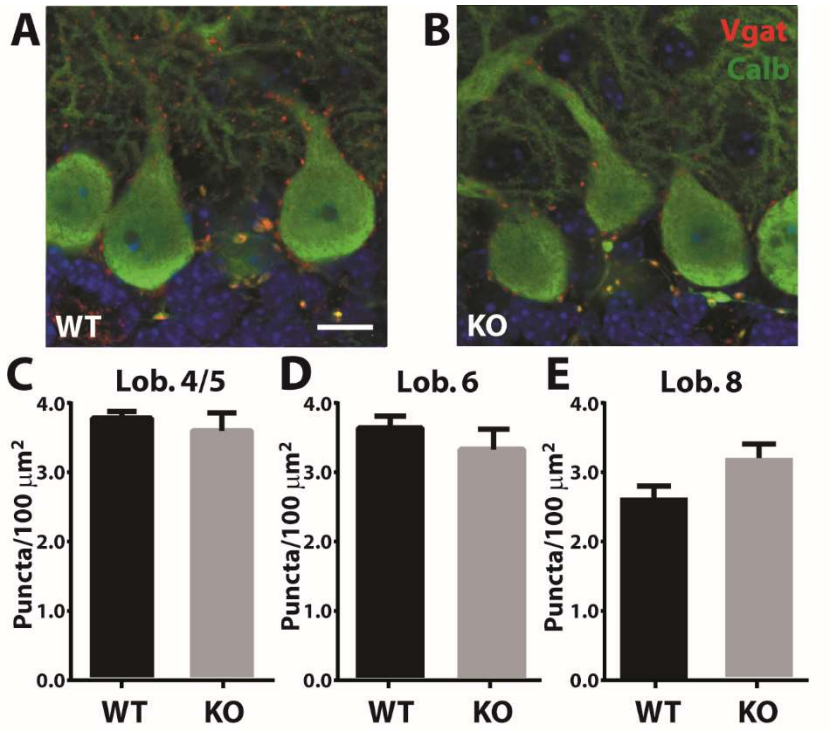

Figure 2.10 *Scn1b*-null mice have comparable densities of GABAergic synapses formed between basket interneurons and Purkinje cell somata at P10. A and B, representative images (180X), labeled with anti-calbindin (green) and anti-Vgat (red) antibodies, showing Purkinje cell somata and proximal dendrites of wildtype and knockout cerebellar cortex, respectively. Scale bar = 20 μm. Graphs C, D, and E show the mean density of Vgat+ puncta per 100um^2 of Purkinje cell somatic surface in wildtype and knockout lobules 4/5, 6, and 8, respectively. N = 6. Error bars represent SEM.

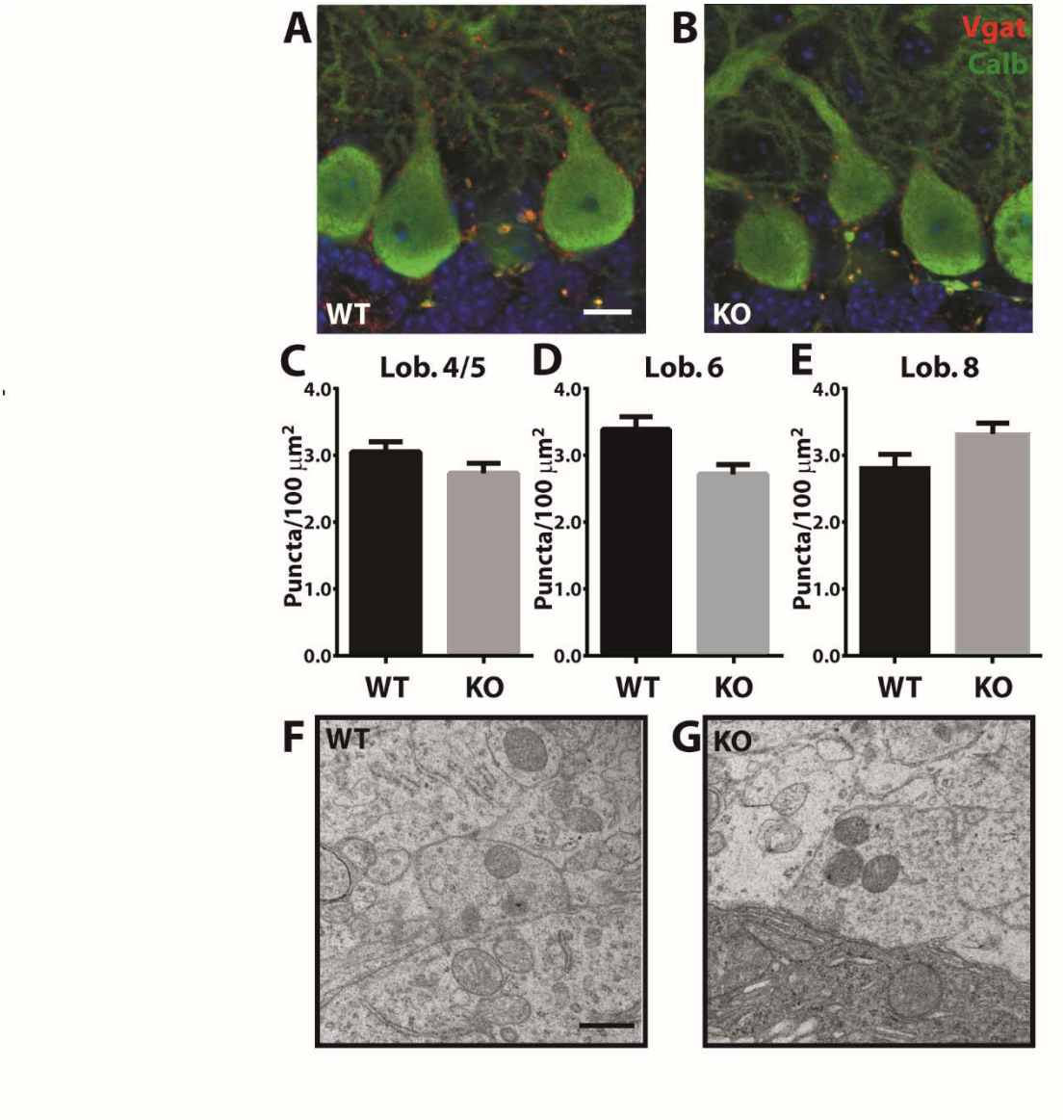

Figure 2.11 *Scn1b*-null mice have comparable densities of GABAergic synapses formed between basket interneurons and Purkinje cell somata at P14. A and B, representative images (180X), labeled with anti-calbindin (green) and anti-Vgat (red) antibodies, showing Purkinje cell somata and proximal dendrites of wildtype and knockout cerebellar cortex, respectively. Scale bar = 20 μm. Graphs C, D, and E show the mean density of Vgat+ puncta per 100um^2 of Purkinje cell somatic surface in wildtype and knockout lobules 4/5, 6, and 8, respectively. N = 6. Error bars represent SEM. F and G show representative TEM images (50,000X) taken of GABAergic synaptic boutons on the surface of wildtype and knockout Purkinje cells, respectively. Scale bar = 500 nm.

9. Molecular layer interneurons exhibit normal migration in the Scn1b-null cerebellar cortex

Previous work has shown that *Scn1b*-null mice have defects in the migration of CGNs (Brackenbury et al., 2008, 2013). It is possible that β1 also plays a role in the migration of other types of neurons. Under normal conditions, interneurons migrate into the cerebellar cortex from the white matter during the first few postnatal days in mouse development. By the end of the first postnatal week, they pass arrive in the ML and differentiate into mature, functional stellate or basket interneurons (Ango, di Cristo, et al., 2004; L. Zhang & Goldman, 1996). Both types of ML interneurons express parvalbumin but not calbindin. By contrast, PCs are detectable using both anti-parvalbumin and anti-calbindin antibodies. Thus, we used these combined staining strategies to discriminate and quantify interneurons in parasagittal cerebellar sections from P14 wildtype and *Scn1b*-null mice. We found no difference in the density of ML interneurons in lobule 4/5 (Figure 2.12C; wildtype, 48.94 $\pm$ 5.05 cells/100,000 μm^2 vs. *Scn1b*-null, 43.18 $\pm$ 4.09 cells/100,000 μm^2; N = 4; P = 0.41), lobule 6 (Figure 2.12D; wildtype, 58.53 $\pm$ 5.25 cells/100,000 μm^2 vs. *Scn1b*-null, 54.16 $\pm$ 2.47 cells/100,000 μm^2; N = 4; P = 0.48), or lobule 8 (Figure 2.10=2E; wildtype, 72.13 $\pm$ 9.34 cells/100,000 μm^2 vs. *Scn1b*-null, 67.09 $\pm$ 1.10 cells/100,000 μm^2; N = 4; P = 0.61). We also measured the distance of migration of the interneurons into the ML. Starting from the base of the PC bodies and expressed as a percentage, we detected no difference in the mean distance between genotypes in lobule 4/5 (Figure 2.12F; wildtype, 37.3 $\pm$ 1.8% vs. *Scn1b*-null, 40.3 $\pm$ 1.3%; N = 4; P = 0.22), lobule 6 (Figure 2.12G; wildtype, 42.8 $\pm$ 2.9% vs. *Scn1b*-null, 40.3 $\pm$ 2.8%; N = 4; P = 0.56), or lobule 8 (Figure 2.12H; wildtype, 40.3 $\pm$ 1.3% vs. *Scn1b*-null, 38.0 $\pm$ 2.4%; N = 4; P = 0.43). Thus, there are no overt migration defects in ML interneurons in the *Scn1b*-null cerebellar cortex.

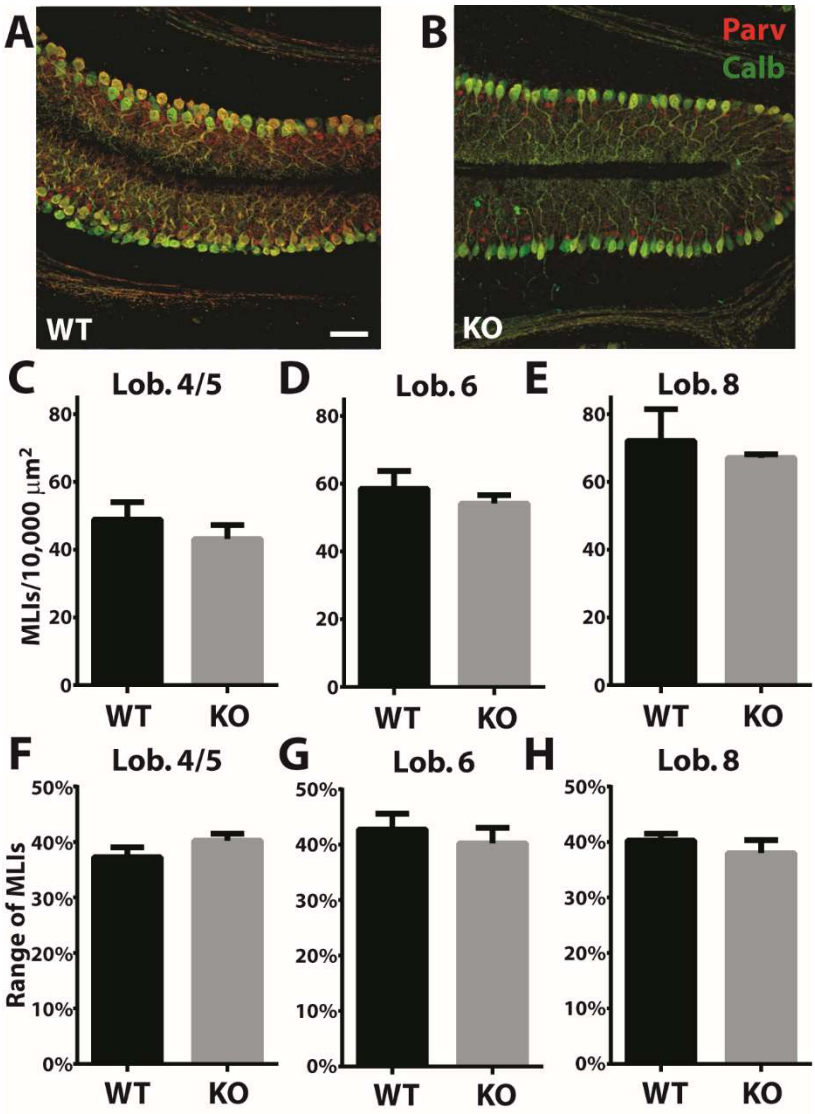

Figure 2.12 Molecular layer interneurons exhibit normal migration in the *Scn1b*-null cerebellar cortex. A and B, representative images (20X), labeled with anti-calbindin (green) and anti-parvalbumin (red) antibodies, from wildtype and null (KO) cerebellar cortex, respectively. Scale bar = 50 μm. Graphs C, D, and E show the mean density of molecular layer interneurons (MLI) in wildtype and knockout lobules 4/5, 6, and 8, respectively. Graphs F, G, and H show the mean range of MLIs measured from the base of the Purkinje cell bodies outward toward the surface of the cerebellar cortex in wildtype and null lobules 4/5, 6, and 8, respectively. N = 4. Error bars represent SEM.

Discussion

As the sole efferent projections from the cerebellar cortical network, Purkinje cells are critical to all cerebellar functions. This is particularly evident when considering spontaneous mutant mice with substantial malformation of the cerebellar cortex. Examples include Lurcher and Staggerer, which carry unrelated mutations that converge upon a profound loss of Purkinje cells (Caddy & Biscoe, 1979; Fortier et al., 1987; Lalonde, 1987; Lalonde et al., 1996; Sonmez & Herrup, 1984; Zuo et al., 1997). Another mutant, Weaver, undergoes early postnatal degeneration of granule neurons, which ultimately exert their effects through stimulation of Purkinje cell activity (Goldowitz & Smeyne, 1995; Signorini et al., 1997). Ataxia is common to all such mutants, and is the most common behavioral outcome associated with cerebellar dysfunction (Lalonde & Strazielle, 2007). Importantly, it is not necessary to lose large quantities of cells within the cerebellar cortex in order to have a consequent ataxic gait. Contactin-null mice, for example, have a progressive ataxic gait which correlates with micro-organizational defects not dissimilar from those observed in *Scn1b*-null mice, namely aberrant axon pathfinding and fasciculation in the parallel fibers (E O Berglund et al., 1999; Brackenbury et al., 2010, 2013). Contactin is an Ig-CAM, a binding partner for β1, and *Cntn1*-null mice have reduced expression of β1 protein in the brain (Brackenbury et al., 2010). It is not clear whether the micro-organizational defects seen in either of these mutants are responsible for the gait abnormalities they exhibit. Indeed, involvement of the cerebellum in the motor phenotypes of DS patients has been questioned (Scheffer, 2012). The main difference between wildtype and *Scn1b*-null walking gait is a significant spreading out of the limbs, especially the forelimbs. This widened stance is a common feature of cerebellar ataxia (Lalonde & Strazielle, 2007), but is not sufficient to directly implicate the cerebellum.

Current clamp experiments in Purkinje cells demonstrate firing deficits in the absence of *Scn1b*. Such hypoexcitability could be the consequence of reduced functional synaptic inputs, a change in the balance between excitation and inhibition at such inputs, or reflect an intrinsic deficit in the Purkinje cells themselves. We also observed bursting activity which could reflect a developmental delay in at least a subset of *Scn1b*-null Purkinje cells. We used immunohistochemistry to distinguish specific classes of synapses converging onto the surface of

Purkinje cells in wildtype and *Scn1b*-null brain sections. We found no reduction in the apparent density of excitatory or inhibitory synapses. This is in agreement with the lack of strong immunoreactivity for β1 in the post-synaptically enriched fraction of cerebellar synaptosomes analyzed by Western blot. β1 localizes to axons, especially at nodes of Ranvier and AISs (Brackenbury et al., 2010; C. Chen et al., 2004; Wimmer et al., 2010). The Purkinje cell AIS, notably, is highly enriched in β1(Brackenbury et al., 2010; Kruger et al., 2016), along with Ig-CAM heterophilic partners such as NF186 and AnkyrinG (Jyoti Dhar Malhotra et al., 2000; McEwen & Isom, 2004). It is also detectable at axon growth cones in developing neurons, including CGNs (Brackenbury et al., 2008). Thus, β1 is likely present at presynaptic terminals. However, in the present study we did not observe a significant reduction in Vglut1+ parallel fiber synaptic specializations. Thus, we conclude that *Scn1b* is not critical for the formation of synapses between Purkinje cells and their most prominent innervating partners. Antibodies which detect β1 are not of sufficiently high affinity to detect low levels of expression outside of the AIS and nodes of Ranvier (C. Chen et al., 2012; Kruger et al., 2016). However, basket interneurons form Vgat+ synapses onto the somata, proximal dendrites, and ultimately the AIS of their target Purkinje cells (Ango, di Cristo, et al., 2004; Buttermore et al., 2012). Thus, β1 is in position to have a post-synaptic adhesive function in the organization of the Pinceau synapse. Because this specialized synapse does not fully form until much later in development than *Scn1b*-null mice survive, we were not able to assess its formation in this model. Finally, β1 is known to have a role in the localization of VGSC α subunits (Brackenbury et al., 2010). Perhaps Purkinje cell hypo-excitability in *Scn1b*-null brain slices can be accounted for by a reduction in the number of functional Na^+ channels on the cell surface and clustered at the AIS, resulting in a failure to produce supra-threshold currents and fire action potentials with fidelity. This is an attractive hypothesis, given the findings of the current study. [^{3}H]-Saxitoxin binding provides a quantitative method for examining the number of VGSC α subunits expressed in a sample (McEwen & Isom, 2004; Patino et al., 2011). Carried out in membranes collected from wildtype and *Scn1b*-null cerebellum, this experiment will be highly informative. A significant reduction in α subunits could, at least in-part, explain the reduced excitability displayed by neurons in the cerebellar cortex in the absence of *Scn1b*.

Homozygous *SCN1B* loss-of-function mutations have been shown to cause the Dravet syndrome in previous reports (Ogiwara et al., 2012; Patino et al., 2009). The *Scn1b*-null mouse is a model of this rare form of Dravet syndrome. It remains unknown whether a common mechanism exists between *SCN1A*- and *SCN1B*-linked syndromes. Under most circumstances, Dravet syndrome presents with febrile seizures during the first years of life. Subsequently, patients exhibit seizures and episodes of status epilepticus even in the absence of fever (Surges & Sander, 2012). Cognitive development slows or stagnates in the young children, and as they age, they show a progressive ataxic gait (Scheffer, 2012). Our previous results showing micro-organizational defects in the *Scn1b*-null cerebellar cortex, together with the mouse's gait defect and dysfunctional Purkinje cell excitability point to the potential for a cerebellar role in the pathology of *SCN1B*-linked epileptic encephalopathy (Brackenbury et al., 2008, 2013). In addition to motor functions, it has become clear in recent years that the cerebellum serves functions in cognition, including language perception, memory, and temporal ordering (Noroozian, 2014). Importantly, clinical evidence has been gathered that suggests a cerebellar role in the neuropsychological profile of Dravet syndrome patients (Battaglia et al., 2013). Substantial deficits are visible in both the form and the function of *Scn1b*-null cerebellar cortex, warranting further investigation into the potential importance of this structure in the pathology of epilepsy disorders including Dravet syndrome.

Acknowledgements

Dr. Yukun Yuan conducted the slice electrophysiology experiments and analyses. Fatima Lima provided excellent technical assistance in 3-D reconstruction and analysis of synapse densities. Dr. Yuan and Fatima Lima are researchers in the laboratory of Dr. Lori Isom, Department of Pharmacology at the University of Michigan. Synaptosomes were prepared in the laboratory of Dr. Roman Giger, Department of Cell and Developmental Biology at the University of Michigan. This project was funded, in part, by a pre-doctoral fellowship granted by the Epilepsy Foundation.

Chapter III

Conclusions and Future Directions

1. *Introduction*

Previous work from our lab showed neuronal migration and fasciculation defects in *Scn1b*-null cerebellum (Brackenbury et al., 2008, 2013). Here, we show that *Scn1b* deletion leads to substantially reduced firing activity in Purkinje cells and interneurons as well as micro-organizational defects in the mouse cerebellar cortex. Consistent with these results, *Scn1b*-null mice exhibit an abnormal gait. In spite of this, our data also suggest that structural formation of the major classes of synapses within this circuit is preserved in *Scn1b*-null mutants. Homozygous *SCN1B* loss-of-function mutations in humans are linked to the severe epileptic encephalopathy Dravet syndrome (O'Malley & Isom, 2015). This chapter will build a case for the possible role of cerebellar dysfunction in the hallmark symptoms of Dravet syndrome and related diseases, namely ataxia, cognitive impairment, and possibly seizures. Further, I will propose potential functional roles for sodium channel β1 subunits with regard to regulating the expression of NaV1.6 at key subcellular locations, because this VGSC α subunit is characterized by the passage of persistent current and has previously been shown to be deficiently-expressed at the *Scn1b*-null Purkinje cell axon initial segment (AIS) (Brackenbury et al., 2010). Finally, a prescription for future studies directed at the cerebellum will be proposed for continued work toward understanding the developmental and functional mechanisms underlying the pathology associated with *SCN1B*-linked epileptic encephalopathy and related disorders.

2. *Scn1b* in cerebellar cortex development

Previous investigations have revealed that *Scn1b*-null mice have micro-organizational defects in the postnatal cerebellar cortex (Brackenbury et al., 2008, 2013). These include a delay in granule cell migration, abnormal axon targeting and fasciculation of the parallel fibers. These processes rely on adhesive interactions between granule cells and Bergmann glia. In *Scn1b*-null mice, the Bergmann glia are similar in density and morphology to those of wildtype mice (unpublished observations). Furthermore, the Purkinje cell layer of *Scn1b*-null mice forms normally by P14, and Purkinje cell morphology does not appear to be significantly different from wildtype (Table 2.1). These cells are comparable in number, and they have similar somatic surface area and primary dendrite width as wildtype littermates. The molecular layer interneurons are also similar in number and position in P14 wildtype and *Scn1b*-null mice (Figure 2.12). Largely, the layers of the cerebellar cortex form on a comparable timeline with that of wildtype mice. Thus, there are specific abnormalities in the organization of the postnatal cerebellar cortex in mice deficient in *Scn1b*, but the layers, cellular constituents, and lobules of these mutants are largely normal.

With spontaneous mutation models such as Lurcher and Staggerer in mind, one might not expect to observe meaningful behavioral phenotypes from the relatively mild developmental abnormalities seen in contactin-null and *Scn1b*-null mice (Lalonde & Strazielle, 2007). Indeed, the former mutants undergo losses of entire classes of cells, including the millions of granule cells and the projectors of the sole output from the cerebellar cortical circuit, the Purkinje cells. As expected, these mice show profound motor abnormalities. Can the axon pathfinding and cell migration defects observed throughout postnatal development in *Scn1b*-null mice fully account for their apparent ataxic gait? Recent data in our laboratory might provide an answer to this question. SLICK mice express Cre-recombinase under the direction of the neuron-specific Thy-promoter, in a tamoxifen-dependent manner (Young et al., 2008). Breeding these mice with our *Scn1b*$^{Flox/Flox}$ mutants (Chen et al., 2007) produces SLICK/ *Scn1b*$^{Flox/Flox}$ pups, which develop and survive with no overt abnormalities. However, injection of tamoxifen at any time point causes a severe and progressive behavioral phenotype and death within two weeks (Chen, Hull, and Isom, unpublished results). This phenotype includes severe, spontaneous seizures, ataxia, and episodic limb paralysis. Importantly, performing this

experiment in adult mice older than P30 allows the cerebellar cortex to develop normally, well after the migration of granule cells into the internal granule layer and the extension and pathfinding of their axonal projections has taken place. This finding strongly suggests that developmental abnormalities in cerebellar micro-organization are not necessary for loss of *Scn1b* to produce motor abnormalities. Thus, it now seems likely that functional deficits in neurons arising from the acute loss of β1, e.g. loss of sodium channels at the cell surface resulting in decreased sodium current, lead directly to circuit-level abnormalities and the severe phenotypes which result in death.

3. Ataxia in Scn1b-null mice

Ataxia, characterized by a significantly widespread walking stance and a lack of motor coordination in humans and in mice, is common to spontaneous and transgenic mutant mice with developmental defects or cell degeneration in the cerebellum (Lalonde & Strazielle, 2007). It also occurs in association with micro-organizational defects such as those seen in contactin-null mice (E O Berglund et al., 1999). Our gait analysis in *Scn1b*-null juvenile mice showed that they walk with a sprawled, widened stance. This is especially apparent with regard to the front paws, which are positioned more closely to the body in control mice. The hind paws, too, show greater width in the walking gait of *Scn1b*-null mice. Together, the developmental defects that have been described in the *Scn1b*-null cerebellar cortex and the functional deficits measured in *Scn1b*-null Purkinje cells, build a compelling case for the involvement of the cerebellum in the ataxic gait seen in these mice.

In addition to gait analysis, a variety of behavioral tests have been developed to investigate the motor coordination of mouse mutants exhibiting ataxia. Among these, the vertical grid, stationary beam, suspended wire, and rotorod tests use the measure of latency to fall from the apparatus to compare motor coordination abilities amongst mice (Lalonde & Strazielle, 2007). Distance travelled along the stationary beam can also be measured. The rotorod requires mice to synchronize their walking pace with the rate of the device's rotation (Lalonde & Strazielle, 2007). These methods have been applied to many spontaneous and

transgenic ataxic mutants at juvenile ages, comparable to the survivable age of *Scn1b*-null mice. Lurcher, Staggerer, Reeler, and Weaver mice all have a reduced latency to fall from round stationary beams when compared to wildtype controls. Furthermore, all four of these spontaneous mutants fell sooner when suspended from a coat-hanger and showed significantly poorer performance on the rotorod (Lalonde & Strazielle, 2007). In contrast to these mutants, *SCA1* transgenic mice begin to show abnormal performance on the rotorod starting at five weeks of age, at the onset of Purkinje cell pathology (H. Clark et al., 1997). Unfortunately, tests such as these are not feasible for evaluating *Scn1b*-null mouse behavior. Their small body size and frequent seizures would provide a considerable confound to such analyses. Later in this discussion, I will propose experiments to address this limitation and permit the evaluation of *Scn1b*'s role in motor and other behavioral phenotypes that may be caused by cerebellar dysfunction.

4. Scn1b in synapse-formation

CAMs are involved in the formation of synapses. These proteins accumulate at presynaptic and postsynaptic sites and direct the formation and stabilization of nascent synapses during development. This is accomplished by means of organizing the assembly of signaling molecules, neurotransmitter receptors, and cytoskeletal components in addition to adhering membrane components between the two cells forming the synapse. Among the CAMs involved in synaptogenesis are cadherins, neurexins and neuroligins, CAMs containing leucine-rich repeats (LRRs), ephrins and Eph receptors, and Ig-CAMs, a family of proteins with particular relevance to the study of VGSC β1 and β1B. Ig-CAMs with important synapse-formation functions include NCAM, L1, CHL1, contactins, and others. These examples are highlighted because they contain extracellular Ig-loops of the V-type, which is also common to the VGSC β subunits (L L Isom et al., 1995). NCAM, neural cell adhesion molecule, plays a number of well-characterized roles at synapses, including in their formation, maturation, and function. NCAM is expressed both pre- and post-synaptically. It interacts homophilically as well as heterophilically with other molecules, including β1-spectrin, and directs the conversion of

cell-cell contacts into functional synapses (Sytnyk et al., 2002). Hippocampal culture experiments from NCAM-null mice revealed reduced excitatory synapse numbers, decreased PSD size, and reduced expression of PSD-associated proteins (Dityatev, Dityateva, & Schachner, 2000; Sytnyk, Leshchyns'Ka, Nikonenko, & Schachner, 2006). L1-null mice have fewer perisomatic inhibitory synapses in the hippocampus and abnormalities at presynaptic terminals when viewed ultrastructurally (Saghatelyan et al., 2004). Like VGSC β1, L1 has been shown to interact intracellularly with ankyrin. Loss of this interaction resulted in impairments in perisomatic GABAergic synapses in the cingulate cortex (Guan & Maness, 2010). Neurofascin is a member of the L1-CAM subfamily that is involved in GABAergic synapse formation between basket interneurons in the cerebellar cortex and Purkinje cells. Like L1, neurofascin-mediated synapse-formation depends on interactions with ankyrin (Ango, di Cristo, et al., 2004). CHL1, close homolog of L1, is another related Ig-CAM with a role in inhibitory synaptogenesis. Unlike L1-null mice, CHL1-null mice have an increased number of inhibitory synapses in the hippocampus. These synapses also have increased size and density of active zones (Nikonenko et al., 2006). Contactins are a subfamily of Ig-CAMs that are GPI-anchored to the extracellular membrane. Contactin-6 is expressed at presynaptic membranes. Mice deficient in contactin-6 were found to have a reduced number of excitatory presynaptic terminals in the hippocampus and cerebellum (K. Sakurai et al., 2009; K. Sakurai, Toyoshima, Takeda, Shimoda, & Watanabe, 2010).

Our investigation into the potential roles of *Scn1b* in the formation of synapses during development was focused on the cerebellar cortex. The decision to examine this brain structure was informed by a number of advantages that it offers. First, the murine cerebellar cortical network largely develops postnatally. This affords the opportunity to characterize the processes of synaptogenesis without sacrificing the pregnant mothers. It also likely limits the investigation to the functions of β1, which is expressed in the postnatal cerebellum at a much higher level than the splice variant β1B (Patino et al., 2011). Second, the cerebellar cortex of the *Scn1b*-null mouse is known to have micro-organizational defects that occur contemporaneously with the formation of synapses during development (Brackenbury et al., 2008, 2013). These abnormalities are especially relevant to the glutamatergic synapses formed

between the parallel fibers and Purkinje cell dendritic spines in the molecular layer because these axonal projections have pathfinding defects and defasciculation in the mutants at the same age-range examined in the present study. Moreover, the granule cells which extend those projections also have delayed migration throughout that age-range (Brackenbury et al., 2008, 2013). This observation might lead to the prediction that fewer parallel fiber synapses would have formed in the *Scn1b* molecular layer than in that of age-matched controls. Cultured cerebellar granule neurons express β1 protein at the axon growth cone, which potentially positions β1 pre-synaptically to interact with postsynaptic targets and play a role in cell-cell adhesion at points of contact (Brackenbury et al., 2010). Third, *Scn1b*-null mice, like contactin-null mice, have an apparent ataxic gait, which could correspond to defects in cerebellar development (E O Berglund et al., 1999). Thus, further investigation of the cerebellum was warranted by the behavioral phenotype exhibited by the mutants. Since Purkinje cell projections represent the only output from the massive circuitry of the cerebellar cortex, and all of the cell types that make up this circuit ultimately influence behavior by means of directly or indirectly acting through synapses with Purkinje cells, it follows that significant differences in the number of one or more classes of these synapses in *Scn1b*-null mutants could contribute to their ataxic gait. Fourth, the simple 3-layered structure and limited number of cell types that make up the cerebellar cortex provide advantages for experimental design. Previous *in vivo* studies have laid the groundwork for studying the various classes of synapses within this structure (Fritschy, 2006; E. M. Johnson, Craig, & Yeh, 2007; Qiao et al., 2013; K. Sakurai et al., 2009; B. Zhang et al., 2015). These studies have identified antibody markers, namely anti-Vglut1, anti-Vglut2, and anti-Vgat, which target distinct classes of presynaptic specializations. These markers label the excitatory parallel fiber synapses formed between granule cells and Purkinje cell dendritic spines, excitatory climbing fiber synapses which initially form on the somatic surface of Purkinje cells and subsequently translocate to the major dendritic branches of Purkinje cells, and the inhibitory synapses formed between stellate and basket cells in the molecular layer and Purkinje cells, respectively. This enables the isolation of distinct classes of synapses composed of known neuronal partners, and a number of researchers have previously taken advantage of this feature.

Our synaptosome-fractionation results strongly suggest that β1 protein is not expressed to a great extent at glutamatergic postsynaptic sites in the cerebellum. The vast majority of synaptically-enriched proteins isolated from the cerebellum should correspond to the excitatory synapses formed between parallel fibers and Purkinje cells. Purkinje cells receive thousands of these connections from the granule cells of the internal granule layer, which are the most densely-populated and numerous neurons in the brain. In contrast, GABAergic synapses, which are far fewer in number, would not be expected to be well represented in postsynaptic fractions collected from synaptosome preparations because they do not possess the insoluble PSD proteins which characterize these fractions. Thus, while it is likely that β1 is not highly present at glutamatergic synapses, we cannot yet make the conclusion that β1 is not enriched at GABAergic synapses, such as those formed between basket cells and Purkinje cell somata. Further, we know that β1 is strongly expressed at the Purkinje cell AIS and likely on the somatic surface, where it may be involved in post-synaptic functions (C. Chen et al., 2012; Kruger et al., 2016). The third class of synapses, those formed by the climbing fibers, would be expected to be represented in the synaptosome fractions enriched for PSD components. However, the relatively small number of climbing fiber synapses may be overwhelmed in the synaptosome preparation by the extremely high density of parallel fiber synapses that a specific expression of β1 at the postsynaptic membrane of climbing fiber synapses would not appear in the results of a Western blot experiment. Thus, we cannot conclude with any confidence that β1 is absent from climbing fiber synapses. With the future development of higher quality anti-β1 antibodies, immuno-EM experiments will be able to solve these important questions.

The expression of β1 protein at pre-synaptic membranes in the cerebellum remains undetermined. Evidence suggests that this is a strong possibility. Cultured CGNs express detectable levels of β1 at the axon growth cone, which would allow it to participate in homophilic or heterophilic adhesive interactions upon contact with a post-synaptic target (Brackenbury et al., 2010). Expression of β1 in axonal projections extended from granule cells *in vivo* is compellingly, though indirectly, indicated by the robust defasciculation visible in IHC-labeled parallel fibers (Brackenbury et al., 2008, 2013).

The inability of available antibodies to detect low or moderate concentrations of β subunit proteins by IHC presents a substantial experimental limitation. Current antibodies are only able to reliably show β1 at nodes of Ranvier and the AIS, where the protein is most densely expressed in neural tissue. A transgenic mouse line being generated in our lab expressing carboxyl-terminal V5 epitope-tagged β1 subunits will enable us to delineate the localization of this protein with much greater acuity than what has been possible up to this point (Chen and Isom, unpublished results). Such a mouse will allow for the dual-labeling of pre- and postsynaptic proteins with an anti-V5 antibody to determine with confidence whether β1 is present at these sites within neurons, including basket cells and Purkinje cells.

We compared the densities of all three classes of synapses formed with Purkinje cells in three separate lobules, lobule IV, lobule VI, and lobule VIII of postnatal *Scn1b*-null and wildtype mice, and found that there were no significant differences. It remains possible that *Scn1b*-encoded proteins have some impact on the formation of cerebellar synapses but that other, perhaps more consequential synaptic organizing molecules have dominant or redundant capacities. Moreover, a role for β1 in organizing or modulating the functional machinery of these synapses remains untested.

Of particular interest are the basket cell synapses that initially form on the somata and proximal dendritic arbors of the Purkinje cells and then subsequently move to construct the elaborate pinceau synapse that engulfs their target's AIS. Because β1 subunits are located at the Purkinje cell axon initial segment (Buffington & Rasband, 2013; C. Chen et al., 2012), pinceau synapses may be affected by *Scn1b* deletion. Importantly, the β1 binding partners neurofascin (McEwen et al., 2004), the VGSC α subunit NaV1.6 (Brackenbury et al., 2010), and the cytoskeletal adaptor protein ankyrin-G that regulates the targeting and formation of this special GABAergic synapse (Ango, di Cristo, et al., 2004; Buttermore et al., 2012) are enriched at the Purkinje cell AIS. Neurofascin, an Ig-CAM related to L1, is expressed in basket cell axonal projections as well as the somatic surface and AIS of developing Purkinje cells, where it coordinates the localization and formation of the pinceau synapse (Ango, di Cristo, et al., 2004; Buttermore et al., 2012). Due to early mortality of *Scn1b*-null mice, the pinceau synapse does not fully form in this model. This prevents us from characterizing the role that *Scn1b*-encoded

proteins may play in development of this synapse. Our recent experiments utilizing SLICK/ *Scn1b*$^{Flox/Flox}$ mice, injected with tamoxifen in young adulthood, result in severe phenotypes, including progressive motor abnormalities (Chen, Hull, and Isom, unpublished observations). Since this experimental model permits normal expression of β1 throughout the time period during which pinceau synapses form, it suggests that their improper development is not responsible for the ataxia that occurs in *Scn1b*-null mutants. Nevertheless, β1 may play an undiscovered role in the formation or maintenance of these synaptic complexes.

5. Scn1b in the function of the cerebellar cortex

It is not necessary for the number of apparent structural synapses to differ significantly between *Scn1b*-null mutants and wildtype littermates in order for there to be a direct or indirect function for β1/β1B at cerebellar synapses. β1/β1B may have roles in synaptic function without being necessary for their structural formation. Precedent for this is found in the Ig-CAM literature. For example, NCAM impacts the targeting of NMDA receptors and other PSD components (O. Bukalo, 2004; Muller et al., 1996). In addition, NMDA receptor-dependent forms of long-term potentiation (LTP) and long-term depression are impaired in some brain areas in NCAM-null mice (O. Bukalo, 2004; Muller et al., 1996). In terms of presynaptic function, NCAM-null mice have defects in some types of neurotransmitter release (Chan et al., 2005). These mutants also have deficits in paired-pulse facilitation (PPF), at least at neuromuscular junctions (Rafuse, Polo-Parada, & Landmesser, 2000). Researchers have observed impairment of LTP at selective perforant path synapses in the hippocampus of L1-null mice (Olena Bukalo & Dityatev, 2012). Mice deficient in the closely related CHL1, have reduced LTP in CA1 (Nikonenko et al., 2006). Contactin-null mice have selective defects that reflect the involvement of contactin in pre- as well as post-synaptic functions. These include impaired LTD in CA1 pyramidal neurons and impaired PPF mediated by AMPA receptors (Murai, Misner, & Ranscht, 2002). Thus, members of the Ig-superfamily of CAMs are widely involved in synaptic functions such as synaptic plasticity.

β1 may be necessary for the normal function of one or more classes of synapses that influence the behavior of Purkinje cells. This is one possible explanation for the reduced excitability seen in *Scn1b*-null Purkinje cell whole-cell recordings, and it is not inconsistent with other data we have collected. First, we found no difference in the number of parallel fiber, climbing fiber, or interneuronal synapses formed with Purkinje cells in wildtype and *Scn1b*-null cerebellar cortex. Secondly, our experiments in SLICK/ *Scn1b*$^{Flox/Flox}$ mice, injected with tamoxifen after postnatal development, could indicate a need for β1 at synapses to regulate their function without having a role in their formation.

Electrophysiological experiments designed to measure synaptic currents will help us to determine whether this is the case. Whole-cell voltage clamp recordings in wildtype and *Scn1b*-null Purkinje cells will be carried out in the presence of pharmacological agents to isolate spontaneous excitatory post-synaptic currents (EPSCs) and inhibitory post-synaptic currents (IPSCs). Specifically, spontaneous EPSCs will be measured in Purkinje cells in the presence of bicuculline in the external solution. The frequency of EPSCs will provide data with regard to the number of action potentials arriving at the presynaptic parallel fiber and climbing fiber terminals. The previous finding that *Scn1b*-null granule cells are hypo-excitable predicts a reduction in the frequency of spontaneous EPSCs in such experiments. However, the firing properties of inferior olive neurons which project the climbing fibers has never been examined. Spontaneous IPSCs will be measured in Purkinje cells in the presence of CNQX and APV to block glutamate-mediated synaptic responses. The finding that *Scn1b*-null molecular layer interneurons have a profoundly reduced capacity to fire action potentials predicts a reduction in the measured frequency of spontaneous IPSCs in *Scn1b*-null Purkinje cells. Reduced amplitude of these spontaneous post-synaptic currents might be caused by a reduction in neurotransmitter receptors situated at the post-synaptic membrane in the *Scn1b*-null Purkinje cells. This would suggest a potential new role for β1 in neuronal physiology. Miniature EPSCs (mEPSCs) and IPSCs (mIPSCs) will be measured in wildtype and *Scn1b*-null Purkinje cells by application of tetrodotoxin (TTX) to the external solution to block synaptic activity. The frequency of these currents provides an indication of the number of functional glutamatergic and GABAergic synapses, respectively. Our immunohistochemistry data strongly suggest that

Scn1b-null mice and wildtype littermate mice form comparable numbers of structural synapses between parallel fibers, climbing fibers, and interneurons and their target Purkinje cells. Thus, a reduction in the frequency of miniature post-synaptic currents could indicate that some of these synapses do not function normally in mice lacking *Scn1b*. Reduced amplitude of mEPSCs or mIPSCs in *Scn1b*-null Purkinje cells could correspond to a reduction in the relevant neurotransmitter receptors concentrated at the post-synaptic membrane.

NaV1.6 has been shown using immuno-EM techniques to be post-synaptically expressed at parallel fiber synapses in Purkinje cells (Caldwell et al., 2000). Because NaV1.6 channels are known to generate persistent sodium currents, their localization in the post-synapse would be expected to amplify local depolarizations resulting from excitatory synaptic activity. This expression could be reduced in or absent from *Scn1b*-null post-synaptic membranes. This would be in agreement with previous evidence of reduced NaV1.6 at the *Scn1b*-null Purkinje cell AIS (Brackenbury et al., 2010). A reduction in the amplitude of spontaneous EPSCs in *Scn1b*-null Purkinje cells would support, though not prove, this hypothesis. A change in the amplitude of mEPSCs would not be expected, however, because of the inclusion of TTX in the external solution. A reduction in both of these EPSC amplitudes might indicate an alternative explanation such as reduced AMPA receptors at the post-synapse. One possible explanation for this alternative result could be aberrant synaptic plasticity as a result of reduced backpropagation of action potentials into somato-dendritic cellular domains. Backpropagation would be expected to be adversely affected by a reduction in NaV1.6.

Parallel fiber-Purkinje cell synaptic plasticity may be important for motor learning. The principle EPSC caused by activity at these synapses is associated with AMPA receptors situated immediately opposite the active zone (Hoxha, Tempia, Lippiello, & Miniaci, 2016). Repeated action potentials arriving at the parallel fiber terminal is sufficient to activate NMDA receptors located nearby. This causes further depolarization and a local increase in Ca^{2+} concentration. Endocytotic mechanisms subsequently reduce AMPA receptor expression on the post-synaptic membrane, leading to LTD (Hoxha et al., 2016). Reduced post-synaptic NaV1.6 in *Scn1b*-null Purkinje cells might lead to a deficit in this function and decrease the cells' capacity for this type of synaptic plasticity. Insufficient backpropagation could further decrease this type of LTD.

Another possibility is that the hypo-excitability associated with *Scn1b* deletion occurs solely as a result of a failure in the proper localization or modulation of voltage-gated Na^+ channel α subunits at the Purkinje cell AIS. This site of action potential initiation requires a spatially and temporally ordered set of molecular components, including the $\beta 1$ binding partners, ankyrin-G and neurofascin (Ango, Di Cristo, et al., 2004; Buttermore et al., 2012; Grubb & Burrone, 2010). The scaffolding protein ankyrin-G is essential for the construction of the AIS (Grubb & Burrone, 2010). Mice with cerebellum-specific ankyrin-G deletion exhibited a disruption of VGSC and neurofascin localization to the Purkinje cell AIS. This resulted in reduced capacity to fire action potentials and an inability to maintain spontaneous bursting activity. Consequently, the mice presented with ataxia and tremor starting at P16 and progressing into adulthood (D. Zhou et al., 1998). Both $\beta 1$ and contactin are important for surface expression of VGSC α subunits (Kazarinova-Noyes et al., 2001; McEwen & Isom, 2004). In agreement with the phenotypes in other mutants, it is conceivable that *Scn1b*-null mice have hypo-excitable Purkinje cells due to a deficiency in the concentration of sodium channels at the AIS. Reduced expression of VGSC α subunits can be quantitatively measured using [^{3}H]-Saxitoxin binding. We recently measured a ~40% reduction in [^{3}H]-Saxitoxin binding in forebrain membranes collected from *Scn1b*-null mice (Hull, Jameson, and Isom, unpublished observations). Conducting [^{3}H]-Saxitoxin binding experiments using membranes collected from wildtype and *Scn1b*-null cerebellum will determine whether this reduction is also seen there, a result which seems probable. We have now seen that cerebellar granule cells, Purkinje cells, and molecular layer interneurons all have reduced excitability (Brackenbury et al., 2010, Figures 2.2-2.6). The density of VGSCs, especially at the AIS, could be sufficient to explain this. However, previous work has demonstrated that resurgent current remains intact in *Scn1b*-null Purkinje cells despite smaller sodium currents (Grieco et al., 2005). This would be expected to counteract the functional impact of reduced VGSC numbers at the AIS. Purkinje cells are massive in size, but their numbers are vastly lower than those of all other cerebellar neurons, especially granule cells, combined. Thus, I will propose a binding experiment later in this chapter that would illuminate the altered numbers of VGSCs to the Purkinje cells and provide valuable data for interpreting the reduced firing activity we have seen in these cells in *Scn1b*-

null cerebellar slices. A more complex mechanism may bear responsibility for hypo-excitability occurring in *Scn1b*-null Purkinje cells. For example, a switch in the relative prominence of specific α subunits, such as NaV1.1 and NaV1.6 could also contribute to a loss in excitability. A reduction in NaV1.6 and concomitant increase in NaV1.1 has been reported at the AIS of *Scn1b*-null Purkinje cells (Brackenbury et al., 2010). This could certainly be of consequence to Purkinje cell firing properties. But, immunohistochemistry is not a quantitative measure, and a comparison of relative immunoreactivity between different antibodies is difficult to extrapolate from. A consequent reduction in NaV1.6-mediated resurgent current, could also provide an explanation for the inability of a high number of *Scn1b*-null Purkinje cells to rapidly fire repeated action potentials. Recall for Chapter II that 12 out of 26 Purkinje cells we measured in *Scn1b*-null cerebellar slices failed to fire repetitively.

I propose two possible explanations for Purkinje cell hypo-excitability in *Scn1b*-null cerebellar slice recordings. First, reduced functionality in one or more classes of synapses which stimulate Purkinje cells could result in their incapacity to fire sufficient action potentials. Second, a reduction in the expression of VGSC α subunits at the Purkinje cell AIS could be the cause. These two possibilities are not mutually exclusive. Perhaps, the localization of NaV1.6 at both the AIS and at post-synaptic membranes relies on β1, at least in Purkinje cells. A concomitant increase in NaV1.1 might also be occurring at these domains, as suggested by previous immunohistochemistry results at the *Scn1b*-null Purkinje cell AIS (Brackenbury et al., 2010). A failure in backpropagation could impact synaptic plasticity and prevent strengthening of active glutamatergic synapses. Thus, *Scn1b*-null mice having reduced NaV1.6 expression throughout Purkinje cells could add up to a pronounced reduction in action potential frequency.

NaV1.6 and β1 are also highly concentrated at nodes of Ranvier in myelinated axons. An interesting and untested hypothesis is whether there are defects in Purkinje cell nodes of Ranvier, which could impact the velocity and reliability of action potentials projected to the deep cerebellar nuclei. If a common mechanism in *Scn1b*-null mice leads to reduced NaV1.6 at the Purkinje cell AIS and at post-synaptic sites, as I have suggested above, it is reasonable to propose that *Scn1b*-null Purkinje cell axon nodes of Ranvier might also show a reduced density

of NaV1.6 channels. *Scn1b*-null optic nerves have fewer nodes of Ranvier and reduced velocity of compound action potential propagation (C. Chen et al., 2004). This could also be the case for Purkinje cell axons. Together with the hypo-excitability of *Scn1b*-null Purkinje neurons, this could exacerbate the behavioral phenotype and lead to more pronounced ataxia and other deficits.

Genetic mutations which lead to changes in Purkinje cell firing, including some channelopathies, have been linked to ataxia in mouse models and human diseases (Rinaldo & Hansel, 2010). Two such channelopathies, spinocerebellar ataxia type 6 (SCA6) and episodic ataxia type 2 (EA2) both result from mutations affecting *CACNA1A*, a gene which encodes for the α-1A subunit of the P/Q-type voltage-gated calcium channel (Rinaldo & Hansel, 2010). Mouse models show that *CACNA1A* is strongly expressed in Purkinje cells, where its mutation results in marked changes in firing properties and motor deficits (Hoebeek et al., 2005). *CACNA1A*-null mutant mice showed an absence of P-type Ca^{2+} currents from Purkinje cells and both P- and Q-type currents from CGNs. In addition, they exhibited ataxia and dystonia and lived for less than 4 weeks (Jun et al., 1999). Some mutations known to impair Purkinje cell synaptic plasticity have also resulted in severely ataxic phenotypes (Rinaldo & Hansel, 2010). These include mice deficient in mGluR1 and βCaMKII (Aiba et al., 1994; van Woerden et al., 2009). Current clamp experiments measured in mouse brain slices show that *Scn1b*-null Purkinje cells are significantly hypo-excitable compared to age-matched wildtype controls, requiring much higher inputs of current to evoke action potentials and then evoking fewer of them (Figures 6.2-6.4). While the number of Purkinje cells is comparable between *Scn1b*-null mice and wildtype littermates (Table 2.1), this reduction in firing may be functionally comparable to other genetic mutants in which a large percentage of the Purkinje cells fail to develop or succumb to degeneration. Whether the cause is reduced cell numbers, abnormal firing patterns, or reduced firing, the cellular targets of Purkinje cell projections in the deep cerebellar nuclei are predicted to receive abnormal signals from the cerebellar cortex that would predict dysfunction in behavioral phenotypes. A reduction in the concentration of NaV1.6 across *Scn1b*-null Purkinje cell domains, resulting in decreased synaptic strength due to smaller depolarization and failed backpropagation, increased threshold to fire action potentials

at the AIS, and sluggish or unreliable saltatory conduction along the axons, could ultimately lead to a heavy loss of Purkinje cell function comparable in severity to mutations with diminished Purkinje cell survival. Deficits in Purkinje cell function, rather than micro-organization defects in the cerebellar cortex, might represent the most parsimonious explanation for cerebellum-associated behavioral phenotypes in the mutants.

6. Cerebellar dysfunction in SCN1B-linked epileptic encephalopathy

The vast majority of cases of Dravet syndrome are linked to haploinsufficiency in *SCN1A*, the gene encoding the α subunit NaV1.1 (L Claes et al., 2001; A Escayg et al., 2000; Meisler & Kearney, 2005; Shi et al., 2009; Sugawara et al., 2001). Loss-of-function of both copies of *SCN1B* has also been shown to cause Dravet syndrome (Ogiwara et al., 2012; Patino et al., 2009). Thus, *Scn1b*-null mice are a model of severe pediatric epileptic encephalopathy, which is clinically diagnosed as Dravet syndrome (O'Malley & Isom, 2015; Ogiwara et al., 2012; Patino et al., 2009). Children with Dravet syndrome often present initially with febrile seizures in the first years of infancy then progress to afebrile seizures and status epilepticus (Surges & Sander, 2012). Extreme cognitive decline often appears around the second year of life (Scheffer, 2012). Ataxia begins in children around nine years old and progresses with age (Scheffer, 2012; Surges & Sander, 2012). Gait abnormalities and a characteristic crouch have been described as Parkinsonian in nature, and cerebellar involvement is questioned (Scheffer, 2012). However, only *SCN1A*- and not *SCN1B*-linked epileptic encephalopathy was included in this clinical characterization. Two cases of *SCN1B*-linked Dravet syndrome have been reported in the literature (Ogiwara et al., 2012; Patino et al., 2009) with two additional cases soon to be reported by our lab. The first case presented early with developmental deterioration and death at just 13 months of age (Patino et al., 2009). In the second case, the patient showed seizure onset at just 6 months of age along with developmental stagnation. At 4 years of age, the patient was reportedly ataxic (Ogiwara et al., 2012). The *Scn1b*-null mouse has a substantially more severe phenotype than *Scn1a* +/- mice, which model the more common genetic cause of disease (C. Chen et al., 2004; Lieve Claes et al., 2003; Fukuma et al., 2004; Sugawara et al.,

2002). *Scna1* +/- Dravet syndrome model mice have reduced firing in Purkinje cells and a mild ataxic phenotype at P21 (Kalume, Yu, Westenbroek, Scheuer, & Catterall, 2007). Perhaps in this mutant, like in patients, the ataxic gait is a progressive phenomenon that would worsen with age.

Evidence has mounted in recent years supporting the importance of the cerebellum in a variety of cognitive functions, including language perception, temporal ordering, implicit memory, and visuospatial attention (Noroozian, 2014). The cerebral cortex sends more projections to the cerebellum than to any other area of the nervous system, and projections from the deep cerebellar nuclei interact, mainly via the thalamus, with cerebral cortical areas beyond just motor areas. These areas include the prefrontal cortex, medial frontal cortex, anterior cingulate cortex, superior temporal cortex, and parietal cortex (Dolan, 1998; Middleton & Strick, 1997). Furthermore, a number of hereditary ataxia disorders, including types of SCA, have symptoms of cognitive dysfunction (Bürk, 2007). Systematic study of a variety of diseases limited to lesions of the cerebellum, especially the posterior cerebellum, led to the discovery of what researchers termed cerebellar cognitive affective syndrome, which is characterized by dysregulation in executive functions such as planning and abstract reasoning, spatial cognition, language processing, and regulation of affect. The features of this syndrome were noted, for example, in a study of children with cerebellar tumor resection (Levisohn, Cronin-Golomb, & Schmahmann, 2000). These findings suggest that disruption of connections between the cerebellum and cerebral cortical areas associated with cognitive functions causes selective deficits that implicate an important role for the cerebellum (Noroozian, 2014). Autism spectrum disorder is widely understood to involve altered connectivity between brain regions, including the cerebellum where abnormalities are seen in neuroimaging studies, animal models, and post-mortem human brains (Becker & Stoodley, 2013). Also, damage to the cerebellum during early development has been linked to symptoms of autism (Crippa et al., 2016). Studies have also highlighted abnormalities in this brain structure in attention deficit hyperactivity disorder, showing reduced cerebellar volume as well as alterations in structural and functional cerebellar connectivity (D'Mello & Stoodley, 2015). Perhaps most significantly, there is clinical evidence for a cerebellar role in neurological and neuropsychological

examination of patients with Dravet syndrome. Cognitive defects detected in Dravet syndrome patients include many which are thought to involve the cerebellum, including in the expression of language, executive functions, and visual-spatial organization (Battaglia et al., 2013). Of note, autistic features and hyperactivity are common behavioral characteristics of Dravet syndrome (Guzzetta, 2011). Furthermore, along with ataxia, cerebellar symptoms including intention tremor, eye movement disorder, and motor speech problems, worsen as Dravet syndrome patients grow into adolescence and adulthood. These symptoms progress even as the incidence of seizures levels off or improves (Genton, Velizarova, & Dravet, 2011). Finally, there is evidence for cerebellar modulation of hippocampal seizures (Krook-Magnuson et al., 2014). There are direct connections between the hippocampus and cerebellum, and recent evidence demonstrates cerebellar involvement in hippocampal processing (Rochefort, Arabo, André, et al., 2011; J. C. Wong & Escayg, 2015). In conclusion, there is sufficient experimental and clinical justification for considering an important cerebellar role in epileptic encephalopathies, including Dravet syndrome. Further research is warranted to examine the potential link between cerebellar dysfunction and the range of pathological phenotypes associated with *SCN1B* mutations.

7. Future directions

Using a transgenic approach to restrict the deletion of *Scn1b* to Purkinje cells, by means of the well characterized Purkinje cell-specific *Pcp2/L7*-Cre mouse line would be highly informative in delineating the contributions of cerebellar dysfunction to the pathological phenotypes modeled in the *Scn1b*-null mouse (Oberdick et al., 2016; Vandaele et al., 1991). It is unlikely that *Pcp2/L7*-Cre/*Scn1b*$^{Flox/Flox}$ mice would exhibit spontaneous seizures or die prior to reaching adulthood. This would permit the examination of a number of significant comorbidities seen in epileptic encephalopathies such as Dravet syndrome. Most obviously, the controversy over the cerebellar nature of the ataxia and tremor could be addressed directly. We limited our ataxia study in *Scn1b*-null mice to footprint analysis of gait because the mutants are small in size, have frequent seizures, and do not survive past ~P21 (C. Chen et al.,

2004). More sophisticated methods such as vertical grid, rotorod, suspended wire, and stationary beam tests, which measure latency to fall, would be much more feasible in *Pcp2/L7*-Cre/*Scn1b*$^{Flox/Flox}$ mice, permitting a more thorough characterization (Lalonde & Strazielle, 2007). Moreover, these phenotypes could be examined at different ages ranging into adulthood. In Dravet syndrome patients, ataxia and cognitive symptoms progress with age starting as children and worsening in adolescence. Behavioral analyses designed to measure cognitive and affective functions would likely be feasible in *Pcp2/L7*-Cre/*Scn1b*$^{Flox/Flox}$ mice, as well, allowing the examination of cerebellar contributions to these symptoms. Examples might include novel object recognition and Morris water maze tests to examine memory, open field and elevated plus maze tests to examine anxiety and activity levels, and approach and avoidance tests to examine social behaviors. By contrast, *Scn1b*-null mice are not healthy enough and do not live long enough for those kinds of experiments. Finally, seizure-susceptibility could be compared between *Pcp2/L7*-Cre/*Scn1b*$^{Flox/Flox}$ and control mice using pharmacological challenges such as kainite, electrical-stimulation, or hyperthermia challenge. These experiments would help determine the contribution of cerebellar dysfunction to this aspect of *SCN1B*-linked epileptic encephalopathy. Since the *Pcp2/L7* promoter is limited in expression to Purkinje cells (Oberdick et al., 2016; Vandaele et al., 1991), the cell-autonomy of developmental and functional properties could be evaluated. [^{3}H]-Saxitoxin binding would permit the evaluation of VGSC a subunit expression in Purkinje cells alone, in order to determine the degree of reduction in these cells. Immuno-EM experiments would permit the evaluation of NaV1.6 localization and expression, in particular. These data would indicate whether loss of *Scn1b* in Purkinje cells results in loss or depletion of NaV1.6 at the AIS, somato-dendritic regions, post-synaptic membranes, and nodes of Ranvier. With regard to expected outcomes, I predict that *Pcp2/L7*-Cre/*Scn1b*$^{Flox/Flox}$ mice would have a comparable lifespan to control animals, exhibit ataxia and selective behavioral abnormalities reflecting cerebellum-dependent cognitive functions such as working memory and hyperactivity and, potentially, a modest increase in seizure susceptibility. I further expect that Purkinje cells would exhibit reduced [^{3}H]-Saxitoxin binding, implicating a decrease in VGSCs in their hypo-excitability. I also anticipate a reduction in NaV1.6 across Purkinje cell domains. This animal model would have

the potential to provide valuable new insights into the mechanisms of *SCN1B*-linked Dravet syndrome and related epileptic encephalopathies, including the spectrum of comorbid symptoms that these disorders manifest.

8. Conclusions

This chapter provides a comprehensive overview of the known cerebellar defects associated with *Scn1b* deletion. Genetic mutations leading to the disruption of cerebellar cortical organization, cellular development and longevity, synaptic connectivity and plasticity, and Purkinje cell intrinsic excitability all converge on motor coordination problems in mice. The cerebellum is now understood to modulate cognition as well. The experimental evidence along with the severe comorbid symptoms observed in epileptic encephalopathies compels researchers who wish to understand their mechanisms to strongly consider a role for the cerebellum. Toward this end, I have proposed a practical next step toward achieving this goal, at least with regard to *SCN1B*. A closer look at the cerebellum may yet lead to valuable and unexpected insights into the catastrophic pathophysiology of these syndromes.

Bibliography

Adams, M. D., Celniker, S. E., Holt, R. a, Evans, C. a, Gocayne, J. D., Amanatides, P. G., … Venter, J. C. (2000). The genome sequence of Drosophila melanogaster. *Science (New York, N.Y.)*, *287*(5461), 2185–2195. https://doi.org/10.1126/science.287.5461.2185

Aiba, A., Kano, M., Chen, C., Stanton, M. E., Fox, G. D., Herrup, K., … Tonegawa, S. (1994). Deficient cerebellar long-term depression and impaie\red motor learning in mGluR1 mutant mice. *Cell*, *79*, 377–388.

Alföldi, J., Di Palma, F., Grabherr, M., Williams, C., Kong, L., Mauceli, E., … Lindblad-Toh, K. (2011). The genome of the green anole lizard and a comparative analysis with birds and mammals. *Nature*, *477*(7366), 587–591. https://doi.org/10.1038/nature10390

Altman, J. (1972). Postnatal Development of the Cerebellar Cortex in the R a t. *Journal of Comparative Neurology*, *145*, 353–398.

Altman, J., & Bayer, S. (1997). *Development of the Cerebellar System in Relation to its Evolution, Structure, and Functions*. New York: CRC Press.

Aman, T. K., Grieco-Calub, T. M., Chen, C., Rusconi, R., Slat, E. a, Isom, L. L., & Raman, I. M. (2009). Regulation of persistent Na current by interactions between beta subunits of voltage-gated Na channels. *The Journal of Neuroscience : The Official Journal of the Society for Neuroscience*, *29*(7), 2027–2042. https://doi.org/10.1523/JNEUROSCI.4531-08.2009

Amemiya, C. T., Alföldi, J., Lee, A. P., Fan, S., Philippe, H., Maccallum, I., … Lindblad-Toh, K. (2013). The African coelacanth genome provides insights into tetrapod evolution. *Nature*, *496*(7445), 311–6. https://doi.org/10.1038/nature12027

Andrikopoulos, P., Fraser, S. P., Patterson, L., Ahmad, Z., Burcu, H., Ottaviani, D., … Djamgoz, M. B. a. (2011). Angiogenic functions of voltage-gated Na+ channels in human endothelial cells: Modulation of vascular endothelial growth factor (VEGF) signaling. *Journal of Biological Chemistry*, *286*(19), 16846–16860. https://doi.org/10.1074/jbc.M110.187559

Ango, F., di Cristo, G., Higashiyama, H., Bennett, V., Wu, P., & Huang, Z. J. (2004). Ankyrin-based subcellular gradient of neurofascin, an immunoglobulin family protein, directs GABAergic innervation at purkinje axon initial segment. *Cell*, *119*(2), 257–72. https://doi.org/10.1016/j.cell.2004.10.004

Ango, F., Di Cristo, G., Higashiyama, H., Bennett, V., Wu, P., & Huang, Z. J. (2004). Ankyrin-based subcellular gradient of neurofascin, an immunoglobulin family protein, directs GABAergic innervation at Purkinje axon initial segment. *Cell*, *119*(2), 257–272. https://doi.org/10.1016/j.cell.2004.10.004

Apps, R., & Garwicz, M. (2005). Anatomical and physiological foundations of cerebellar information processing. *Nature Reviews Neuroscience*, *6*(4), 297–311. https://doi.org/10.1038/nrn1646

Aronica, E., Troost, D., Rozemuller, A. J., Yankaya, B., Jansen, G. H., Isom, L. L., & Gorter, J. a. (2003). Expression and regulation of voltage-gated sodium channel beta1 subunit protein in human gliosis-associated pathologies. *Acta Neuropathologica*, *105*(5), 515–23. https://doi.org/10.1007/s00401-003-0677-2

Audenaert, D., Claes, L., Ceulemans, B., Löfgren, a, Van Broeckhoven, C., & De Jonghe, P. (2003). A deletion in SCN1B is associated with febrile seizures and early-onset absence epilepsy. *Neurology*, *61*(6), 854–856. https://doi.org/10.1212/01.WNL.0000080362.55784.1C

Auld, V. J., Goldin, a L., Krafte, D. S., Marshall, J., Dunn, J. M., Catterall, W. a, … Dunn, R. J. (1988). A rat brain Na+ channel alpha subunit with novel gating properties. *Neuron*, *1*(6), 449–461. https://doi.org/10.1016/0896-6273(88)90176-6

Azumi, K., De Santis, R., De Tomaso, A., Rigoutsos, I., Yoshizaki, F., Pinto, M. R., … Nonaka, M. (2003). Genomic analysis of immunity in a Urochordate and the emergence of the vertebrate immune system: "waiting for Godot." *Immunogenetics*, *55*(8), 570–581. https://doi.org/10.1007/s00251-003-0606-5

Bant, J. S., & Raman, I. M. (2010). Control of transient, resurgent, and persistent current by open-channel block by Na channel beta4 in cultured cerebellar granule neurons. *Proceedings of the National Academy of Sciences of the United States of America*, *107*(27), 12357–12362. https://doi.org/10.1073/pnas.1005633107

Battaglia, D., Chieffo, D., Siracusano, R., Waure, C. de, Brogna, C., Ranalli, D., … Guzzetta, F. (2013). Cognitive decline in Dravet syndrome: Is there a cerebellar role? *Epilepsy Research*, *106*(1–2), 211–221. https://doi.org/10.1016/j.eplepsyres.2013.03.012

Bayer, S., & Altman, J. (1987). Directions in neurogenetic gradients and patterns of anatomical connections in the telencephalon. *Prog. Nerobiol.*, *29*, 57–106.

Bean, B. P. (2005). Progress in realizing the promise of microarrays in systems neurobiology. *Neuron*, *45*(2), 183–185. https://doi.org/10.1016/j.neuron.2005.01.007

Becker, E. B. E., & Stoodley, C. J. (2013). *Autism spectrum disorder and the cerebellum*. *International Review of Neurobiology* (1st ed., Vol. 113). Elsevier Inc. https://doi.org/10.1016/B978-0-12-418700-9.00001-0

Beckers, M.-C., Bar, I., Huynh-Thu, T., Dernoncourt, C., Brunialti, A. L., Montagutelli, X., … Goffinet, A. M. (1994). A High-Resolution Genetic Map of Mouse Chromosome 5 Encompassing the Reeler (rl) Locus. *Genomics*, *23*, 685–690.

Beneski, D. a, & Catterall, W. a. (1980). Covalent labeling of protein components of the sodium channel with a photoactivable derivative of scorpion toxin. *Proceedings of the National Academy of Sciences of the United States of America*, *77*(1), 639–643. https://doi.org/10.1073/pnas.77.1.639

Bennett, P. B., Makita, N., & George, a L. (1993). A molecular basis for gating mode transitions in human skeletal muscle Na+ channels. *FEBS Letters*, *326*(1–3), 21–24.

https://doi.org/10.1016/0014-5793(93)81752-L

Berglund, E. O., Murai, K. K., Fredette, B., Sekerková, G., Marturano, B., Weber, L., … Ranscht, B. (1999). Ataxia and abnormal cerebellar microorganization in mice with ablated contactin gene expression. *Neuron*, *24*(3), 739–750. https://doi.org/10.1016/S0896-6273(00)81126-5

Berglund, E. O., & Ranscht, B. (1994). Molecular Cloning and in Situ Localization of the Human Contactin Gene (CNTN1) on Chromosome 12q11-q12. *Genomics*, *21*, 571–582.

Brackenbury, W. J., Calhoun, J. D., Chen, C., Miyazaki, H., Nukina, N., Oyama, F., … Isom, L. L. (2010). Functional reciprocity between Na+ channel Nav1.6 and beta1 subunits in the coordinated regulation of excitability and neurite outgrowth. *Proceedings of the National Academy of Sciences of the United States of America*, *107*(5), 2283–8. https://doi.org/10.1073/pnas.0909434107

Brackenbury, W. J., Davis, T. H., Chen, C., Slat, E. a, Detrow, M. J., Dickendesher, T. L., … Isom, L. L. (2008). Voltage-gated Na+ channel beta1 subunit-mediated neurite outgrowth requires Fyn kinase and contributes to postnatal CNS development in vivo. *The Journal of Neuroscience : The Official Journal of the Society for Neuroscience*, *28*(12), 3246–56. https://doi.org/10.1523/JNEUROSCI.5446-07.2008

Brackenbury, W. J., & Isom, L. L. (2011a). Na+ channel β subunits: Overachievers of the ion channel family. *Frontiers in Pharmacology*, *2*, 1–11. https://doi.org/10.3389/fphar.2011.00053

Brackenbury, W. J., & Isom, L. L. (2011b). Na Channel β Subunits: Overachievers of the Ion Channel Family. *Frontiers in Pharmacology*, *2*(September), 53. https://doi.org/10.3389/fphar.2011.00053

Brackenbury, W. J., Yuan, Y., O'Malley, H. a, Parent, J. M., & Isom, L. L. (2013). Abnormal neuronal patterning occurs during early postnatal brain development of Scn1b-null mice and precedes hyperexcitability. *Proceedings of the National Academy of Sciences of the United States of America*, *110*(3), 1089–94. https://doi.org/10.1073/pnas.1208767110

Brette, F., & Orchard, C. (2003). T-tubule function in mammalian cardiac myocytes. *Circulation Research*, *92*(11), 1182–1192. https://doi.org/10.1161/01.RES.0000074908.17214.FD

Brümmendorf, T., Michael Wolff, J., Frank, R., & Rathjen, F. G. (1989). Neural cell recognition molecule F11: Homology with fibronectin type III and immunoglobulin type C domains. *Neuron*, *2*(4), 1351–1361. https://doi.org/10.1016/0896-6273(89)90073-1

Buffington, S. a, & Rasband, M. N. (2013). Na+ channel-dependent recruitment of Navβ4 to axon initial segments and nodes of Ranvier. *The Journal of Neuroscience : The Official Journal of the Society for Neuroscience*, *33*(14), 6191–202. https://doi.org/10.1523/JNEUROSCI.4051-12.2013

Bukalo, O. (2004). Conditional Ablation of the Neural Cell Adhesion Molecule Reduces Precision of Spatial Learning, Long-Term Potentiation, and Depression in the CA1 Subfield of Mouse

Hippocampus. *Journal of Neuroscience*, *24*(7), 1565–1577. https://doi.org/10.1523/JNEUROSCI.3298-03.2004

Bukalo, O., & Dityatev, A. (2012). *Synaptic Plasticity*. (M. R. Kreutz & C. Sala, Eds.) (Vol. 970). Vienna: Springer Vienna. https://doi.org/10.1007/978-3-7091-0932-8

Burgess, D. L., Kohrman, D. C., Galt, J., Plummer, N. W., Jones, J. M., Spear, B., & Meisler, M. H. (1995). Mutation of a new sodium channel gene, Scn8a, in the mouse mutant "motor endplate disease." *Nature Genetics*, *10*, 196–201.

Bürk, K. (2007). Cognition in hereditary ataxia. *Cerebellum (London, England)*, *6*(3), 280–286. https://doi.org/10.1080/14734220601115924

Burright, E. N., Brent Clark, H., Servadio, A., Matilla, T., Feddersen, R. M., Yunis, W. S., … Orr, H. T. (1995). SCA1 transgenic mice: A model for neurodegeneration caused by an expanded CAG trinucleotide repeat. *Cell*, *82*(6), 937–948. https://doi.org/10.1016/0092-8674(95)90273-2

Buttermore, E. D., Piochon, C., Wallace, M. L., Philpot, B. D., Hansel, C., & Bhat, M. a. (2012). Pinceau organization in the cerebellum requires distinct functions of neurofascin in Purkinje and basket neurons during postnatal development. *The Journal of Neuroscience : The Official Journal of the Society for Neuroscience*, *32*(14), 4724–42. https://doi.org/10.1523/JNEUROSCI.5602-11.2012

Buttiglione, M., Revest, J. M., Pavlou, O., Karagogeos, D., Furley, a, Rougon, G., & Faivre-Sarrailh, C. (1998). A functional interaction between the neuronal adhesion molecules TAG-1 and F3 modulates neurite outgrowth and fasciculation of cerebellar granule cells. *The Journal of Neuroscience : The Official Journal of the Society for Neuroscience*, *18*(17), 6853–6870.

Caddy, K., & Biscoe, T. (1979). Structural and quantitative studies on the normal C3H and Lurcher mutant mouse. *Philos. Trans. R. Soc. London*, *287*, 167–201.

Cahoy, J. D., Emery, B., Kaushal, a., Foo, L. C., Zamanian, J. L., Christopherson, K. S., … Barres, B. a. (2008). A Transcriptome Database for Astrocytes, Neurons, and Oligodendrocytes: A New Resource for Understanding Brain Development and Function. *Journal of Neuroscience*, *28*(1), 264–278. https://doi.org/10.1523/JNEUROSCI.4178-07.2008

Caldwell, J. H., Schaller, K. L., Lasher, R. S., Peles, E., & Levinson, S. R. (2000). Sodium channel Na(v)1.6 is localized at nodes of ranvier, dendrites, and synapses. *Proceedings of the National Academy of Sciences of the United States of America*, *97*(10), 5616–5620. https://doi.org/10.1073/pnas.090034797

Calhoun, J. D., & Isom, L. L. (2014). The Role of Non-pore-Forming b subunits in Physiology and Pathophysiology of Voltage-Gated Sodium Channels. In *Voltage-Gated Sodium Channels* (Vol. 221, pp. 111–135). https://doi.org/10.1007/978-3-642-41588-3

Catterall, W. A. (2000). From ionic currents to molecular mechanisms: the structure and function of voltage-gated sodium channels. *Neuron*, *26*(1), 13–25.

https://doi.org/10.1016/s0896-6273(00)81133-2

Caviness Jr, V. S., & Rakic, P. (1978). Mechanisms of Cortical Development: a View from Mutations in Mice. *Ann. Rev. Neuroscience*, *1*(Table 1), 297–326. https://doi.org/10.1146/annurev.ne.01.030178.001501

Chen, C., Bharucha, V., Chen, Y., Westenbroek, R. E., Brown, A., Malhotra, J. D., … Isom, L. L. (2002). Reduced sodium channel density, altered voltage dependence of inactivation, and increased susceptibility to seizures in mice lacking sodium channel beta 2-subunits. *Proceedings of the National Academy of Sciences of the United States of America*, *99*(26), 17072–17077. https://doi.org/10.1073/pnas.212638099

Chen, C., Calhoun, J. D., Zhang, Y., Lopez-Santiago, L., Zhou, N., Davis, T. H., … Isom, L. L. (2012). Identification of the cysteine residue responsible for disulfide linkage of Na+ channel α and β2 subunits. *Journal of Biological Chemistry*, *287*(46), 39061–39069. https://doi.org/10.1074/jbc.M112.397646

Chen, C., Westenbroek, R. E., Xu, X., Edwards, C. a, Sorenson, D. R., Chen, Y., … Isom, L. L. (2004). Mice lacking sodium channel beta1 subunits display defects in neuronal excitability, sodium channel expression, and nodal architecture. *The Journal of Neuroscience : The Official Journal of the Society for Neuroscience*, *24*(16), 4030–42. https://doi.org/10.1523/JNEUROSCI.4139-03.2004

Chen, Y., Yu, F. H., Sharp, E. M., Beacham, D., Scheuer, T., & Catterall, W. a. (2008). Functional properties and differential neuromodulation of Nav1.6 channels. *Molecular and Cellular Neuroscience*, *38*(4), 607–615. https://doi.org/10.1016/j.mcn.2008.05.009

Chioni, A.-M., Brackenbury, W. J., Calhoun, J. D., Isom, L. L., & Djamgoz, M. B. a. (2009). A novel adhesion molecule in human breast cancer cells: voltage-gated Na+ channel beta1 subunit. *The International Journal of Biochemistry & Cell Biology*, *41*(5), 1216–1227. https://doi.org/10.1016/j.biocel.2008.11.001

Chopra, S. S., Watanabe, H., Zhong, T. P., & Roden, D. M. (2007). Molecular cloning and analysis of zebrafish voltage-gated sodium channel beta subunit genes: implications for the evolution of electrical signaling in vertebrates. *BMC Evolutionary Biology*, *7*, 113. https://doi.org/10.1186/1471-2148-7-113

Cingolani, L. A., Gymnopoulos, M., Boccaccio, A., Stocker, M., & Pedarzani, P. (2002). Developmental regulation of small-conductance Ca2+-activated K+ channel expression and function in rat Purkinje neurons. *J Neurosci*, *22*(11), 4456–4467. https://doi.org/20026415

Claes, L., Ceulemans, B., Audenaert, D., Smets, K., Löfgren, A., Del-Favero, J., … De Jonghe, P. (2003). De novo SCN1A mutations are a major cause of severe myoclonic epilepsy of infancy. *Human Mutation*, *21*(6), 615–621. https://doi.org/10.1002/humu.10217

Claes, L., Del-Favero, J., Ceulemans, B., Lagae, L., Van Broeckhoven, C., & De Jonghe, P. (2001). De novo mutations in the sodium-channel gene SCN1A cause severe myoclonic epilepsy of infancy. *American Journal of Human Genetics*, *68*(6), 1327–1332.

https://doi.org/10.1086/320609

Clark, H. B., & Orr, H. T. (2000). Spinocerebellar ataxia type 1--modeling the pathogenesis of a polyglutamine neurodegenerative disorder in transgenic mice. *Journal of Neuropathology and Experimental Neurology*, *59*(4), 265–270.

Clark, H., Burright, E., Yunis, W., Larson, S., Wilcox, C., Hartman, B., … Orr, H. (1997). Purkinje cell expression of a mutant allele of SCA1 in transgenic mice leads to disparate effects on motor behaviors, followed by a progressive cerebellar dysfunction and histological alterations. *The Journal of Neuroscience : The Official Journal of the Society for Neuroscience*, *17*(19), 7385–7395. Retrieved from http://www.ncbi.nlm.nih.gov/pubmed/9295384%5Cnhttp://discovery.ucl.ac.uk/184549/

Crepel, F. (1972). Maturation of the cerebellar Purkinje cells I. Postnatal evolution of the Purkinje cell spontaneous firing in the rat. *Experimental Brain Research*, *14*, 463–471.

Crippa, A., Del Vecchio, G., Ceccarelli, S. B., Nobile, M., Arrigoni, F., & Brambilla, P. (2016). Cortico-cerebellar connectivity in Autism Spectrum Disorder: What do we know so far? *Frontiers in Psychiatry*, *7*(FEB), 1–7. https://doi.org/10.3389/fpsyt.2016.00020

Crossin, K. L., & Krushel, L. A. (2000). Cellular Signaling by Neural Cell Adhesion Molecules of the Immunoglobulin Superfamily. *Developmental Dynamics*, *279*(January), 260–279.

Cummins, T. R., Dib-Hajj, S. D., Herzog, R. I., & Waxman, S. G. (2005). Nav1.6 channels generate resurgent sodium currents in spinal sensory neurons. *FEBS Letters*, *579*(10), 2166–2170. https://doi.org/10.1016/j.febslet.2005.03.009

D'arcangelo, G., Miao, G. G., Chen, S.-C., Soares, H. D., Morgan, J. I., & Curran, T. (1995). A protein related to extracellular matrix proteins deleted in the mouse mutant reeler. *Nature*, *374*, 719–723.

D'Mello, A. M., & Stoodley, C. J. (2015). Cerebro-cerebellar circuits in autism spectrum disorder. *Frontiers in Neuroscience*, *9*(NOV). https://doi.org/10.3389/fnins.2015.00408

Davis, T. H., Chen, C., & Isom, L. L. (2004). Sodium channel beta1 subunits promote neurite outgrowth in cerebellar granule neurons. *The Journal of Biological Chemistry*, *279*(49), 51424–32. https://doi.org/10.1074/jbc.M410830200

De Zeeuw, C. I., Hoebeek, F. E., Bosman, L. W. J., Schonewille, M., Witter, L., & Koekkoek, S. K. (2011). Spatiotemporal firing patterns in the cerebellum. *Nature Reviews Neuroscience*, *12*(6), 327–344. https://doi.org/10.1038/nrn3011

Deschenes, I., & Tomaselli., G. F. (2002). Modulation of Kv4 . 3 current by accessory subunits. *FEBS Letters*, *528*, 183–188.

Diss, J. K. J., Fraser, S. P., Walker, M. M., Patel, a, Latchman, D. S., & Djamgoz, M. B. a. (2008). Beta-subunits of voltage-gated sodium channels in human prostate cancer: quantitative in vitro and in vivo analyses of mRNA expression. *Prostate Cancer and Prostatic Diseases*, *11*(4), 325–333. https://doi.org/10.1038/sj.pcan.4501012

Dityatev, A., Dityateva, G., & Schachner, M. (2000). Synaptic Strength as a Function of Post- versus Presynaptic Expression of the Neural Cell Adhesion Molecule NCAM. *Neuron*, *26*(1), 207–217. https://doi.org/10.1016/S0896-6273(00)81151-4

Dolan, R. J. (1998). A cognitive affective role for the cerebellum [editorial; comment]. *Brain*, *121*(Pt 4), 545–546.

Dravet, C., Bureau, M., Oguni, H., Fukuyama, Y., & Cokar, O. (2005). Severe myoclonic epilepsy in infancy: Dravet syndrome. *Advances in Neurology*, *95*, 71–102. Retrieved from http://www.ncbi.nlm.nih.gov/entrez/query.fcgi?cmd=Retrieve&db=PubMed&dopt=Citation&list_uids=15508915

Du Pasquier, L., Zucchetti, I., & De Santis, R. (2004). Immunoglobulin superfamily receptors in protochordates: Before RAG time. *Immunological Reviews*, *198*, 233–248. https://doi.org/10.1111/j.0105-2896.2004.00122.x

Durbec, P., Gennarini, G., Goridis, C., & Rougon, G. (1992). A soluble form of the F3 neuronal cell adhesion molecule promotes neurite outgrowth. *J Cell Biol*, *117*(4), 877–887. Retrieved from http://www.ncbi.nlm.nih.gov/entrez/query.fcgi?cmd=Retrieve&db=PubMed&dopt=Citation&list_uids=1315782

Eccles, J. C. (1967). Circuits in the cerebellar conrtol of movement. *Physiology*, *58*.

Eisenberg, B., & Messer, A. (1989). Tonic/clonic seizures in a mouse mutant carrying the weaver gene. *Neuroscience Letters*, *96*(2), 168–172. https://doi.org/10.1016/0304-3940(89)90052-9

Escayg, A., & Goldin, A. L. (2010). Sodium channel SCN1A and epilepsy: mutations and mechanisms. *Epilepsia*, *51*(9), 1650–1658. Retrieved from http://www.pubmedcentral.nih.gov/articlerender.fcgi?artid=2937162&tool=pmcentrez&rendertype=abstract

Escayg, A., MacDonald, B., Meisler, M., Baulac, S., Huberfeld, G., An-Gourfinkel, I., … Malafosse, A. (2000). Mutations of SCN1A, encoding a neuronal sodium channel, in two families with GEFS+2. *Nature Genetics*, *24*(4), 343–345. https://doi.org/10.1111/j.1095-8649.2006.01157.x

Faivre-Sarrailh, C., Gennarini, G., Goridis, C., & Rougon, G. (1992). F3/F11 cell surface molecule expression in the developing mouse cerebellum is polarized at synaptic sites and within granule cells. *The Journal of Neuroscience : The Official Journal of the Society for Neuroscience*, *12*(1), 257–67. Retrieved from http://www.ncbi.nlm.nih.gov/pubmed/1729438

Fein, A. J., Meadows, L. S., Chen, C., Slat, E. a, & Isom, L. L. (2007). Cloning and expression of a zebrafish SCN1B ortholog and identification of a species-specific splice variant. *BMC Genomics*, *8*, 226. https://doi.org/10.1186/1471-2164-8-226

Fein, A. J., Wright, M. a, Slat, E. a, Ribera, A. B., & Isom, L. L. (2008). scn1bb, a zebrafish ortholog

of SCN1B expressed in excitable and nonexcitable cells, affects motor neuron axon morphology and touch sensitivity. *The Journal of Neuroscience : The Official Journal of the Society for Neuroscience*, *28*(47), 12510–12522. https://doi.org/10.1523/JNEUROSCI.4329-08.2008

Filbin, M. T., & Tennekoon, G. I. (1993). Homophilic adhesion of the myelin Po protein requires glycosylation of both molecules in the homophilic pair. *Journal of Cell Biology*, *122*(2), 451–459. https://doi.org/10.1083/jcb.122.2.451

Fortier, P., Smith, A., & Rossignol, S. (1987). Locomotor deficits in the mutant mouse, Lurcher. *Experimental Brain Research*, *66*, 271–286.

Fritschy, J.-M. (2006). Differential Dependence of Axo-Dendritic and Axo-Somatic GABAergic Synapses on GABAA Receptors Containing the 1 Subunit in Purkinje Cells. *Journal of Neuroscience*, *26*(12), 3245–3255. https://doi.org/10.1523/JNEUROSCI.5118-05.2006

Fukuma, G., Oguni, H., Shirasaka, Y., Watanabe, K., Miyajima, T., Yasumoto, S., … Hirose, S. (2004). Mutations of Neuronal Voltage-gated Na+ Channel α1 Subunit Gene SCN1A in Core Severe Myoclonic Epilepsy in Infancy (SMEI) and in Borderline SMEI (SMEB). *Epilepsia*, *45*(2), 140–148. https://doi.org/10.1111/j.0013-9580.2004.15103.x

Gallant, J. R., Traeger, L. L., Volkening, J. D., Moffett, H., Chen, P., Novina, C. D., … Albert, J. S. (2014). Genomic basis for the convergent evolution of electric organs. *Science*, *344*(6191), 1522–1525.

Gennarini G, Durbec P, Boned A, Rougon G, G. C. (1991). Transfected F3/F11 neuronal cell surface protein mediates intercellular adhesion and promotes neurite outgrowth. *Neuron*, *6*, 595–606.

Genton, P., Velizarova, R., & Dravet, C. (2011). Dravet syndrome: The long-term outcome. *Epilepsia*, *52*(SUPPL. 2), 44–49. https://doi.org/10.1111/j.1528-1167.2011.03001.x

Gibbs, R. A., Rogers, J., Katze, M. G., Bumgarner, R., Weinstock, G. M., Mardis, E. R., … Zwieg, A. S. (2007). Evolutionary and Biomedical Insights. *Science*, (April), 222–234.

Gilchrist, J., Das, S., Van Petegem, F., & Bosmans, F. (2013). Crystallographic insights into sodium-channel modulation by the β4 subunit. *Proceedings of the National Academy of Sciences of the United States of America*, *110*(51), E5016-24. https://doi.org/10.1073/pnas.1314557110

Goldin, a L. (2001). Resurgence of sodium channel research. *Annual Review of Physiology*, *63*, 871–894. https://doi.org/10.1146/annurev.physiol.63.1.871\r63/1/871 [pii]

Goldin, a L., Snutch, T., Lübbert, H., Dowsett, a, Marshall, J., Auld, V., … Dunn, R. (1986). Messenger RNA coding for only the alpha subunit of the rat brain Na channel is sufficient for expression of functional channels in Xenopus oocytes. *Proceedings of the National Academy of Sciences of the United States of America*, *83*(19), 7503–7507. https://doi.org/10.1073/pnas.83.19.7503

Goldowitz, D., & Smeyne, R. J. (1995). Tune into the weaver channel. *Nature Genetics*, *11*, 107–109. https://doi.org/10.1038/ng0595-111

Gorter, J. a., van Vliet, E. a., da Silva, F. H. L., Isom, L. L., & Aronica, E. (2002). Sodium channel beta1-subunit expression is increased in reactive astrocytes in a rat model for mesial temporal lobe epilepsy. *European Journal of Neuroscience*, *16*(2), 360–364. https://doi.org/10.1046/j.1460-9568.2002.02078.x

Grieco, T. M., Malhotra, J. D., Chen, C., Isom, L. L., & Raman, I. M. (2005). Open-channel block by the cytoplasmic tail of sodium channel β4 as a mechanism for resurgent sodium current. *Neuron*, *45*(2), 233–244. https://doi.org/10.1016/j.neuron.2004.12.035

Grubb, M. S., & Burrone, J. (2010). Building and maintaining the axon initial segment. *Current Opinion in Neurobiology*, *20*(4), 481–488. https://doi.org/10.1016/j.conb.2010.04.012

Guan, H., & Maness, P. F. (2010). Perisomatic GABAergic innervation in prefrontal cortex is regulated by ankyrin interaction with the L1 cell adhesion molecule. *Cerebral Cortex*, *20*(11), 2684–2693. https://doi.org/10.1093/cercor/bhq016

Guzzetta, F. (2011). Cognitive and behavioral characteristics of children with Dravet syndrome: An overview. *Epilepsia*, *52*(SUPPL. 2), 35–38. https://doi.org/10.1111/j.1528-1167.2011.02999.x

Hakim, P., Brice, N., Thresher, R., Lawrence, J., Zhang, Y., Jackson, a. P., … Huang, C. L. H. (2010). Scn3b knockout mice exhibit abnormal sino-atrial and cardiac conduction properties. *Acta Physiologica*, *198*(1), 47–59. https://doi.org/10.1111/j.1748-1716.2009.02048.x

Hakim, P., Gurung, I. S., Pedersen, T. H., Thresher, R., Brice, N., Lawrence, J., … Huang, C. L. H. (2008). Scn3b knockout mice exhibit abnormal ventricular electrophysiological properties. *Progress in Biophysics and Molecular Biology*, *98*(2–3), 251–266. https://doi.org/10.1016/j.pbiomolbio.2009.01.005

Hamilton, B. A., Frankel, W. N., Kerrebrock, A. W., Hawkins, T. L., FitzHugh, W., Kusumi, K., … Lander, E. S. (1996). Disruption of the nuclear hormone receptor ROR alpha in staggerer mice. *Nature*, *379*, 736–739.

Hartshorne, R. P., & Catterall, W. a. (1981). Purification of the saxitoxin receptor of the sodium channel from rat brain. *Proceedings of the National Academy of Sciences of the United States of America*, *78*(7), 4620–4624. https://doi.org/10.1073/pnas.78.7.4620

Hartshorne, R. P., & Catterall, W. A. (1984). The Sodium Channel from Rat Brain: Purification and Subunit Composition. *Journal of Biological Chemistry*, *259*(3), 1667–1675.

Hartshorne, R. P., Messner, D. J., Coppersmith, J. C., & Catterall, W. A. (1982). The Saxitoxin Receptor of the Sodium Channel from Rat Brain. *Journal of Biological Chemistry*, 1667–1675.

Hashimoto, K., Ichikawa, R., Kitamura, K., Watanabe, M., & Kano, M. (2009). Translocation of a

"winner" climbing fiber to the Purkinje cell dendrite and subsequent elimination of "losers" from the soma in developing cerebellum. *Neuron*, *63*(1), 106–18. https://doi.org/10.1016/j.neuron.2009.06.008

Hashimoto, K., & Kano, M. (2003). Functional differentiation of multiple climbing fiber inputs during synapse elimination in the developing cerebellum. *Neuron*, *38*(5), 785–796. https://doi.org/10.1016/S0896-6273(03)00298-8

Hatten, M. E., & Heintz, N. (1995). Mechanisms of neural patterning and specification in the developing cerebellum. *Annual Review of Neuroscience*, *18*(1), 385–408. https://doi.org/10.1146/annurev.neuro.18.1.385

Heckroth, J. A., Goldowitz, D., & Eisenman, L. M. (1989). Purkinje Cell Reduction in the Reeler Mutant Mouse: A Quantitative Immunohistochemical Study. *The Journal of Comparative Neurology*, *279*, 546–555. https://doi.org/10.1002/cne.902790404

Hellsten, U., Harland, R. M., Gilchrist, M. J., Hendrix, D., Jurka, J., Blitz, I. L., … Amaya, E. (2010). The Genome of the Western Clawed Frog Xenopus tropicalis. *Science*, *328*(April), 633–636.

Hillier, L. W., Miller, W., Birney, E., Warren, W., & Hardison, R. C. (2004). Sequence and comparative analysis of the chicken genome provide unique perspectives on vertebrate evolution. *Nature*, *432*(7018), 695–716. https://doi.org/10.1038/nature03394

Hodgkin, A. L., & Huxley, A. F. (1952). A quantitative description of membrane current and its application to conduction in nerve. *Journal of Physiology*, 500–544.

Hoebeek, F. E., Stahl, J. S., Van Alphen, A. M., Schonewille, M., Luo, C., Rutteman, M., … De Zeeuw, C. I. (2005). Increased noise level of Purkinje cell activities minimizes impact of their modulation during sensorimotor control. *Neuron*, *45*(6), 953–965. https://doi.org/10.1016/j.neuron.2005.02.012

Hoxha, E., Tempia, F., Lippiello, P., & Miniaci, M. C. (2016). Modulation , Plasticity and Pathophysiology of the Parallel Fiber-Purkinje Cell Synapse, *8*(November), 1–16. https://doi.org/10.3389/fnsyn.2016.00035

Hu, W., Tian, C., Li, T., Yang, M., Hou, H., & Shu, Y. (2009). Distinct contributions of Na(v)1.6 and Na(v)1.2 in action potential initiation and backpropagation. *Nature Neuroscience*, *12*(8), 996–1002. https://doi.org/10.1038/nn.2359

Ino, H. (2004). Immunohistochemical characterization of the orphan nuclear receptor ROR alpha in the mouse nervous system. *The Journal of Histochemistry and Cytochemistry : Official Journal of the Histochemistry Society*, *52*(3), 311–323. https://doi.org/10.1177/002215540405200302

Ishikawa, T., & Takahashi, N. (2012). Novel SCN3B Mutation Associated With Brugada Syndrome Affects Intracellular Trafficking and Function of Nav1. 5. *Circulation Journal Official Journal of the Japanese Circulation Society*, *77*(4), 959–967. https://doi.org/10.1253/circj.CJ-12-0995

Islam, R., Kristiansen, L. V., Romani, S., Garcia-Alonso, L., & Hortsch, M. (2004). Activation of EGF Receptor Kinase by L1-mediated Homophilic Cell Interactions. *Molecular Biology of the Cell*, *15*(4), 2003–2012. https://doi.org/10.1091/mbc.E03

Isom, L. L. (2001). Sodium channel beta subunits: anything but auxiliary. *The Neuroscientist : A Review Journal Bringing Neurobiology, Neurology and Psychiatry*, *7*(1), 42–54. https://doi.org/10.1177/107385840100700108

Isom, L. L., & Catterall, W. A. (1996). Na+ channel subunits and Ig domains. *Nature*, *383*, 307–308.

Isom, L. L., De Jongh, K. S., Patton, D. E., Reber, B. F., Offord, J., Charbonneau, H., … Catterall, W. a. (1992). Primary structure and functional expression of the beta 1 subunit of the rat brain sodium channel. *Science*, *256*(5058), 839–42. Retrieved from http://www.ncbi.nlm.nih.gov/pubmed/1375395

Isom, L. L., Ragsdale, D. S., De Jongh, K. S., Westenbroek, R. E., Reber, B. F., Scheuer, T., & Catterall, W. a. (1995). Structure and function of the beta 2 subunit of brain sodium channels, a transmembrane glycoprotein with a CAM motif. *Cell*, *83*(3), 433–42. Retrieved from http://www.ncbi.nlm.nih.gov/pubmed/8521473

Isom, L. L., Scheuer, T., Brownstein, A. B., Ragsdale, D. S., Murphy, B. J., & Catterall, W. A. (1995). Functional co-expresson of the b1 and type IIA a subunits of sodium channels in a mammalian cell line. *Journal of Biological Chemistry*, *270*(7), 3306–3312.

Johnson, D., & Bennett, E. S. (2006). Isoform-specific effects of the b2 subunit on voltage-gated sodium channel gating. *Journal of Biological Chemistry*, *281*(36), 25875–25881. https://doi.org/10.1074/jbc.M605060200

Johnson, D., Montpetit, M. L., Stocker, P. J., & Bennett, E. S. (2004). The sialic acid component of the b1 subunit modulates voltage-gated sodium channel function. *Journal of Biological Chemistry*, *279*(43), 44303–44310. https://doi.org/10.1074/jbc.M408900200

Johnson, E. M., Craig, E. T., & Yeh, H. H. (2007). TrkB is necessary for pruning at the climbing fibre-Purkinje cell synapse in the developing murine cerebellum. *The Journal of Physiology*, *582*, 629–646. https://doi.org/10.1113/jphysiol.2007.133561

Joho, R. H., Moorman, J. R., VanDongen, a M., Kirsch, G. E., Silberberg, H., Schuster, G., & Brown, a M. (1990). Toxin and kinetic profile of rat brain type III sodium channels expressed in Xenopus oocytes. *Brain Research. Molecular Brain Research*, *7*(2), 105–113.

Jun, K., Piedras-Rentería, E. S., Smith, S. M., Wheeler, D. B., Lee, S. B., Lee, T. G., … Shin, H. S. (1999). Ablation of P/Q-type Ca(2+) channel currents, altered synaptic transmission, and progressive ataxia in mice lacking the alpha(1A)-subunit. *Proceedings of the National Academy of Sciences of the United States of America*, *96*(26), 15245–50. https://doi.org/10.1073/pnas.96.26.15245

Kalume, F., Yu, F. H., Westenbroek, R. E., Scheuer, T., & Catterall, W. A. (2007). Reduced Sodium Current in Purkinje Neurons from Na V 1 . 1 Mutant Mice : Implications for Ataxia in Severe

Myoclonic Epilepsy in Infancy. *Neuroscience*, *27*(41), 11065–11074. https://doi.org/10.1523/JNEUROSCI.2162-07.2007

Kano, M., Hashimoto, K., Chen, C., Abeliovich, a, Aiba, a, Kurihara, H., … Tonegawa, S. (1995). Impaired Synapse Elimination during Cerebellar Development in PKCγ Mutant Mice. *Cell*, *83*(7), 1223–1231. Retrieved from file://d/okujeni/literature/Papers/Kano95_1223.pdf

Kaplan, M., Cho, M., Ullian, E., & Isom, L. (2001). Differential Control of Clustering of the Sodium Channels Na v 1.2 and Na v 1.6 at Developing CNS Nodes of Ranvier. *Neuron*, *30*(1), 105–119. https://doi.org/10.1016/S0896-6273(01)00266-5

Kashiwabuchi, N., Ikeda, K., Araki, K., Hirano, T., Shibuki, K., Takayama, C., … et al. (1995). Impairment of motor coordination, Purkinje cell synapse formation, and cerebellar long-term depression in GluR delta 2 mutant mice. *Cell*, *81*(2), 245–252. https://doi.org/10.1016/0092-8674(95)90334-8

Kaufmann, S. G., Westenbroek, R. E., Maass, A. H., Lange, V., Renner, A., Wischmeyer, E., … Maier, S. K. G. (2013). Distribution and function of sodium channel subtypes in human atrial myocardium. *Journal of Molecular and Cellular Cardiology*, *61*, 133–141. https://doi.org/10.1016/j.yjmcc.2013.05.006

Kazarinova-Noyes, K., Malhotra, J. D., McEwen, D. P., Mattei, L. N., Berglund, E. O., Ranscht, B., … Xiao, Z. C. (2001). Contactin associates with Na+ channels and increases their functional expression. *The Journal of Neuroscience : The Official Journal of the Society for Neuroscience*, *21*(19), 7517–25. Retrieved from http://www.ncbi.nlm.nih.gov/pubmed/11567041

Kazen-Gillespie, K. a, Ragsdale, D. S., D'Andrea, M. R., Mattei, L. N., Rogers, K. E., & Isom, L. L. (2000a). Cloning, localization, and functional expression of sodium channel beta1A subunits. *The Journal of Biological Chemistry*, *275*(2), 1079–1088. https://doi.org/10.1074/jbc.275.2.1079

Kazen-Gillespie, K. a, Ragsdale, D. S., D'Andrea, M. R., Mattei, L. N., Rogers, K. E., & Isom, L. L. (2000b). Cloning, localization, and functional expression of sodium channel beta1A subunits. *The Journal of Biological Chemistry*, *275*(2), 1079–88. Retrieved from http://www.ncbi.nlm.nih.gov/pubmed/10625649

Kim, D. Y., Carey, B. W., Wang, H., Ingano, L. a M., Binshtok, A. M., Wertz, M. H., … Kovacs, D. M. (2007). BACE1 regulates voltage-gated sodium channels and neuronal activity. *Nature Cell Biology*, *9*(7), 755–764. https://doi.org/10.1038/ncb1602

Ko, S. H., Lenkowski, P. W., Lee, H. C., Mounsey, J. P., & Patel, M. K. (2005). Modulation of Nav1.5 by β1- and β3-subunit co-expression in mammalian cells. *Pflugers Archiv European Journal of Physiology*, *449*(4), 403–412. https://doi.org/10.1007/s00424-004-1348-4

Krafte, D. S., Goldin, a L., Auld, V. J., Dunn, R. J., Davidson, N., & Lester, H. a. (1990). Inactivation of cloned Na channels expressed in Xenopus oocytes. *The Journal of General Physiology*, *96*(4), 689–706. https://doi.org/10.1085/jgp.96.4.689

Krämer, E., Klein, C., Boytinck, M., Kra, E., Koch, T., & Trotter, J. (1999). Compartmentation of Fyn Kinase with Molecules in Oligodendrocytes Facilitates Kinase Activation during Myelination. *Journal of Biological Chemistry*, *274*(41), 29042–29049.

Krook-Magnuson, E., Szabo, G. G., Armstrong, C., Oijala, M., & Soltesz, I. (2014). Cerebellar Directed Optogenetic Intervention Inhibits Spontaneous Hippocampal Seizures in a Mouse Model of Temporal Lobe Epilepsy. *eNeuro*, *1*(1), 1–27. https://doi.org/10.1523/ENEURO.0005-14.2014

Kruger, L. C., O'Malley, H. A., Hull, J. M., Kleeman, A., Patino, G. A., & Isom, L. L. (2016). β1-C121W Is Down But Not Out: Epilepsy-Associated Scn1b-C121W Results in a Deleterious Gain-of-Function. *The Journal of Neuroscience : The Official Journal of the Society for Neuroscience*, *36*(23), 6213–24. https://doi.org/10.1523/JNEUROSCI.0405-16.2016

Lalonde, R. (1987). Exploration and spatial learning in staggerer mutant mice. *Journal of Neurogenetics*, *4*, 285–292.

Lalonde, R., Bensoula, N., & Filali, M. (1995). Neuroscienc£ research, *22*, 423–426.

Lalonde, R., Hayzoun, K., Derer, M., Mariani, J., & Strazielle, C. (2004). Neurobehavioral evaluation of Relnrl-orl mutant mice and correlations with cytochrome oxidase activity. *Neuroscience Research*, *49*(3), 297–305. https://doi.org/10.1016/j.neures.2004.03.012

Lalonde, R., Lalonde, R., Filali, M., Filali, M., Bensoula, a N., Bensoula, a N., … Lestienne, F. (1996). Sensorimotor learning in three cerebellar mutant mice. *Neurobiol Learn Mem*, *65*(2), 113–120. https://doi.org/10.1006/nlme.1996.0013

Lalonde, R., & Strazielle, C. (2007). Spontaneous and induced mouse mutations with cerebellar dysfunctions: Behavior and neurochemistry. *Brain Research*, *1140*(1), 51–74. https://doi.org/10.1016/j.brainres.2006.01.031

Larsell, O. (1970). The Comparative Anatomy and Histology of the Cerebellum from Monotremes through Apes (pp. 31–58). Minneapolis, MN: Univ. Minnesota Press.

Levisohn, L., Cronin-Golomb, A., & Schmahmann, J. D. (2000). Neuropsychological consequences of cerebellar tumour resection in children: cerebellar cognitive affective syndrome in a paediatric population. *Brain: A Journal of Neurology*, *123 (Pt 5*, 1041–1050. https://doi.org/10.1093/brain/123.5.1041

Li, J., Waterhouse, R. M., & Zdobnov, E. M. (2011). A remarkably stable TipE gene cluster: evolution of insect Para sodium channel auxiliary subunits. *BMC Evolutionary Biology*, *11*(1), 337. https://doi.org/10.1186/1471-2148-11-337

Li, R. G., Wang, Q., Xu, Y. J., Zhang, M., Qu, X. K., Liu, X., … Yang, Y. Q. (2013). Mutations of the SCN4B-encoded sodium channel b4 subunit in familial atrial fibrillation. *International Journal of Molecular Medicine*, *32*(1), 144–150. https://doi.org/10.3892/ijmm.2013.1355

Lin, X., O'Malley, H., Chen, C., Auerbach, D., Foster, M., Shekhar, A., … Delmar, M. (2015). Scn1b deletion leads to increased tetrodotoxin-sensitive sodium current, altered intracellular

calcium homeostasis and arrhythmias in murine hearts. *The Journal of Physiology*, *593*(6), 1389–1407. https://doi.org/10.1113/jphysiol.2014.277699

Liu, H., Ming-Ming, W., & Zakon, H. H. (2007). Individual Variation and Hormonal Modulation of a Sodium Channel b Subunit in the Electric Organ Correlate with Variation in a Social Signal. *Developmental Neurobiology*, 1289–1304. https://doi.org/10.1002/dneu

Lopez-Santiago, L. F., Brackenbury, W. J., Chen, C., & Isom, L. L. (2011). Na+ channel Scn1b gene regulates dorsal root ganglion nociceptor excitability in vivo. *Journal of Biological Chemistry*, *286*(26), 22913–22923. https://doi.org/10.1074/jbc.M111.242370

Lopez-Santiago, L. F., Meadows, L. S., Ernst, S. J., Chen, C., Malhotra, J. D., McEwen, D. P., … Isom, L. L. (2007). Sodium channel Scn1b null mice exhibit prolonged QT and RR intervals. *Journal of Molecular and Cellular Cardiology*, *43*(5), 636–647. https://doi.org/10.1016/j.yjmcc.2007.07.062

Lopez-Santiago, L. F., Pertin, M., Morisod, X., Chen, C., Hong, S., Wiley, J., … Isom, L. L. (2006). Sodium channel beta2 subunits regulate tetrodotoxin-sensitive sodium channels in small dorsal root ganglion neurons and modulate the response to pain. *The Journal of Neuroscience : The Official Journal of the Society for Neuroscience*, *26*(30), 7984–7994. https://doi.org/10.1523/JNEUROSCI.2211-06.2006

Lowery, L. A., & Van Vactor, D. (2009). The trip of the tip: understanding the growth cone machinery. *Nature Reviews. Molecular Cell Biology*, *10*(5), 332–343. https://doi.org/10.1038/nrm2679

Maier, S. K. G., Westenbroek, R. E., McCormick, K. a., Curtis, R., Scheuer, T., & Catterall, W. a. (2004). Distinct Subcellular Localization of Different Sodium Channel a and b Subunits in Single Ventricular Myocytes from Mouse Heart. *Circulation*, *109*(11), 1421–1427. https://doi.org/10.1161/01.CIR.0000121421.61896.24

Malhotra, J. D., Chen, C., Rivolta, I., Abriel, H., Malhotra, R., Mattei, L. N., … Isom, L. L. (2001). Characterization of sodium channel alpha- and beta-subunits in rat and mouse cardiac myocytes. *Circulation*, *103*(9), 1303–1310. https://doi.org/10.1161/01.cir.103.9.1303

Malhotra, J. D., Kazen-Gillespie, K., Hortsch, M., & Isom, L. L. (2000). Sodium channel β subunits mediate homophilic cell adhesion and recruit ankyrin to points of cell-cell contact. *Journal of Biological Chemistry*, *275*(15), 11383–11388. https://doi.org/10.1074/jbc.275.15.11383

Malhotra, J. D., Koopmann, M. C., Kazen-Gillespie, K. a, Fettman, N., Hortsch, M., & Isom, L. L. (2002). Structural requirements for interaction of sodium channel beta 1 subunits with ankyrin. *The Journal of Biological Chemistry*, *277*(29), 26681–26688. https://doi.org/10.1074/jbc.M202354200

Malhotra, J. D., Thyagarajan, V., Chen, C., & Isom, L. L. (2004). Tyrosine-phosphorylated and nonphosphorylated sodium channel beta1 subunits are differentially localized in cardiac myocytes. *The Journal of Biological Chemistry*, *279*(39), 40748–54. https://doi.org/10.1074/jbc.M407243200

Maness, P. F., & Schachner, M. (2007). Neural recognition molecules of the immunoglobulin superfamily: signaling transducers of axon guidance and neuronal migration. *Nature Neuroscience*, *10*(1), 19–26. https://doi.org/10.1038/nn1827

Marionneau, C., Carrasquillo, Y., Norris, a. J., Townsend, R. R., Isom, L. L., Link, a. J., & Nerbonne, J. M. (2012). The Sodium Channel Accessory Subunit Nav 1 Regulates Neuronal Excitability through Modulation of Repolarizing Voltage-Gated K+ Channels. *Journal of Neuroscience*, *32*(17), 5716–5727. https://doi.org/10.1523/JNEUROSCI.6450-11.2012

Mason, C. A., & Gregory, E. (1984). Postnatal maturation of cerebellar mossy and climbing fibers: transient expression of dual features on single axons. *The Journal of Neuroscience : The Official Journal of the Society for Neuroscience*, *4*(7), 1715–35. Retrieved from http://www.ncbi.nlm.nih.gov/pubmed/6737039

McCormick, K. a, Isom, L. L., Ragsdale, D., Smith, D., Scheuer, T., & Catterall, W. a. (1998). Molecular determinants of Na+ channel function in the extracellular domain of the beta1 subunit. *The Journal of Biological Chemistry*, *273*(7), 3954–3962. https://doi.org/10.1074/jbc.273.7.3954

McEwen, D. P., Chen, C., Meadows, L. S., Lopez-Santiago, L., & Isom, L. L. (2009). The voltage-gated Na+ channel β3 subunit does not mediate trans homophilic cell adhesion or associate with the cell adhesion molecule contactin. *Neuroscience Letters*, *462*(3), 272–275. https://doi.org/10.1016/j.neulet.2009.07.020

McEwen, D. P., & Isom, L. L. (2004). Heterophilic interactions of sodium channel beta1 subunits with axonal and glial cell adhesion molecules. *The Journal of Biological Chemistry*, *279*(50), 52744–52. https://doi.org/10.1074/jbc.M405990200

McEwen, D. P., Meadows, L. S., Chen, C., Thyagarajan, V., & Isom, L. L. (2004). Sodium Channel β1 Subunit-mediated Modulation of Nav1.2 Currents and Cell Surface Density Is Dependent on Interactions with Contactin and Ankyrin. *Journal of Biological Chemistry*, *279*(16), 16044–16049. https://doi.org/10.1074/jbc.M400856200

Meadows, L., Malhotra, J. D., Stetzer, a, Isom, L. L., & Ragsdale, D. S. (2001). The intracellular segment of the sodium channel beta 1 subunit is required for its efficient association with the channel alpha subunit. *Journal of Neurochemistry*, *76*(6), 1871–1878. https://doi.org/10.1046/j.1471-4159.2001.00192.x

Meadows, L. S., Chen, Y. H., Powell, a J., Clare, J. J., & Ragsdale, D. S. (2002). Functional modulation of human brain Nav1.3 sodium channels, expressed in mammalian cells, by auxiliary beta 1, beta 2 and beta 3 subunits. *Neuroscience*, *114*(3), 745–753. https://doi.org/10.1016/s0306-4522(02)00242-7

Meadows, L. S., Malhotra, J., Loukas, A., Thyagarajan, V., Kazen-Gillespie, K. a, Koopman, M. C., … Ragsdale, D. S. (2002). Functional and biochemical analysis of a sodium channel beta1 subunit mutation responsible for generalized epilepsy with febrile seizures plus type 1. *The Journal of Neuroscience : The Official Journal of the Society for Neuroscience*, *22*(24), 10699–709. Retrieved from http://www.ncbi.nlm.nih.gov/pubmed/12486163

Medeiros-Domingo, A., Kaku, T., Tester, D. J., Iturralde-Torres, P., Itty, A., Ye, B., … Ackerman, M. J. (2007). SCN4B-encoded sodium channel β4 subunit in congenital long-QT syndrome. *Circulation*, *116*(2), 134–142. https://doi.org/10.1161/CIRCULATIONAHA.106.659086

Meisler, M. H., & Kearney, J. a. (2005). Sodium channel mutations in epilepsy and other neurological disorders. *Journal of Clinical Investigation*, *115*(8). https://doi.org/10.1172/JCI25466.2010

Messner, D. J., & Catterall, W. A. (1985). The Sodium Channel from Rat Brain: Separation and Characterization of Subunits. *Journal of Biological Chemistry*, *260*(19), 1667–1675.

Middleton, F. A., & Strick, P. L. (1997). Dentate output channels: motor and cognitive components. *Progress in Brain Research*, *114*, 553–566.

Mikkelsen, T. S., Wakefield, M. J., Aken, B., Amemiya, C. T., Chang, J. L., Duke, S., … Lindblad-Toh, K. (2007). Genome of the marsupial Monodelphis domestica reveals innovation in non-coding sequences. *Nature*, *447*(7141), 167–177. https://doi.org/10.1038/nature05805

Miller, J. a, Agnew, W. S., & Levinson, S. R. (1983). Principal glycopeptide of the tetrodotoxin/saxitoxin binding protein from Electrophorus electricus: isolation and partial chemical and physical characterization. *Biochemistry*, *22*(2), 462–470.

Morales, G., Hubert, M., Brümmendorf, T., Treubert, U., Tárnok, A., Schwarz, U., & Rathjen, F. G. (1993). Induction of axonal growth by heterophilic interactions between the cell surface recognition proteins Fll and Nr-CAM/Bravo. *Neuron*, *11*(6), 1113–1122. https://doi.org/10.1016/0896-6273(93)90224-F

Morgan, K., Stevens, E. B., Shah, B., Cox, P. J., Dixon, a K., Lee, K., … Jackson, a P. (2000). Beta 3: an Additional Auxiliary Subunit of the Voltage-Sensitive Sodium Channel That Modulates Channel Gating With Distinct Kinetics. *Proceedings of the National Academy of Sciences of the United States of America*, *97*(5), 2308–2313. https://doi.org/10.1073/pnas.030362197

Muller, D., Wang, C., Skibo, G., Toni, N., Cremer, H., Calaora, V., … Kiss, J. Z. (1996). PSA – NCAM Is Required for Activity-Induced Synaptic Plasticity. *Cell*, *17*, 413–422. https://doi.org/10.1016/S0896-6273(00)80174-9

Murai, K. K., Misner, D., & Ranscht, B. (2002). Associated with Hippocampal Long-Term Depression but Not Potentiation, *12*(2), 181–190.

Nakagawa, S., Watanabe, M., & Inoue, Y. (1997). Prominent expression of nuclear hormone receptor ROR alpha in Purkinje cells from early development. *Neurosci.Res.*, *28*(0168–0102 SB–M), 177–184.

Namadurai, S., Balasuriya, D., Rajappa, R., Wiemhöfer, M., Stott, K., Klingauf, J., … Jackson, A. P. (2014). Crystal structure and molecular imaging of the Nav channel β3 subunit indicates a trimeric assembly. *The Journal of Biological Chemistry*, *289*(15), 10797–811. https://doi.org/10.1074/jbc.M113.527994

Nelson, M., Millican-Slater, R., Forrest, L. C., & Brackenbury, W. J. (2014). The sodium channel

β1 subunit mediates outgrowth of neurite-like processes on breast cancer cells and promotes tumour growth and metastasis. *International Journal of Cancer. Journal International Du Cancer*, *135*, 2338–2351. https://doi.org/10.1002/ijc.28890

Nguyen, H. M., Miyazaki, H., Hoshi, N., Smith, B. J., Nukina, N., Goldin, a. L., & Chandy, K. G. (2012). Modulation of voltage-gated K+ channels by the sodium channel 1 subunit. *Proceedings of the National Academy of Sciences*, *109*(45), 18577–18582. https://doi.org/10.1073/pnas.1209142109

Niethammer, P., Delling, M., Sytnyk, V., Dityatev, A., Fukami, K., & Schachner, M. (2002). Cosignaling of NCAM via lipid rafts and the FGF receptor is required for neuritogenesis. *Journal of Cell Biology*, *157*(3), 521–532. https://doi.org/10.1083/jcb.200109059

Nikonenko, A. G., Sun, M., Lepsveridze, E., Apostolova, I., Petrova, I., Irintchev, A., … Schachner, M. (2006). Enhanced perisomatic inhibition and impaired long-term potentiation in the CA1 region of juvenile CHL1-deficient mice. *European Journal of Neuroscience*, *23*(7), 1839–1852. https://doi.org/10.1111/j.1460-9568.2006.04710.x

Noda, M., Ikeda, T., Suzuki, H., Takeshima, H., Takahashi, T., Kuno, M., & Numa, S. (1986). Expression of functional sodium channels from cloned cDNA. *Nature*, *322*, 826–828.

Noroozian, M. (2014). The role of the cerebellum in cognition: Beyond coordination in the central nervous system. *Neurologic Clinics*, *32*(4), 1081–1104. https://doi.org/10.1016/j.ncl.2014.07.005

O'Malley, H. a., & Isom, L. L. (2015). Sodium Channel β Subunits: Emerging Targets in Channelopathies. *Annual Review of Physiology*, *77*(1), 481–504. https://doi.org/10.1146/annurev-physiol-021014-071846

O'Malley, H. a, Shreiner, A. B., Chen, G.-H., Huffnagle, G. B., & Isom, L. L. (2009). Loss of Na+ channel beta2 subunits is neuroprotective in a mouse model of multiple sclerosis. *Molecular and Cellular Neurosciences*, *40*(2), 143–55. https://doi.org/10.1016/j.mcn.2008.10.001

Oberdick, J., Smeyne, R. J., Mann, J. R., Zackson, S., James, I., Oberdick, J., … Morgan, J. I. (2016). A Promoter that Drives Transgene Expression in Cerebellar Purkinje and Retinal Bipolar Neurons Published by : American Association for the Advancement of Science Stable URL : http://www.jstor.org/stable/2873940 JSTOR is a not-for-profit service that helps, *248*(4952), 223–226.

Ogiwara, I., Nakayama, T., Yamagata, T., Ohtani, H., Mazaki, E., Tsuchiya, S., … Yamakawa, K. (2012). A homozygous mutation of voltage-gated sodium channel βi gene SCN1B in a patient with Dravet syndrome. *Epilepsia*, *53*(12), 200–203. https://doi.org/10.1111/epi.12040

Oh, Y., & Waxman, S. G. (1995). Differential Na+ channel beta 1 subunit mRNA expression in stellate and flat astrocytes cultured from rat cortex and cerebellum: a combined in situ hybridization and immunocytochemistry study. *Glia*, *13*(3), 166–173.

https://doi.org/10.1002/glia.440130303

Olesen, M. S., Jespersen, T., Nielsen, J. B., Liang, B., Møller, D. V., Hedley, P., … Svendsen, J. H. (2011). Mutations in sodium channel β-subunit SCN3B are associated with early-onset lone atrial fibrillation. *Cardiovascular Research*, *89*(4), 786–793. https://doi.org/10.1093/cvr/cvq348

Palay, S., & Chan-Palay, V. (1974). *Cerebellar Cortex, Cytology, and Organization*. Berilin: Springer-Verlag.

Patel, F., & Brackenbury, W. J. (2015). Dual roles of voltage-gated sodium channels in development and cancer. *The International Journal of Developmental Biology*, (April). https://doi.org/10.1387/ijdb.150171wb

Patil, N., Cox, D. R., Bhat, D., Faham, M., Myers, R. M., & Peterson, A. S. (1995). A potassium channel mutation in weaver mice implicates membrane excitability in granule cell differentiation. *Nature Genetics*, *10*, 196–201. https://doi.org/10.1038/ng0595-111

Patino, G. a, Brackenbury, W. J., Bao, Y., Lopez-Santiago, L. F., O'Malley, H. a, Chen, C., … Isom, L. L. (2011). Voltage-gated Na+ channel β1B: a secreted cell adhesion molecule involved in human epilepsy. *The Journal of Neuroscience : The Official Journal of the Society for Neuroscience*, *31*(41), 14577–91. https://doi.org/10.1523/JNEUROSCI.0361-11.2011

Patino, G. a, Claes, L. R. F., Lopez-Santiago, L. F., Slat, E. a, Dondeti, R. S. R., Chen, C., … Isom, L. L. (2009). A functional null mutation of SCN1B in a patient with Dravet syndrome. *The Journal of Neuroscience : The Official Journal of the Society for Neuroscience*, *29*(34), 10764–78. https://doi.org/10.1523/JNEUROSCI.2475-09.2009

Peles, E., Nativ, M., Campbell, P. L., Sakurai, T., Martinez, R., Lev, S., … Schlessinger, J. (1995). The carbonic anhydrase domain of receptor tyrosine phosphatase beta is a functional ligand for the axonal cell recognition molecule contactin. *Cell*, *82*(2), 251–260. https://doi.org/10.1016/0092-8674(95)90312-7

Qiao, S., Kim, S. H., Heck, D., Goldowitz, D., LeDoux, M. S., & Homayouni, R. (2013). Dab2IP GTPase Activating Protein Regulates Dendrite Development and Synapse Number in Cerebellum. *PLoS ONE*, *8*(1), 1–12. https://doi.org/10.1371/journal.pone.0053635

Qin, N., D'Andrea, M. R., Lubin, M.-L., Shafaee, N., Codd, E. E., & Correa, A. M. (2003). Molecular cloning and functional expression of the human sodium channel b1B subunit, a novel splicing variant of the b1 subunit. *European Journal of Biochemistry*, *270*(23), 4762–4770. https://doi.org/10.1046/j.1432-1033.2003.03878.x

Rafuse, V. F., Polo-Parada, L., & Landmesser, L. T. (2000). Structural and functional alterations of neuromuscular junctions in NCAM-deficient mice. *The Journal of Neuroscience : The Official Journal of the Society for Neuroscience*, *20*(17), 6529–6539.

Raman, I. M., & Bean, B. P. (1997). Resurgent sodium current and action potential formation in dissociated cerebellar Purkinje neurons. *The Journal of Neuroscience : The Official Journal of the Society for Neuroscience*, *17*(12), 4517–4526.

Raman, I. M., Sprunger, L. K., Meisler, M. H., & Bean, B. P. (1997). Altered Subthreshold Sodium Currents and Disrupted Firing Patterns in Purkinje Neurons of< i> Scn8a</i> Mutant Mice. *Neuron*, *19*(4), 881–891. Retrieved from http://www.sciencedirect.com/science/article/pii/S0896627300809691%5Cnpapers2://publication/uuid/0AF4D5FE-16DE-4CBA-B6C3-FE9218B02C85

Ratcliffe, C. F., Qu, Y., McCormick, K. a, Tibbs, V. C., Dixon, J. E., Scheuer, T., & Catterall, W. a. (2000). A sodium channel signaling complex: modulation by associated receptor protein tyrosine phosphatase beta. *Nature Neuroscience*, *3*(5), 437–444. https://doi.org/10.1038/74805

Ratcliffe, C. F., Westenbroek, R. E., Curtis, R., & Catterall, W. A. (2001). Sodium channel beta1 and beta3 subunits associate with neurofascin through their extracellular immunoglobulin-like domain. *The Journal of Cell Biology*, *154*(2), 427–434. https://doi.org/10.1083/jcb.200102086

Reid, C. a., Leaw, B., Richards, K. L., Richardson, R., Wimmer, V., Yu, C., … Petrou, S. (2014). Reduced dendritic arborization and hyperexcitability of pyramidal neurons in a Scn1b-based model of Dravet syndrome. *Brain*, *137*(6), 1701–1715. https://doi.org/10.1093/brain/awu077

Remme, C. A., & Bezzina, C. R. (2010). Sodium channel (Dys)function and cardiac arrhythmias. *Cardiovascular Therapeutics*, *28*(5), 287–294. https://doi.org/10.1111/j.1755-5922.2010.00210.x

Ren, D., Navarro, B., Xu, H., Yue, L., Shi, Q., & Clapham, D. E. (2001). A Prokaryotic Voltage-Gated Sodium Channel. *Science*, *294*(December), 2372–2375.

Rinaldo, L., & Hansel, C. (2010). Ataxias and cerebellar dysfunction: Involvement of synaptic plasticity deficits? *Functional Neurology*, *25*(3), 135–139. https://doi.org/4587 [pii]

Riuró, H., Beltran-Alvarez, P., Tarradas, A., Selga, E., Campuzano, O., Vergés, M., … Brugada, R. (2013). A Missense Mutation in the Sodium Channel β2 Subunit Reveals SCN2B as a New Candidate Gene for Brugada Syndrome. *Human Mutation*, *34*(7), 961–966. https://doi.org/10.1002/humu.22328

Rochefort, C., Arabo, A., Andre, M., Poucet, B., Save, E., & Rondi-Reig, L. (2011). Cerebellum Shapes Hippocampal Spatial Code. *Science*, *311*(October), 385–390.

Rochefort, C., Arabo, A., André, M., Poucet, B., Save, E., & Rondi-Reig, L. (2011). Cerebellum Shapes Hippocampal Spatial Code. *Science*, *311*(October), 385–390. https://doi.org/10.1126/science.1207403

Saghatelyan, A. K., Nikonenko, A. G., Sun, M., Rolf, B., Putthoff, P., Kutsche, M., … Schachner, M. (2004). Reduced GABAergic transmission and number of hippocampal perisomatic inhibitory synapses in juvenile mice deficient in the neural cell adhesion molecule L1. *Molecular and Cellular Neuroscience*, *26*(1), 191–203. https://doi.org/10.1016/j.mcn.2004.01.008

Sakurai, K., Toyoshima, M., Takeda, Y., Shimoda, Y., & Watanabe, K. (2010). Synaptic formation in subsets of glutamatergic terminals in the mouse hippocampal formation is affected by a deficiency in the neural cell recognition molecule NB-3. *Neuroscience Letters*, *473*(2), 102–106. https://doi.org/10.1016/j.neulet.2010.02.027

Sakurai, K., Toyoshima, M., Ueda, H., Matsubara, K., Takeda, Y., Karagogeos, D., … Watanabe, K. (2009). Contribution of the neural cell recognition molecule NB-3 to synapse formation between parallel fibers and Purkinje cells in mouse. *Developmental Neurobiology*, *69*(12), 811–824. https://doi.org/10.1002/dneu.20742

Sakurai, T., Lustig, M., Nativ, M., Hemperly, J. J., Schlessinger, J., Peles, E., & Grumet, M. (1997). Induction of neurite outgrowth through contactin and Nr-CAM by extracellular regions of glial receptor tyrosine phosphatase β. *Journal of Cell Biology*, *136*(4), 907–918. https://doi.org/10.1083/jcb.136.4.907

Sashihara, S., Felts, P. A., Waxman, S. G., & Matsui, T. (1996). Orphan nuclear reportor ROR alpha gene: isoform-specific spatiotemporal expression during postnatal development of brain. *Molecular Brain Research*, *42*, 109–117.

Scheffer, I. E. (2012). Diagnosis and long-term course of Dravet syndrome. *European Journal of Paediatric Neurology*, *16*(SUPPL. 1), S5–S8. https://doi.org/10.1016/j.ejpn.2012.04.007

Scheffer, I. E., Harkin, L. a., Grinton, B. E., Dibbens, L. M., Turner, S. J., Zielinski, M. a., … Berkovic, S. F. (2007). Temporal lobe epilepsy and GEFS+ phenotypes associated with SCN1B mutations. *Brain*, *130*(1), 100–109. https://doi.org/10.1093/brain/awl272

Schiffmann, S. N., Bernier, B., & Goffinet, a M. (1997). Reelin mRNA Expression During Mouse Brain Development. *European Journal of Neuroscience*, *9*, 1055–1077. https://doi.org/10.1111/j.1460-9568.1997.tb01456.x

Seyfried, T. N., & Glaser, G. H. (1985). A review of mouse mutants as genetic models of epilepsy. *Epilepsia*, *26*(2), 143–50. Retrieved from http://www.ncbi.nlm.nih.gov/pubmed/4039253

Shah, B. S., Stevens, E. B., Pinnock, R. D., Dixon, a K., & Lee, K. (2001). Developmental expression of the novel voltage-gated sodium channel auxiliary subunit beta3, in rat CNS. *The Journal of Physiology*, *534*(Pt 3), 763–776. https://doi.org/10.1111/j.1469-7793.2001.t01-1-00763.x

Shi, X., Yasumoto, S., Nakagawa, E., Fukasawa, T., Uchiya, S., & Hirose, S. (2009). Missense mutation of the sodium channel gene SCN2A causes Dravet syndrome. *Brain and Development*, *31*(10), 758–762. https://doi.org/10.1016/j.braindev.2009.08.009

Shin, S. C., Ahn, D. H., Kim, S. J., Pyo, C. W., Lee, H., Lee, H., … Park, H. (2014). The genome sequence of the Antarctic bullhead notothen reveals evolutionary adaptations to a cold environment. *Genome Biology*, *15*, 1–14. https://doi.org/10.1186/s13059-014-0468-1

Signorini, S., Liao, Y. J., Duncan, S. a, Jan, L. Y., & Stoffel, M. (1997). Normal cerebellar development but susceptibility to seizures in mice lacking G protein-coupled, inwardly rectifying K+ channel GIRK2. *Proceedings of the National Academy of Sciences of the*

United States of America, *94*(3), 923–927. https://doi.org/10.1073/pnas.94.3.923

Sillitoe, R., & Joyner, A. (2007). Morphology, molecular codes, and circuitry produce the three-dimensional complexity of the cerebellum. *Annual Review of Cell and Developmental Biology*, *23*, 549–577. https://doi.org/10.1146/annurev.cellbio.23.090506.123237 [doi]

Smith, J. J., Kuraku, S., Holt, C., Sauka-Spengler, T., Jiang, N., Campbell, M. S., … Li, W. (2013). Sequencing of the sea lamprey (Petromyzon marinus) genome provides insights into vertebrate evolution. *Nature Genetics*, *45*(4), 415–21, 421–2. https://doi.org/10.1038/ng.2568

Sodergren, E., Weinstock, G., Davidson, E., Cameron, R., Gibbs, R., Angerer, R., … Wright, R. (2006). The Genome of the Sea Urchin. *Science*, *314*(February), 941–952. https://doi.org/10.1126/science.1133609

Somogyi, P., & Hámori, J. (1976). A quantitative electron microscopic study of the Purkinje cell axon initial segment. *Neuroscience*, *1*(5), 361–5. Retrieved from http://www.ncbi.nlm.nih.gov/pubmed/1004711

Sonmez, E., & Herrup, K. (1984). Role of staggerer gene in determining cell number in cerebellar cortex. II. Granule cell death and persistence of the external granule cell layer in young mouse chimeras. *Developmental Brain Research*, *12*(2), 271–283. https://doi.org/10.1016/0165-3806(84)90049-X

Spampanato, J., Kearney, J. a, de Haan, G., McEwen, D. P., Escayg, a, Aradi, I., … Meisler, M. H. (2004). A novel epilepsy mutation in the sodium channel SCN1A identifies a cytoplasmic domain for beta subunit interaction. *The Journal of Neuroscience : The Official Journal of the Society for Neuroscience*, *24*(44), 10022–10034. https://doi.org/10.1523/JNEUROSCI.2034-04.2004

Srinivasan, J., Schachner, M., & Catterall, W. a. (1998). Interaction of voltage-gated sodium channels with the extracellular matrix molecules tenascin-C and tenascin-R. *Proceedings of the National Academy of Sciences of the United States of America*, *95*(26), 15753–15757. https://doi.org/10.1073/pnas.95.26.15753

Stafstrom, C. E., & Carmant, L. (2015). Seizures and Epilepsy : An Overview for Neuroscientists. *Cold Spring Harb Perspect Med*, *5*, 1–18.

Sugawara, T., Mazaki-Miyazaki, E., Fukushima, K., Shimomura, J., Fujiwara, T., Hamano, S., … Yamakawa, K. (2002). Frequent mutations of SCN1A in severe myoclonic epilepsy in infancy. *Neurology*, *58*(7), 1122–4. https://doi.org/10.1212/WNL.58.7.1122

Sugawara, T., Tsurubuchi, Y., Agarwala, K. L., Ito, M., Fukuma, G., Mazaki-Miyazaki, E., … Yamakawa, K. (2001). A missense mutation of the Na+ channel alpha II subunit gene Na(v)1.2 in a patient with febrile and afebrile seizures causes channel dysfunction. *Proceedings of the National Academy of Sciences of the United States of America*, *98*(11), 6384–6389. https://doi.org/10.1073/pnas.111065098

Surges, R., & Sander, J. (2012). Sudden unexpected death in epilepsy: mechanisms, prevalence,

and prevention. *Current Opinion in Neurology*, *25*(2), 201–207. https://doi.org/10.1097/WCO.0b013e3283506714

Sutkowski, E. M., & Catterall, W. A. (1990). b1 Subunits of Sodium Channels. *Journal of Biological Chemistry*, *265*(21), 12393–12399.

Sytnyk, V., Leshchyns'ka, I., Delling, M., Dityateva, G., Dityatev, A., & Schachner, M. (2002). Neural cell adhesion molecule promotes accumulation of TGN organelles at sites of neuron-to-neuron contacts. *Journal of Cell Biology*, *159*(4), 649–661. https://doi.org/10.1083/jcb.200205098

Sytnyk, V., Leshchyns'Ka, I., Nikonenko, A. G., & Schachner, M. (2006). NCAM promotes assembly and activity-dependent remodeling of the postsynaptic signaling complex. *Journal of Cell Biology*, *174*(7), 1071–1085. https://doi.org/10.1083/jcb.200604145

Takahashi, N., Kikuchi, S., Dai, Y., Kobayashi, K., Fukuoka, T., & Noguchi, K. (2003). Expression of auxiliary β subunits of sodium channels in primary afferent neurons and the effect of nerve injury. *Neuroscience*, *121*(2), 441–450. https://doi.org/10.1016/S0306-4522(03)00432-9

Takayama, C. (2005). Formation of GABAergic synapses in the cerebellum. *Cerebellum (London, England)*, *4*(April), 171–177. https://doi.org/10.1080/14734220510008012

The C. elegans Sequencing Consortium. (1998). Genome sequence of the nematode C. elegans: a platform for investigating biology. *Science (New York, N.Y.)*, *282*(5396), 2012–2018. https://doi.org/10.1126/science.282.5396.2012

Theile, J. W., & Cummins, T. R. (2011). Inhibition of Nav beta4 Peptide-Mediated Resurgent Sodium Currents in Nav1 . 7 Channels by Carbamazepine , Riluzole ,. *Molecular Pharmacology*, 724–734. https://doi.org/10.1124/mol.111.072751.

Trinidad, J. C., Barkan, D. T., Gulledge, B. F., Thalhammer, a., Sali, a., Schoepfer, R., & Burlingame, a. L. (2012). Global Identification and Characterization of Both O-GlcNAcylation and Phosphorylation at the Murine Synapse. *Molecular & Cellular Proteomics*, *11*(8), 215–229. https://doi.org/10.1074/mcp.O112.018366

van Woerden, G. M., Hoebeek, F. E., Gao, Z., Nagaraja, R. Y., Hoogenraad, C. C., Kushner, S. A., … Elgersma, Y. (2009). betaCaMKII controls the direction of plasticity at parallel fiber-Purkinje cell synapses. *Nat Neurosci*, *12*(7), 823–825. https://doi.org/10.1038/nn.2329

Vandaele, S., Nordquist, D. T., Feddersen, R. M., Tretjakoff, I., Peterson, A. C., & Orr, H. T. (1991). Purkinje cell protein-2 regulatory regions and transgene expression in cerebellar compartments. *Genes and Development*, *5*(7), 1136–1148. https://doi.org/10.1101/gad.5.7.1136

Vaughn, D. E., & Bjorkman, P. J. (1996). The (Greek) key to structures of neural adhesion molecules. *Neuron*, *16*(2), 261–273. https://doi.org/10.1016/S0896-6273(00)80045-8

Venkatesh, B., Lee, A. P., Ravi, V., Maurya, A. K., Lian, M. M., Swann, J. B., … Warren, W. C. (2014). Elephant shark genome provides unique insights into gnathostome evolution.

Nature, *505*(7482), 174–9. https://doi.org/10.1038/nature12826

Vig, P. J., Subramony, S. H., Burright, E. N., Fratkin, J. D., McDaniel, D. O., Desaiah, D., & Qin, Z. (1998). Reduced immunoreactivity to calcium-binding proteins in Purkinje cells precedes onset of ataxia in spinocerebellar ataxia-1 transgenic mice. *Neurology*, *50*(1), 106–13. Retrieved from http://www.ncbi.nlm.nih.gov/pubmed/9443466

Vilella, A. J., Severin, J., Ureta-Vidal, A., Heng, L., Durbin, R., & Birney, E. (2009). EnsemblCompara GeneTrees: Complete, duplication-aware phylogenetic trees in vertebrates. *Genome Research*, *19*(2), 327–335. https://doi.org/10.1101/gr.073585.107

Wallace, R. H., Scheffer, I. E., Parasivam, G., Barnett, S., Wallace, G. B., Sutherland, G. R., … Mulley, J. C. (2002). Generalized epilepsy with febrile seizures plus: mutation of the sodium channel subunit SCN1B. *Neurology*, *58*(9), 1426–1429. https://doi.org/10.1212/WNL.58.9.1426

Wallace, R. H., Wang, D. W., Singh, R., Scheffer, I. E., George, a L., Phillips, H. a, … Mulley, J. C. (1998). Febrile seizures and generalized epilepsy associated with a mutation in the Na+-channel beta1 subunit gene SCN1B. *Nature Genetics*, *19*(4), 366–370. https://doi.org/10.1038/1252

Warren, W. C., Hillier, L. W., Marshall Graves, J. a, Birney, E., Ponting, C. P., Grützner, F., … Wilson, R. K. (2008). Genome analysis of the platypus reveals unique signatures of evolution. *Nature*, *453*(7192), 175–183. https://doi.org/10.1038/nature07253

Watanabe, H., Darbar, D., Kaiser, D. W., Jiramongkolchai, K., Chopra, S., Donahue, B. S., … Roden, D. M. (2009). Mutations in Sodium Channel β1- and β2-Subunits Associated With Atrial Fibrillation. *Circulation: Arrhythmia and Electrophysiology*, *2*(3), 268–275. https://doi.org/10.1161/CIRCEP.108.779181

Watanabe, H., Koopmann, T. T., Scouarnec, S. Le, Yang, T., Ingram, C. R., Schott, J., … Wiesfeld, A. C. P. (2008). Sodium channel β1 subunit mutations associated with Brugada syndrome and cardiac conduction disease in humans. *Structure*, *118*(6), 268–75. https://doi.org/10.1172/JCI33891.2260

Watanabe, M., & Kano, M. (2011). Climbing fiber synapse elimination in cerebellar Purkinje cells. *European Journal of Neuroscience*, *34*(10), 1697–1710. https://doi.org/10.1111/j.1460-9568.2011.07894.x

Williams, a F., & Barclay, a N. (1988). The immunoglobulin superfamily--domains for cell surface recognition. *Annual Review of Immunology*, *6*, 381–405. https://doi.org/10.1146/annurev.iy.06.040188.002121

Wimmer, V. C., Reid, C. a., Mitchell, S., Richards, K. L., Scaf, B. B., Leaw, B. T., … Petrou, S. (2010). Axon initial segment dysfunction in a mouse model of genetic epilepsy with febrile seizures plus. *Journal of Clinical Investigation*, *120*(8), 2661–2671. https://doi.org/10.1172/JCI42219

Wong, H. K., Sakurai, T., Oyama, F., Kaneko, K., Wada, K., Miyazaki, H., … Nukina, N. (2005). b

subunits of voltage-gated sodium channels are novel substrates of b-site amyloid precursor protein-cleaving enzyme (BACE1) and g-secretase. *Journal of Biological Chemistry*, *280*(24), 23009–23017. https://doi.org/10.1074/jbc.M414648200

Wong, J. C., & Escayg, A. (2015). Illuminating the cerebellum as a potential target for treating epilepsy. *Epilepsy Currents*, *15*(5), 277–278. https://doi.org/10.5698/1535-7511-15.5.277

Xiao, Z. C., Ragsdale, D. S., Malhotra, J. D., Mattei, L. N., Braun, P. E., Schachner, M., & Isom, L. L. (1999). Tenascin-R is a functional modulator of sodium channel beta subunits. *The Journal of Biological Chemistry*, *274*(37), 26511–7. Retrieved from http://www.ncbi.nlm.nih.gov/pubmed/10473612

Xiao, Z., Ragsdale, D. S., Malhotra, D., Mattei, L. N., Peter, E., Schachner, M., … Braun, P. E. (1999). Tenascin-R Is a Functional Modulator of Sodium Channel β Subunits. *Journal of Biological Chemistry*, *274*(37), 26511–26517.

Yereddi, N. R., Cusdin, F. S., Namadurai, S., Packman, L. C., Monie, T. P., Slavny, P., … Jackson, A. P. (2013). The immunoglobulin domain of the sodium channel b3 subunit contains a surface-localized disulfide bond that is required for homophilic binding. *FASEB Journal*, *27*(2), 568–580. https://doi.org/10.1096/fj.12-209445

Yoshimura, T., & Rasband, M. N. (2014). Axon initial segments: Diverse and dynamic neuronal compartments. *Current Opinion in Neurobiology*, *27*, 96–102. https://doi.org/10.1016/j.conb.2014.03.004

Young, P., Qiu, L., Wang, D., Zhao, S., Gross, J., & Feng, G. (2008). Single-neuron labeling with inducible Cre-mediated knockout in transgenic mice. *Nature Neuroscience*, *11*(6), 721–8. https://doi.org/10.1038/nn.2118

Yu, F. H., Westenbroek, R. E., Silos-Santiago, I., McCormick, K. a, Lawson, D., Ge, P., … Curtis, R. (2003). Sodium channel beta4, a new disulfide-linked auxiliary subunit with similarity to beta2. *The Journal of Neuroscience : The Official Journal of the Society for Neuroscience*, *23*(20), 7577–7585. https://doi.org/23/20/7577 [pii]

Zalc, B., Goujet, D., & Colman, D. (2008). The origin of the myelination program in vertebrates. *Current Biology*, *18*(12), 511–512. https://doi.org/10.1016/j.cub.2008.04.010

Zhang, B., Chen, L. Y., Liu, X., Maxeiner, S., Lee, S. J., Gokce, O., & Südhof, T. C. (2015). Neuroligins Sculpt Cerebellar Purkinje-Cell Circuits by Differential Control of Distinct Classes of Synapses. *Neuron*, *87*(4), 781–796. https://doi.org/10.1016/j.neuron.2015.07.020

Zhang, L., & Goldman, J. E. (1996). Generation of cerebellar interneurons from dividing progenitors in white matter. *Neuron*, *16*(1), 47–54. https://doi.org/10.1016/S0896-6273(00)80022-7

Zhou, D., Lambert, S., Malen, P. L., Carpenter, S., Boland, L. M., & Bennett, V. (1998). Ankyrin(G) is required for clustering of voltage-gated Na channels at axon initial segments and for normal action potential firing. *Journal of Cell Biology*, *143*(5), 1295–1304.

https://doi.org/10.1083/jcb.143.5.1295

Zhou, J., Potts, J. F., Trimmer, J. S., Agnew, W. S., & Sigworth, F. J. (1991). Multiple Gating Modes and the Effect of Modulating Factors on the ul Sodium Channel. *Neuron*, *7*, 775–785.

Zuo, J., Jager, P. L. D., Takhashi, K. A., Jiang, W., Linden, D. J., & Heinz, N. (1997). Neurodegeneration in Lurcher mice caused by mutation in d2 glutamate receptor gene. *Nature*, *388cell de*(August), 769–773.